

**DEVELOPMENT OF READY-TO-USE
BIOSENSORS FOR DIAGNOSTICS
AND BIOSENSING**

DEVELOPMENT OF READY-TO-USE BIOSENSORS FOR DIAGNOSTICS AND BIOSENSING

By
SANA JAHANSHAHI-ANBUHI, B.Eng., M.A.Sc

A Thesis

Submitted to the School of Graduate Studies
in Partial Fulfillment of the Requirements
for the Degree
Doctor of Philosophy

McMaster University

© Copyright by Sana Jahanshahi-Anbuhi, 2014

PhD Candidate (2014)

McMaster University

Chemical Engineering

Hamilton, Ontario

TITLE: Development of Ready-to-Use Biosensors for
Diagnostics and Biosensing

AUTHOR: Sana Jahanshahi-Anbui
B.Eng. (Sharif University of Technology)
M.A.Sc (Tarbiat Modares University)

SUPERVISORS: Professor Robert Pelton
Professor Carlos Filipe

NUMBER OF PAGES: ix, 105

Abstract

Ideally, every person in the world should have access to a safe and clean water supply; if not all sources of water are clean and safe, at the very least, an effective method to detect water contamination should be readily available. An effective detection method should not only be sensitive, rapid, robust, and affordable, but, ideally, it should also be equipment-free and easy to transport and deliver to the end-users.

The main goal of this project is to develop a variety of bits and pieces of bioassay systems, with a particular focus on paper-based bioactive devices in order to provide portable and ready-to-use biosensors which can be useable by anyone anywhere around the world without requiring formal training.

According to the World Health Organization (WHO), 76,000 people each year die in India alone because of pesticide poisoning. Long term exposure to organophosphate pesticides is known to have adverse effects on neurological function and can lead to Alzheimer's Disease, Attention Deficit Hyperactivity Disorder (ADHD), and reduced Intelligence Quotient (IQ). The likelihood of long term exposure to pesticides is heightened in developing countries, so a reliable and inexpensive pesticide sensor is a much-needed device in the developing world. To address this need, this project reports on the development of a fully-automated bioactive paper-based sensor for the detection of organophosphate pesticides. In the proposed biosensor, two innovations were implemented to achieve a full-automated format for the pesticide sensor: (I) First is a *PUMP ON A PAPER* (Jahanshahi-Anbuhi et al., *LOC*, 2012) that increases the flow rate of fluids within paper-based microfluidic analytical devices and sequentially brings two separate liquid streams to the enzyme test zone on the paper sensor, and (II) the second innovation is a *PIPETTE ON A PAPER* (Jahanshahi-Anbuhi et al., *LOC*, 2014) that involved the creation of a pullulan (a natural non-ionic polysaccharide) temporary bridge-system to transfer a known amount of solution to the sensing zone that, gives the enzyme zone a chance to dry and accept the substrate solution from the slow channel after a fixed period of time. This proposed format results in a simplified assay that detects the presence of pesticides automatically without any further manipulation from the user.

However, the shelf life of this assay kit is challenging due to instability of both enzyme (AChE) and substrate (IDA) at room temperature. AChE loses its enzymatic activity when stored at room temperature and IDA becomes oxidized quickly. This problem is not unique to these two bio reagents, however; almost all bioassays which use bio-reagents (such as enzymes and small-molecular substrates) are unstable to varying degrees and require special shipping and storage. The instability of these molecules can arise from either thermal denaturation or chemical modification, such as oxidation or hydrolysis. Because of these issues, they often have to be shipped on dry ice with special packaging, which is costly. The cost of maintaining a cold chain for distributing bio-reagents accounts for up to 80% of the cost.

Aside from the cost, these reagents also have to be stored in bulk in refrigerators or freezers to minimize the loss of activity, but they must be thawed and aliquoted for their intended tests. Repeated freezing and thawing can result in a significant loss of activity, which often leads to less reliable test results. These issues make running such assays in resource-limited settings a significant challenge. There is, therefore, an urgent need for an assay system with stable reagents that is easy to use, simple to read, inexpensive, and that includes a method for the long-term stabilization of enzymes and other unstable reagents in pre-

measured quantities.

To overcome to all these issues, pullulan is utilized for the development of pill-based-biosensors. Pullulan dissolves quickly in aqueous solutions and shows very high oxygen barrier properties in its film form. Considering the unique properties of pullulan, it is hypothesized that pullulan may be suitable for producing assay pills with encapsulated enzymes or other unstable molecules and may provide a simplified platform for carrying out bioassays in resource-limited settings. The application of these pill-based-biosensors is shown via the entrapment of AChE and IDA for the creation of an assay kit that can detect organophosphate pesticides (Jahanshahi-Anbuhi et al., *Angew. Chem.*, 2014). Moreover, this thesis reports on the stabilization of highly unstable firefly luciferase for the detection of microorganisms and, more particularly, ATP. Through the use of pullulan, this thesis demonstrates that both the enzyme and the substrate can be protected, immobilized, and stabilized at room temperature, instead of the existing storage methods, which require temperatures $<-20^{\circ}\text{C}$. This innovation allows for a more convenient method of shipping the bioassay kits around the world without any extra care.

Furthermore, pullulan-based films are utilized for the development of a method for controlled multidirectional flow within paper-based biosensors. This method provides the possibility of trapping labile and volatile reagents and stabilizing them by forming thin films with pullulan. The trapped reagents within pullulan films can be strategically stacked and assembled on a paper strip in different directions. Furthermore, should the need arise, these reagents can be released and delivered sequentially or simultaneously in both vertical and lateral directions through the paper. The application of this method is shown for: (I) creation of "ready-to-use" assay kit for the detection of *Escherichia coli* (*E. Coli*). This assay kit has the step of cell lysing and proceeds automatically to the step in which enzymes react. The second application (II) shows the trapping of Simon's reagents, which is widely used for methamphetamine detection.

Overall, these unique fabrication techniques can be widely used for the preparation of highly stable, ready-to-use, and user-friendly biosensors. We are currently working on the detection of other contaminants such as heavy metals, and we are starting on vaccine stabilization and delivery, which would have a tremendous impact for society.

Acknowledgements

Firstly, I would like to express my gratitude to my PhD supervisors, Prof. Robert Pelton and Prof. Carlos Filipe for their continual support and mentorship throughout my research work. Many thanks to Prof. Pelton for his invaluable guidance while providing me with a remarkable freedom to research and explore new ideas in my own way. I am grateful for his generous support. Many thanks to Prof. Filipe who kept me motivated with his constant encouragement, positive attitude, and confidence in my ideas. I especially appreciate the way that he encouraged me to share my ideas and the opportunities to share my work and ideas with others that he provided me.

I would also like to thank Prof. Kari Dalnoki-Veress from the Department of Physics & Astronomy and my supervisory committee member Prof. Ravi Selvaganapthay from the Mechanical Engineering Department for contributing valuable suggestions and advice. I am also very grateful for Prof. John Brennan from the Department of Chemistry & Chemical Biology, and Prof. Yingfu Li from the Biochemistry Department for providing me with excellent suggestions and help on effective scientific writing as well as experimental work.

Special thanks is also due to the Mechanical Technician of the Chemical Engineering Department, Mr. Paul Gatt who was always ready to give his fast and friendly assistance in the design and fabrication of any apparatus required for my research. Thanks also to the Lab Manager, Mr. Doug Keller, as the distance between thinking of a material and having it on the way to the lab was made easy by simply emailing him a note. I also would like to thank Ms. Sally Watson for handling all the administrative work and paperwork required by my project and Mr. Dan Wright for his technical support in instrumentation.

Furthermore, I am extremely thankful to my undergrad summer students, Ms. Aleah Henry, Mr. Kevin Pennings, Ms. Karen Giang, and Ms. Samantha Dobkowicz, as well as my Research Assistant Mr. Vince Leung, as many of the experiments would not have been completed as easily without their hard work and contributions.

I also would also like to thank all my colleagues and group members for their valuable discussion and support. I appreciate all instrument training and fruitful discussion from Dr. Songtao Yang, Dr. Yuguo Cui, Dr. Kevin Zuohe Wang, Mr. Justin Zhen Hu, Mr. Behnam Naderi Zand, Mr. Roozbeh Mafi, and Dr. Tracy Jingyun Wang. I would also like to thank Dr. Zakir Hossain, Dr. Clemence Sicard, Dr. Si Amar Dahoumane, Dr. Balamurali Kannan, Dr. Meng Liu, Ms. Dawn White, and Ms. Carmen Carrasquilla for sharing their chemistry and bioanalytical knowledge.

Last but not least, I would like to thank my family and express my love and gratitude to my husband, my parents, and my lovely grandma for their endless love and for supporting me spiritually throughout my life, and, finally, thanks to God for giving me the opportunity and the ability to proceed with my doctoral research work.

Table of Contents

Abstract.....	iii
Acknowledgements.....	v
Table of Contents	vi
List of Acronyms and Notation.....	viii
Chapter 1 Introduction.....	1
1.1 Biosensor.....	1
1.2 Contaminants in Drinking Water and Importance of Detection	3
1.2.1 Pesticides	5
Conventional Techniques for Assessment of Pesticide Contamination in Surface Water	6
1.2.2 E. coli & Microorganisms	7
Conventional Techniques for Assessment of Bacterial Contamination	8
1.2.3 Heavy Metals.....	10
Conventional Techniques for Assessment of Heavy Metal Pollution in Surface Water	11
1.3 Paper Based Biosensors and Detection of Water Contamination	12
1.3.1 Microfluidic Paper-Based Analytical Devices (μ PADs)	12
Detection of Analytes in Paper-Based Biosensors.....	13
Creation of Patterned Paper-Based Microfluidic Biosensors	14
1.3.2 Controlling the Flow, and Valve Developed within the Channels in Microfluidic Biosensors.....	20
Temperature Actuation.....	21
Manual Actuation.....	21
Electrical Actuation.....	22
Depositions on the Channel	23
Paper Shaping	25
1.3.3 Paper Based Bioassays for Detecting Pathogens and Toxins in Water.....	26
1.4 Pullulan	31
1.4.1 Pullulan Properties.....	33
Roughness and Hydrophilicity.....	34
Solution Properties.....	36
Solid Properties.....	41
Chemical Modification	45
1.5 Objectives, and Report Outline.....	46

1.6	References.....	48
Chapter 2	Flow Speeding-Up System for Paper- Based Microfluidics Devises	55
2.1	Introduction 1	56
2.2	Experimental section 2.....	57
2.3	Results and discussion 3	58
2.4	Conclusions 7.....	62
2.5	References 7.....	62
Chapter 3	Automatic Flow Shut-Off Valve for Paper-Based Microfluidics Devices.....	63
3.1	Introduction 1	64
3.2	Experimental section 2.....	65
3.3	Results and discussion 3	66
3.4	Conclusions 7.....	70
3.5	References 8.....	71
3.6	Supplementary Information 9	72
Chapter 4	Biolab-on-Pills	75
4.1	Supplementary Information 5	80
4.1.1	A. Experimental Details 6	81
4.1.2	B. Supporting Figures 7.....	82
Chapter 5	‘All-in-One’ Luminescent Pullulan Pills	84
Chapter 6	Automatic Time Dependent Reagent Delivery in Paper-Based Microfluidics Devices	92
Chapter 7	Concluding Remarks.....	102

List of Acronyms and Notation

<i>A. Pullulans</i>	<i>Aureobasidium pullulans</i>
AChE	Acetylcholinesterase
ATP	Adenosine triphosphate
B-PER	Bacterial Protein Extraction Reagent
CA	Contact Angle
cfu	Colony-forming units
CI	Color Intensity
CoA	Co-enzyme A
CPRG	Chlorophenol Red- β -D-galactopyranoside
CPS	Count Per Second
dL	Deciliters
DNA	Deoxyribonucleic Acid
DTT	DL-Dithiothreitol
<i>E. coli</i>	<i>Escherichia coli</i>
EDTA	Ethylenediaminetetraacetic acid
IDA	Indoxyl Acetate
LOD	Limit of Detection
MW	Molecular Weight

OP	Organophosphate
PCR	Polymerase Chain Reaction
PEG	Polyethylene glycol
PET	Polyester
PVAm	Polyvinylamine
RLU	Relative Light Units
SDS	Sodium Dodecyl Sulphate
TaqDP	Taq DNA Polymerase
TSB	Tryptic Soy Broth
β -Gal	Beta-galactosidase

Chapter 1 Introduction

Between 2014 and 2050, the world's population is predicted to climb by about 2 billion; from 7.1 billion today to 9.1 billion in 2050. Significantly, most of this increase is occurring in middle- and low-income countries. [1-4] This population and demographic change will have several implications for public health, and if people are to retain their independence while being involved in both family and community life, good health is crucial. [3, 5-7]

In the context of global public health, effective and early diagnostic of toxic agents in our food, water and air is critical. In recent years, biological assay (shortened into bioassay) has engaged considerable attention to a growing number of biologists and related scientists. Bioassays are widely used in toxicology to determine the relative toxicity of chemicals and therefore may be an effective means of diagnosing and environmental analysis. A bioassay typically involves the use of a biological reagent used to test for chemical or biological activity and is often used to evaluate the biological effects of chemical compounds being considered for healthcare or pharmaceutical applications. [8-12]

In this work, we focus on developing simple, safe, sensitive, quick, reliable, cost-effective, and ideally “ready-to-use” bioassay systems/biosensors for point-of-care diagnostic and environmental analysis. Ready-to-use biosensors have the potential to provide high throughput, easy-to-use and innovative assays, well suited for use in demanding applications ranging from pharmacology, environmental biology, and toxicology to packaging and even labeling.

1.1 Biosensor

Biosensor = Bioreceptor element + transducer \Rightarrow quantifiable signal. A biosensor which converts biological activity into a quantifiable signal, basically consists of two components: a bioreceptor and a transducer. The bioreceptor or biorecognition element is a biomolecule (e.g. enzyme, antibodies, microorganisms, nucleic acids, etc.) that is capable of recognizing a specific target analyte. The transducer or the detector element transforms the recognition event resulting from the analyte of interest interacting with the bioreceptor element into a measurable signal. Typically, this step is done by measuring the change that occurs in the bioreceptor reaction. [3,

13-16] The uniqueness of a biosensor is that it combines the two components into one single sensor. So that, the target analyte can be measured without using extra reagents.

One major requirement for a biosensor is that the bioreceptor molecule has to be stabilized/immobilized in the biosensor system. Bioreceptor immobilization/stabilization is a central requirement as the retention of the biological activity and surface regeneration affects the sensitivity of the system in detecting the target analyte. [17, 18]

The immobilization is done either by physical entrapment or chemical attachment. As illustrated in **Figure 1.1**, the enzyme may be immobilized by: [17]

- Entrapment: Enzymes immobilization in three-dimensional matrices
- Adsorption: Adsorption of the enzyme onto solid supports
- Cross-linking: Crosslinking enzymes with glutaraldehyde, or other bifunctional agents such as glyoxal or hexamethylenediamine
- Covalent immobilization: Covalently coupled enzyme to a polymeric support structure
- Affinity: Enzyme is specifically oriented and immobilized by site-specific interaction between a segment of the protein sequence (e.g. biotin, histidine) and an activated support (e.g. avidin, lectin, metal chelates)

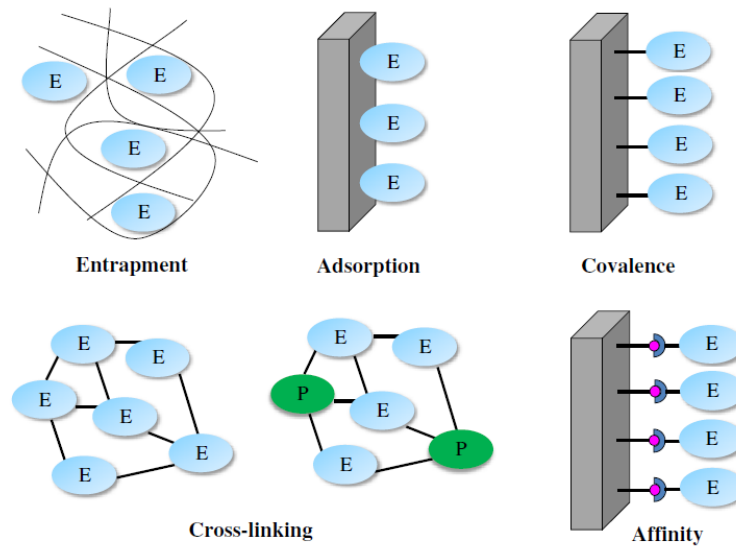


Figure 1.1 Different methods for immobilization of enzymes. E: enzyme, and P: inert protein. Adapted from Ref. [17].

Parameters such as shelf-life, stability of the biosensor, and more importantly, making the biosensor deliverable to end-users also depend on the bioreceptor stabilization. So, in development of powerful biosensors, achieving an efficient immobilization/stabilization procedures is highly important.

1.2 Contaminants in Drinking Water and Importance of Detection

Water is used every day for drinking, cooking, bathing, and cleaning. Tap water is typically obtained from one of two sources, either a public water supply, such as a municipal facility, or a private water supply, such as a private well. [16, 19, 20]

The public supply system facilities provide water for entire communities and are required to meet certain standards; however, for the private water systems, which are generally in rural areas, the owner of the well is responsible for the treatment, testing, and quality of the water. There can be many sources (such as agriculture run-off, animal waste, chemicals and road salts, gasoline leaks, etc.) that can cause contaminants to enter the well. [19]

Even though the public water supply is monitored regularly to ensure maximum contaminant levels are not exceeded, it has often been reported that the quality of water actually delivered to

the end user is lower than that at the source in the municipal facility. This is due to contaminants that may be introduced into the tap from household plumbing and distribution pipes. [1, 2, 21]

Effects of Contaminated Water on Health

Water-related diseases are one of the major health problems in the world. Health risks may arise from consumption of contaminated water. [22, 23]

Each contaminant in water is caused by a different source as shown in **Figure 1.2**. *E. coli* and other micro-organisms which are found in fecal material may move into the water due to a leakage in a sewage tank, or agricultural run-off can bring harmful pesticides into the well water. Different impurities and contaminants can have different health effects. While some impurities are minor contaminants (e.g. the ones that make water a bit smelly, dirty, or discolored), there are contaminants that can cause serious health problems such as Alzheimer's Disease, Cholera, Hepatitis, and even death. Chlorine, a typical disinfectant, can result in skin rashes. Nitrates, which are known to inhibit cellular oxygen levels, are deadly for young children. [19, 24] Exposure to low levels of arsenic can cause stomach issues, and arsenic at high levels is known to lead to cancer. [25]

The more serious contaminants to drinking water include pesticides, human and animal waste, micro-organisms, heavy metals, and improperly disposed chemicals, as well as naturally-occurring substances (such as arsenic).

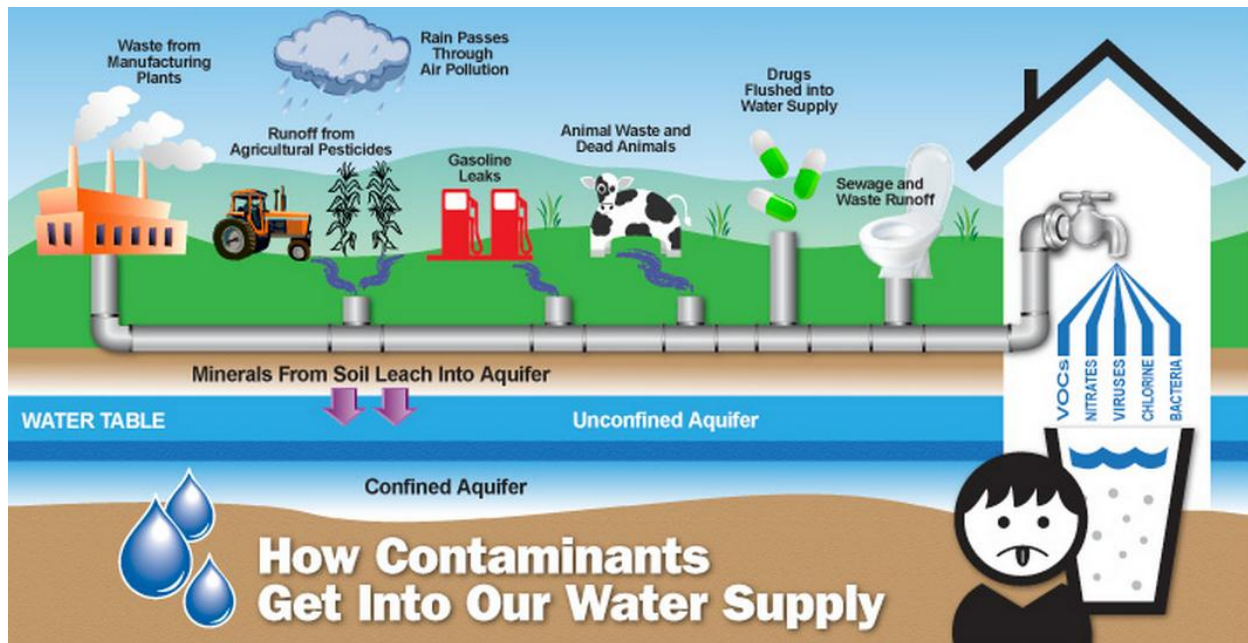


Figure 1.2 Potential sources of water contamination. Adapted from Ref. [19].

1.2.1 Pesticides

Pesticide refers to any compound or mixture of compounds meant for destroying, preventing, or mitigating any pest (insects, weeds, mites, nematodes, rats, etc.) (EPA, 2009). All pesticides act by interfering with the normal metabolism of the target insects. [26-28]

While pesticides are intended to destroy target species, other organisms in the environment including humans and other animals are also affected or even killed. [27] For example, Atrazine is an herbicide widely used to kill weeds. Atrazine is moderately soluble in water, and therefore favours being dissolved by soil in the presence of crop watering or natural rain. Atrazine inhibits photosynthesis and is subject to both biotic and abiotic breakdown. If the water becomes contaminated, it may inhibit the ability to sustain aquatic habitat and sustain life. The dire effects on aquatic plants may also negatively impact the aquatic life. **Figure 1.3** demonstrates the pesticide operations through inhibiting the enzyme. [26]

Malathion, which is classified as an organophosphate insecticide, has the same dire effects as atrazine if it contaminates water supplies as well as soil. Organophosphate pesticides (OP) are a class of pesticides which are widely used in agriculture and homes, and their effects have been

linked to damage brain and neurological function. Long term exposure to organophosphate pesticides can lead to Alzheimer's Disease, Attention Deficit Hyperactivity Disorder (ADHD), reduced IQ scores, or even death. Even extremely low concentrations of these pesticides can harm many species and affect an ecosystem's natural balance. [28-33]

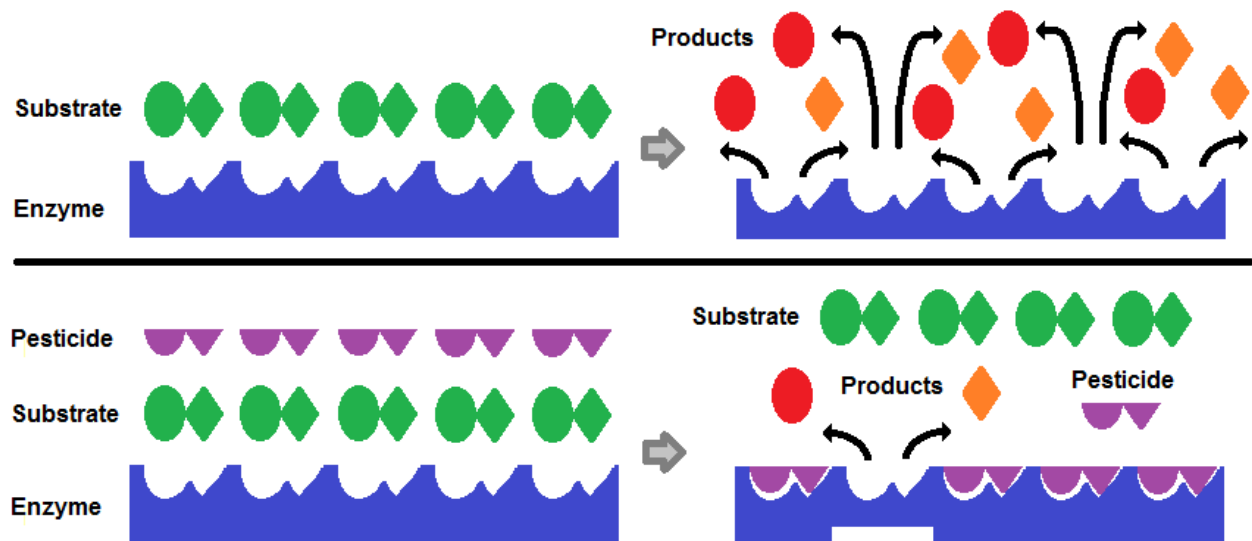


Figure 1.3 Inhibition of the catalytic reaction by means of pesticides: (upper) in the absence of pesticide, and (lower) in presence of pesticide in biosensor. Adapted from Ref. [26].

Conventional Techniques for Assessment of Pesticide Contamination in Surface Water

Pesticide detection is a large issue in places that obtain their drinking water from ground sources due to how complex the process of detection can be. The degradation products that are formed by most modern pesticides are usually polar, non-volatile and thermolabile. Analytical methods of detection commonly use mass spectrometry or gas chromatography with specific detectors; however, they are extremely time-consuming. Liquid Chromatography (LC) as well as Diode Array Detection (DAD) have been increasing in popularity; however, they are not sensitive or selective enough. [34] **Table 1-1** summarizes different analytical techniques for the detection of pesticides in aqueous and soil samples along with advantages and disadvantages of each method. [35]

Prior to the analytical determination of pesticide trace in aqueous samples, low concentrations of analytes must be recovered. Liquid-Liquid Extraction (LLE) is the traditional approach to

preparing water samples for testing; however, it is time consuming and generally involves large volumes of expensive solvents, which limit this method's practicality. Due to the many shortcomings with LLE, liquid-solid extractions using small sorbent cartridges have been developed. One of the most popular is octadecyl (C-18) bonded porous silica. Similarly, carbopack B is a graphitized carbon black with a nonporous, nonpolar homogeneous surface which is utilized in capillary gas chromatography columns. A sample is passed through the cartridge and due to its positively charged center, the base-neutral pesticides are separated from the acidic ones. [36]

Table 1-1 Techniques to determine pesticide residues. [35]

Technique	Advantage	Disadvantage
Gas chromatography (GC)	<ul style="list-style-type: none"> - High resolving power - High sensitivity and selectivity 	<ul style="list-style-type: none"> - Inadequate for polar, thermo labile and low volatility compounds - High consumption of expensive gasses
Gas chromatography (GC) / Mass spectrometers (MS)	<ul style="list-style-type: none"> - High resolving power - High sensitivity and selectivity - Mass spectrum libraries for analyzing unknown samples 	<ul style="list-style-type: none"> - Inadequate for polar, thermo labile and low volatility compounds - High consumption of expensive gasses
Liquid chromatography (LC) - UV	<ul style="list-style-type: none"> - Used for any organic solute - Can use both mobile and stationary phases - Low price - Automated and miniaturized - Lack of matrix interference 	<ul style="list-style-type: none"> - Insufficient separation efficiency and selectivity - Large amounts of expensive, toxic, organic solvents for mobile phase
Liquid chromatography (LC) - Fluorescence	<ul style="list-style-type: none"> - High separation efficiency 	<ul style="list-style-type: none"> - Not many fluorescent compounds
Liquid chromatography (LC) - Mass spectrometers (MS)	<ul style="list-style-type: none"> - Used for any organic solute - Automated and miniaturized - Can use both mobile and stationary phases 	<ul style="list-style-type: none"> - Strongly affected by matrix interferences - Identification difficult using interfaces that provide soft ionization - Lack of spectral libraries

1.2.2 *E. coli* & Microorganisms

Strains of *Escherichia coli* (*E. coli*) have been known to be detrimental to human health and may cause diarrhea, hemolytic-uremic, and hemorrhagic colitis syndrome. Typically, these symptoms

are from the production of the shiga toxin (Stx 1, and Stx 2) but can also be from enterohemorrhagic *E. coli* hemolysin and intimin. [37] There have been many outbreaks that affect people worldwide and have contaminated food and water sources. It is important to detect the presence of *E. coli* early on in order to maintain human health.

Walkerton Tragedy. In the town of Walkerton, Ontario an *E. coli* O157:H7 outbreak caused an estimated 2300 to become seriously ill and seven deaths in May 2000. The source of the contamination was discovered to be manure that had been spread on a farm near a well which was used to supply the town with water. The incident could have been prevented with better efforts to have safe drinking water and continuous monitoring. [38]

Conventional Techniques for Assessment of Bacterial Contamination

Prior detection methods for bacterial pathogens are based on being very selective and using standard biochemical methods. Drawbacks of these methods include large sampling errors, time consuming, and mono-specific and low throughput. Most bacteria are also difficult to culture, which makes most tests unviable. For this purpose many bacteria are not tested for during routine water quality assessments. For a long time, *E. coli* has been used as the primary indicator of water pollution; however, this has recently come into question amongst researchers due to the fact that the presence of *E. coli* does not correlate with water contamination caused by other waterborne pathogens. Alternatively, nucleic acid probes and Polymerase Chain Reaction (PCR) techniques have been demonstrated to provide a high enough sensitivity for detecting specific pathogens. More recently, multiplex Polymerase Chain Reaction (m-PCR) has provided a high sensitivity for detection of specific microorganisms in aquatic life. Current applications use m-PCR to detect six different waterborne pathogens in a single tube. Six sets of primers were developed to detect each of the six pathogens simultaneously, and the primer sequences were compared against each other using the GenBank database. This method provides a high throughput and cost effective m-PCR system that increases the accuracy of detection and limits the risk involved with testing for pathogenic bacteria in marine environments. [39]

ATP and Detection of Microorganisms

Adenosine triphosphate (ATP), which is known as the source of energy for living things, is used for many biological functions like cellular energetics, metabolic regulation, and cell signaling. ATP has three major components: ribose sugar moiety, an adenine-base, and a string of phosphate groups. The energy component of ATP is stored within the phosphate bonds. In a biological context, many energetically unfavourable reactions proceed when linked to ATP or ADP through hydrolysis. [40] ATP, until recently, was only considered important for its role as the primary source of energy. It has since been demonstrated that ATP is also significant as a pleiotropic extracellular messenger, used for cell to cell communication by acting as plasma membrane receptors. [41]

The quantification of ATP is necessary for many purposes. ATP, which is utilized by almost all living things, is degraded when no organism is present; therefore, ATP can be used to determine the presence of living organisms. The measurement of ATP can, therefore, be used to detect bacteria on different surfaces, in water, as well as in somatic cells in culture. [40]

There are many complications with the analysis of relevant ATP release. The fact ATP is present in all cell types makes it difficult to determine whether extracellular ATP is derived from a cellular release mechanism or due to accidental cell lysis during experimental procedures. Most cells also express ectonucleotidases, which hydrolyzes extracellular ATP on the cell surface. These nucleotides may be confined between cells or diluted, which affects the dynamic concentration of ATP and presents further challenges with properly measuring its extracellular levels. [42]

Firefly Luciferase for ATP Detection

Firefly Luciferase catalyzes a chemi-luminescent reaction in the presence of ATP, luciferin, Mg^{2+} , and molecular oxygen. Luciferase is a monomeric 61 kD enzyme that, when oxidized, produces light at 560 nm. ATP activates the protein to produce a mixed hydride intermediate. This intermediate then reacts with oxygen to create a transient dioxetane, which degrades to oxyluciferin and carbon dioxide along with a burst of light. The intensity of the light produced in

this reaction is proportional to the amount of ATP present. [40]

This bioluminescent reaction is therefore ideal for detecting the presence of ATP; however, luciferase is highly unstable and cannot be reused, making it an expensive and inefficient option. This technique is sensitive enough to detect ATP at the nanomolar level, but is stable only when kept in proper storage at temperatures of -80°C . A need for better immobilization is needed since these conditions are not ideal for transporting the luciferase sensor. [43]

1.2.3 Heavy Metals

Heavy metal pollution can come from many different sources, from natural processes to industrial waste. The metal that leaks into the water can affect the wildlife with which it comes in contact or can be consumed by humans and cause detrimental effects. Heavy metals are a large issue to society because they are non-biodegradable and have long half-lives for elimination. This means that they can have longer term health effects since heavy metals can accumulate in the fatty tissue of our body and affect our central nervous system, and they are responsible for the degradation of many important internal organ functions. [44]

Cadmium and mercury can impair kidney function, cause tumours and hypertension, and reduce reproductive capacity. [45] Cobalt has been shown to provoke the generation of reactive oxygen species that damage DNA and increase the amount of cancerous cells. Copper is actually key in both normal and abnormal cells but is known to have an important role in many neurodegenerative diseases like Alzheimer's and Parkinson's. [46]

Lead poisoning only normally occurs where water is exposed to lead pipes either in older buildings or if older pipes have yet to be replaced. Lead, like many heavy metals, causes damage to the nervous and reproductive system as well as causing high blood pressure and anemia. At very high concentrations, lead can cause comas or death. [47]

Minamata disease: Mercury poisoning in Japan. Minamata disease is caused by methyl mercury poisoning that occurs when humans ingest fish or seafood contaminated with waste water. The disease was first discovered in the 1950s in Japan, where marine products were tested for high

concentrations of mercury (5.61-35.7 ppm). Citizens who ingested these products showed symptoms like auditory disturbances, ataxia, dysathria, sensory disturbances, and tremors. The mercury also travelled from mother to fetus, and these babies showed signs of extensive brain lesions. Over the past 36 years, of the 2252 patients officially recognized with M.d, 1043 have died. [48]

Conventional Techniques for Assessment of Heavy Metal Pollution in Surface Water

One conventional method in detecting heavy metals is the use of Atomic Absorption Spectrophotometer (AAS). AAS uses wavelengths of light specific to each element to determine the concentration of an element at parts-per-billion (ppb) levels. AAS is used to determine the quantity of metals based on blood or urine samples, in pharmaceutical manufacturing processes, and for testing elements from environmental samples. [49-51] The concentration of element in the sample is determined based on the absorption of optical radiation from free atoms and uses the Beer-Lambert law to convert absorbancy to concentration.

Figure 1.4 demonstrates a simplified diagram of the AAS Equipment for detection of heavy metal. [49]

Ganga is the most important river of India and supplies 29 cities, 7 towns and thousands of villages with water. The river is contaminated with inorganic pollutants as well as heavy metal toxins and agricultural pesticides. Water samples were collected once a month and kept in polythene containers with concentrated HNO_3 in order to preserve the sample. To test for heavy metals, the samples were digested with di-acid mixture on a hot plate and filtered. These filtered samples were analyzed using AAS. [50] A similar method and AAS is utilized in Korea for the detection of Cd, Cu, Pb and Zn to determine how far waste has travelled around the metal mines and the severity of the metal concentrations. [51]

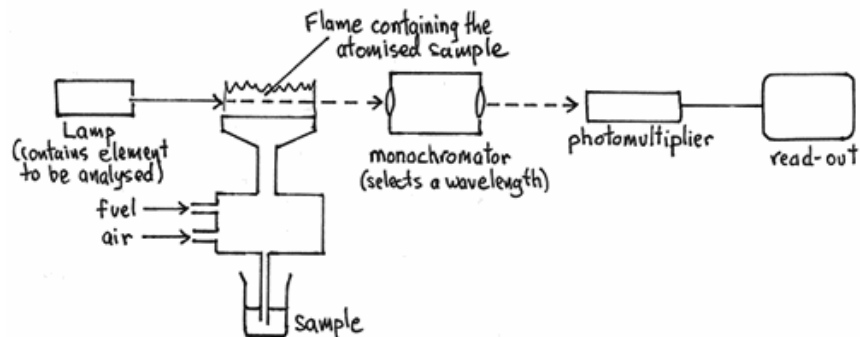


Figure 1.4 Simplified diagram of the Atomic Absorption Spectroscopy Equipment for heavy metal detection. Adapted from Ref. [49].

In general, the conventional methods for detection of contamination in water are not appropriate for society's needs, as the methods are expensive, time consuming, and require trained personnel. [34-36, 49]

Therefore, development of a reliable sensor for detection of such contaminations is needed, especially in the developing world. Requirements of such devices are in line with the WHO's ASSURED criteria for low-cost sensors:

- Affordable
- Sensitive
- Specific
- User-friendly
- Rapid
- Equipment-Free
- Deliverable to end-users

Giving a brief introduction to the paper-based microfluidic biosensors, the following section presents some of the recent research done on the creation, development, and improvement of these devices as well as techniques developed for simple detection of water contamination particularly pesticides, bacteria, and heavy metals.

1.3 Paper-Based Biosensors and Detection of Water Contamination

1.3.1 Microfluidic Paper-Based Analytical Devices (μ PADs)

Microfluidic technology has become an essential part of biosensors and point of care diagnostics as well as becoming more useful in healthcare contexts due to its ability to use extremely small sample quantities of liquid to produce rapid test results.

Lab on a Chip is the current method used for microfluidic analytical sensors and is advantageous because of its high sensitivity. However increased cost and uneasy operation require further research to be done in order to expand its application. Paper-based sensors are widely recognized as a cheaper alternative for low-cost, low-volume bioassays. [8, 52-54]

The primary advantages of paper-based microfluidic sensors are that they are easy to use, low cost, disposable, and equipment-free. These characteristics make this technology perfect for detecting disease and improving healthcare, particularly in developing countries, especially for those with minimal infrastructure and inexperienced healthcare staff.

Detection of Analytes in Paper-Based Biosensors

Four main methods are used for the detection of analytes in paper-based microfluidics: calorimetric detection, electrochemical (EC) detection, electrochemiluminescence (ECL) detection, and chemiluminescence (CL) detection. Calorimetric detection typically utilizes enzymes or colour-changing reactions and can be visually detected. EC detection is more sensitive than calorimetric detection, is not affected by local lighting conditions, and is therefore affected less by contaminants. An example of glucose detection in paper-based biosensors via calorimetric, electrochemical, and electrochemiluminescence detection methods is demonstrated in **Figure 1.5**.

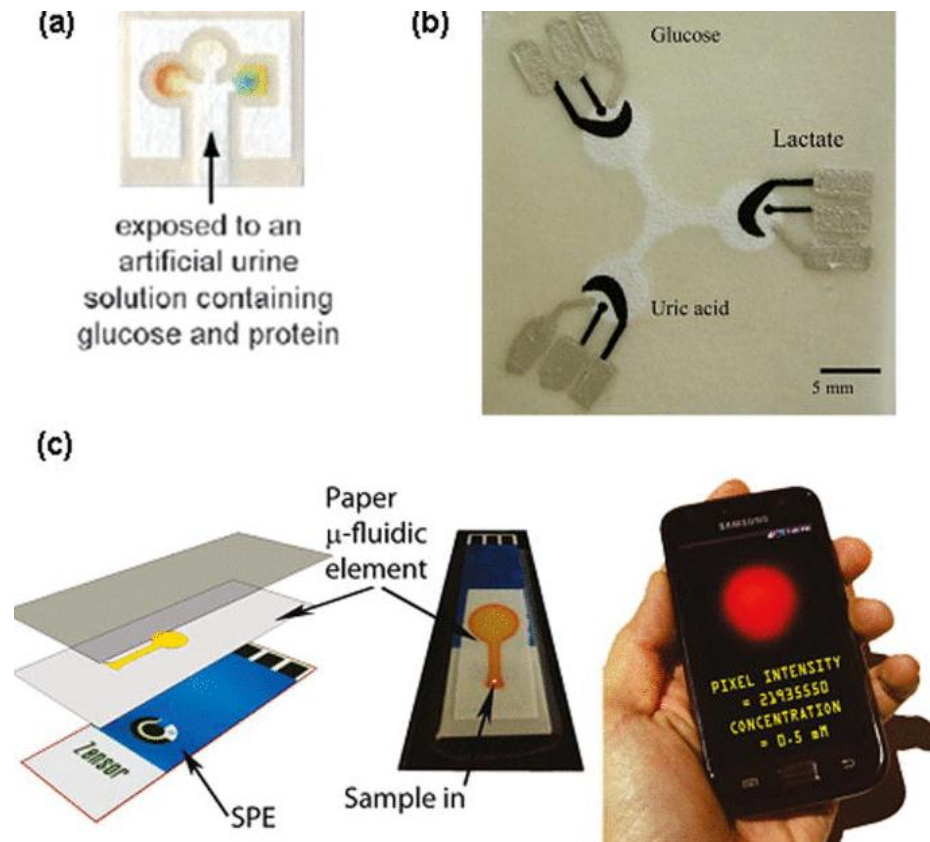


Figure 1.5 a) Calorimetric detection of glucose; b) EC detection using silver electrode contact pads on a three-electrode paper fluidic device; c) ECL detection of DBAE using emitted light from a sample. Adapted from Ref. [55].

Creation of Patterned Paper-Based Microfluidic Biosensors

Cellulose paper is hydrophilic and allows easy penetration of aqueous liquid. Physical or chemical barriers must be put on the paper in order to create the microfluidic channels needed for testing; this can be done by using hydrophobic polymers as walls of the channels.

Hydrophobic photoresist polymers are excellent for creating this hydrophobic wall. However, photolithography poses two major challenges: hardening of the barrier as well as its susceptibility to bending and damage. Printed polydimethylsiloxane (PDMS) on paper was used to overcome the inflexibility of previous devices; however, the barrier deteriorated due to inaccuracy in controlling where the PDMS penetrated the paper. The next step towards

improving this method is using paper sizing chemistry to generate hydrophilic and hydrophobic patterns on paper in order to create a microfluidic sensor using alkyl ketene dimer (AKD) and alkenyl succinic acid anhydride (ASA). These chemicals are commercially used in paper making and as such represent the most inexpensive paper patterning materials currently available.

Combining printing methods and patterned sizing to create paper-based microfluidic sensors help retain original flexibility of the paper; this combination also allows functional reagents to be easily incorporated into the device. [56] Different techniques for fabrication of paper-based microfluidic devices are summarized below in **Table 1-2**.

Table 1-2 Comparison of patterning techniques to create paper-based microfluidics.[55]

Fabrication Technique	Patterning Agents	Patterning Principles	Patterning Approaches
Photolithography	Photoresist (Eg. SU-8)	Physical blocking of pores in paper	Entire hydrophobization followed by selective dehydration
Plotting	PDMS	Physical blocking of pores in paper	Selective hydrophobization
Ink Jet Etching	Polystyrene	Deposit reagent on fiber surface	Entire hydrophobization followed by selective dehydration
Plasma Treatment	AKD	Chemical modification of fiber surface	Entire hydrophobization followed by selective dehydration
Wax Printing	Wax	Deposit reagent on fiber surface	Selective hydrophobization
Ink Jet Printing	AKD	Chemical modification of fiber surface	Selective hydrophobization
Flexography Printing	Polystyrene	Deposit reagent on fiber surface	Selective hydrophobization
Screen Printing	Wax	Deposit reagent on fiber surface	Selective hydrophobization
Laser Treatment	Paper type dependent	Physical blocking of pores in paper	Entire hydrophobization followed by selective dehydration

All techniques include fabricating a hydrophobic–hydrophilic pattern on a sheet of paper to fabricate capillary channels. The only exception to this is the paper cutting technique, which uses a computer to cut out a pattern and encase it with sticky tape; creating a template for the microfluidic device.

There are three categories of techniques: Physical blocking of the pores in paper (e.g. PDMS), physical deposition of a hydrophobizing reagent on the cellulose fiber surfaces (polystyrene/wax), and chemical modification of fiber surfaces (e.g. AKD). Physical surface modification of fibers and physical pore blocking do not involve chemical reactions between the cellulose fibers in the paper and the hydrophobic reagents. These two techniques change the liquid wetting properties of the paper, creating the hydrophobic regions. Chemical modification uses cellulose reactive agents of paper, which react with the alcohol group in the cellulose to create hydrophobicity amongst the fibers.

Wax printing, and inkjet printing use selective hydrophobization (one step fabrication), which directly deposits the hydrophobic agent to the selected area of paper while leaving the remaining area hydrophilic. Photolithography, ink jet etching and patterned plasma oxidation consists of two step fabrication: (I) entire hydrophobization of paper followed by (II) selective dehydrophobization. This approach makes the entire sheet of cellulose paper hydrophobic and then etches hydrophilic regions into it.

Photolithography, as shown in **Figure 1.6**, involves impregnating the hydrophilic paper with photoresist, then selectively exposing the paper to UV light. The unexposed photoresist is then removed through washing with organic solvents. This method produces high resolution barriers, but is more expensive and contains more steps than other available methods. [57]

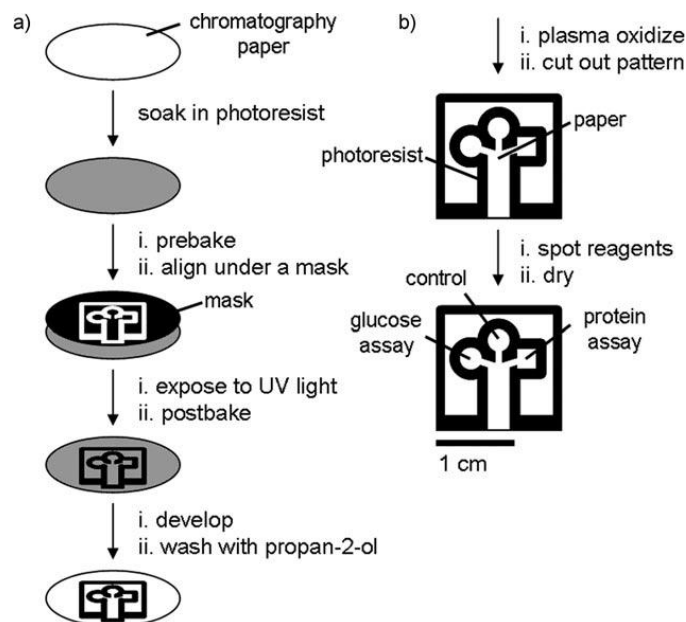


Figure 1.6 Photolithography process and use of SU-8 photoresist to fabricate patterned paper-based microfluidic device. Adapted from Ref. [58].

In contrast, wax printing (**Figure 1.7**) is a simpler and less expensive micro-patterning process for paper-based microfluidics. The wax printing technique is frequently used in paper-based bio-devices due to its low cost and ease of use. A pattern can be printed out using special printers that have the ability to print wax onto paper, which is followed by baking the patterned paper at 120°C for about 10 minutes to melt the wax through the entire thickness of the paper. [57] This process creates a hydrophobic barrier in the paper and outlines hydrophilic channels, fluid reservoirs and reaction zones. This technique can be utilized in paper-based microfluidics. [8] However, this technique is not applicable for the cases that the tested solution sample includes surfactants or organic solvents.

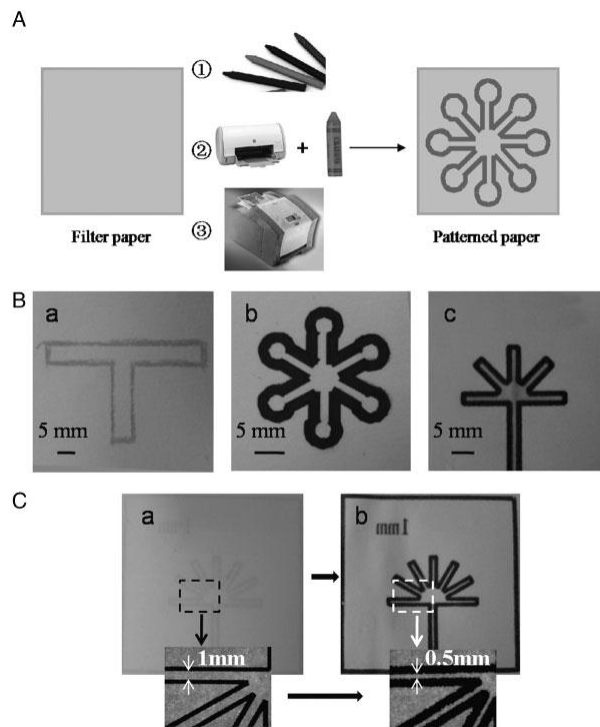


Figure 1.7 Schematic representation of patterns that can be reproduced using wax to create microfluidic channels. Can also hand draw with a wax pen. Adapted from Ref. [59].

Hydrophobic Sol-Gel Channel Patterning Strategies. When acid hydrolyzed, Methyltrimethoxysilane (MTMS) produces a hydrophobic material, methylsilsequioxane (MSQ), and it can be used as a new printed barrier on paper-based microfluidic devices. See **Figure 1.8**. Chromatographic paper could either be impregnated with MSQ or could undergo ink jet printing in order to produce the hydrophobic regions necessary. Techniques of wax and AKD barriers are simple and inexpensive; however, they fail when the sample to be tested has a surfactant component. Using an MSQ barrier alleviates this issue and is a safe, viable, and inexpensive resource for making microfluidic devices. No such barrier has been found to contain samples containing alcohol, and more research needs to be done in order to create a microfluidic device that can address this need. [60]

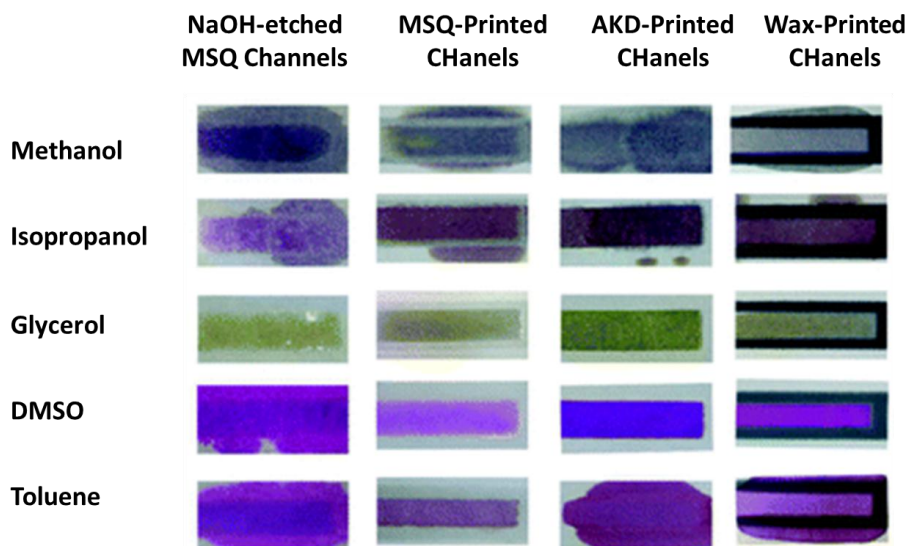


Figure 1.8 Flow of organic solvents through various channels with different hydrophobic barriers. Adapted from Ref. [60].

Later on in 2014, to make the paper-based device compatible with organic solvents, Derda's group from University of Alberta reported a method for patterning the paper by deposition of Teflon on paper. In this method, as demonstrated in **Figure 1.9**, first the pattern is determined by wax printing, then a solution of sucrose (60% w/v) is added to the patterned area to be kept solvophilic, following by deposition of Teflon AF solution (6.4 mg/mL in HFE-7100) onto the remaining area to create solvophobic barriers, it air dries. Finally, after it is dried, the paper should be washed in order to wash away the deposited sucrose from the patterned zones. [61]

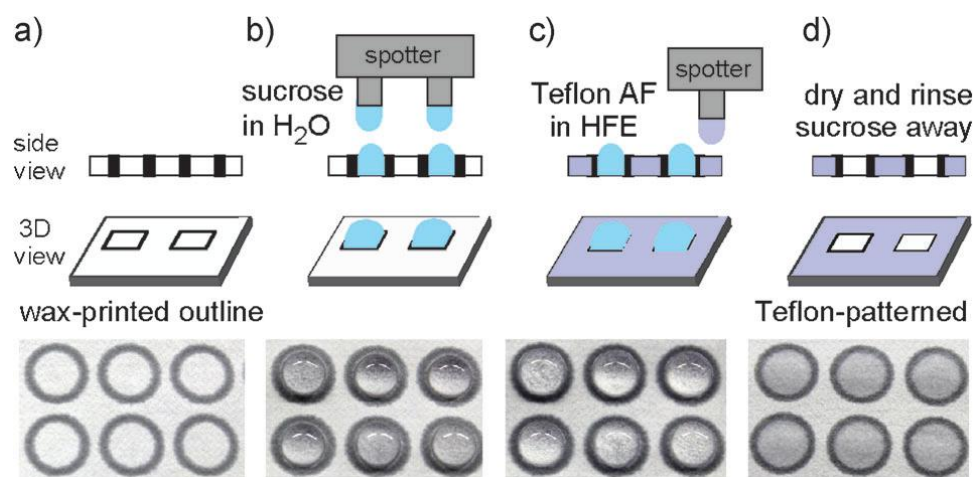


Figure 1.9 Teflon-patterning on Paper Based Biosensors. Adapted from Ref. [61].

Because paper-based microfluidic devices need to be easy to use, portable, and able to provide quantitative results, there are two different types of devices, depending on the needed application. On-demand devices have blank microfluidic platforms that are without indication reactions. These reagents can be chosen on an individual test basis and can either be added before or after the sample depending on the sample being tested. Ready-to-use devices are designed as a complete sensor with an indication reagent implanted in the detection zone of the device.

Current limitations are still present with paper-based microfluidic devices, particularly the features of the paper, fabrication methods, or detection method incorporated into the device. For example, some hydrophobic agents do not create a strong enough hydrophobic barrier to withstand samples with low surface tension. Some devices created with wax, AKD or MSQ allow liquids with surface tension lower than a critical value (biological samples with surfactants) to pass through both the hydrophilic and hydrophobic region. The limit of detection with paper-based devices is also relatively high and therefore insufficient when extremely low concentrations need to be detected. The other important challenging point with paper-based microfluidic devices is the instability of sensitive bio reagents on paper porous media and the limitations of paper-based devices for multiple steps and complex reactions. Previously, Sol-Gel derived materials had been used to trap enzymes and substrates to preserve their activities.[11, 62] Acetylcholinesterase (AChE) entrapped in Sol-Gel demonstrated significantly higher stability with only a slight decrease in activity when compared to the solution. However, protection of highly oxygen sensitive reagents such as Indoxyl Acetate (IDA) is still very challenging.

1.3.2 Controlling the Flow, and Valve Developed within the Channels in Microfluidic Biosensors

One of the major focuses of paper-based microfluidics has been controlling flow through the device. Many different valve configurations currently exist to stop flow, but most are not automatically actuated, and many present significant problems. Researchers are currently developing ways to automatically stop and start flow through paper channels. Valves open the

potential for pumping, multiple liquid use, and reaction timing. [63]

Some valves developed for the traditional PDMS-based microfluidics have the potential to be used in paper-based systems.

Mechanical valves function by compressing a channel to either eliminate or slow flow. A microfluidic pinch valve, used in PDMS-based microfluidics, has a moveable finger that pushes a flexible membrane on one side of a channel against the opposite wall. This is easily transferable to 2D paper-based systems, and the moveable finger provides a method for multi-use flow control. [64]

These valves, however, come with a high operating cost which creates difficulty when implementing them in point of care (POC) devices. [63] Creating an inexpensive device that can be operated by untrained personnel outside of a lab setting is essential to have a greater impact on society.

Temperature Actuation

Wax plug valves function by melting pre-deposited wax to allow for flow through a path. They are difficult to actuate, and the required heating can negatively affect samples or reactions. Ice-valves freeze a local section of the liquid to inhibit flow and can be reversed through melting. Although this is a multi-use valve, its temperature sensitive nature can interfere with samples, and it is not as applicable outside of a lab setting. Additionally, for use outside of the laboratory, valves for paper-based microfluidics should be stable over a wide temperature range during both use and storage. [63]

Manual Actuation

Capillary valves are founded on the pressure differences present in a channel due to an abrupt widening. The expansion forms capillary pressure which poses a temporary barrier to flow. Capillary soft valves operate by releasing pressure in the channel to initiate flow. This is done by manual actuation (**Figure 1.10**), and does not have the potential for multiple uses. [63]

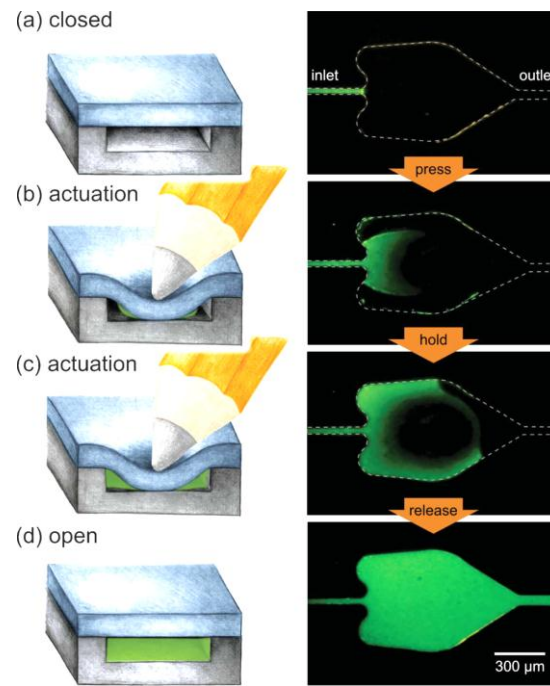


Figure 1.10 Actuation of a Capillary Soft Valve. Adapted from Ref. [63].

A very simple flap valve design provides an easy flow cut-off method. Lifting a physical flap in the paper channel immediately and efficiently stops flow (seen in **Figure 1.11 (b)**). This valve, although inexpensive, must be user actuated which is less user-friendly for untrained individuals. [65]

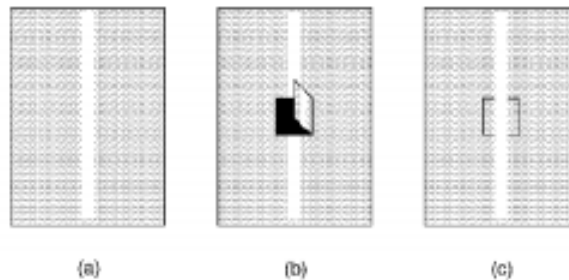


Figure 1.11 Manually actuated flap valves can be lifted to stop flow, and replaced to allow continuation of flow. Adapted from Ref. [66].

Electrical Actuation

A strip of conductive material (metal or polymer) is used to regulate flow through the paper by

controlling analyte concentration to act as a switch or valve (**Figure 1.12**). This type of valve has the ability to stop and start flow as well as the ability to control flow rate. Despite this flexibility, it is not an automatic valve and requires the use of electrical components. [67]

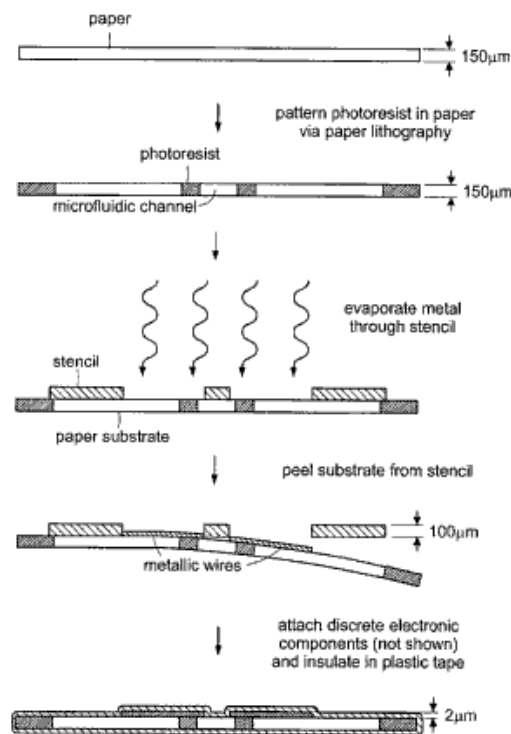


Figure 1.12 Assembly of an electrically actuated valve. Adapted from Ref. [67].

Depositions on the Channel

Fluidic diode valves have the ability to form complex circuits within paper and are capable of controlling the direction of flow. They are single-use valves consisting of both a cathode and an anode separated via a hydrophobic gap (**Figure 1.13**). The fluid direction is limited to flow from the anode to the cathode. A surfactant deposited in the anode is dissolved as the fluid approaches, and the dissolved surfactant is able to reduce surface tension between fluid-air and fluid-solid interfaces. This dissolution stimulates fluid spreading along the hydrophobic barrier. Surfactant is not present in the cathode part of the diode and, therefore, cannot flow past the barrier. These components are strategically shaped to release and capture the spreading fluid. [68]

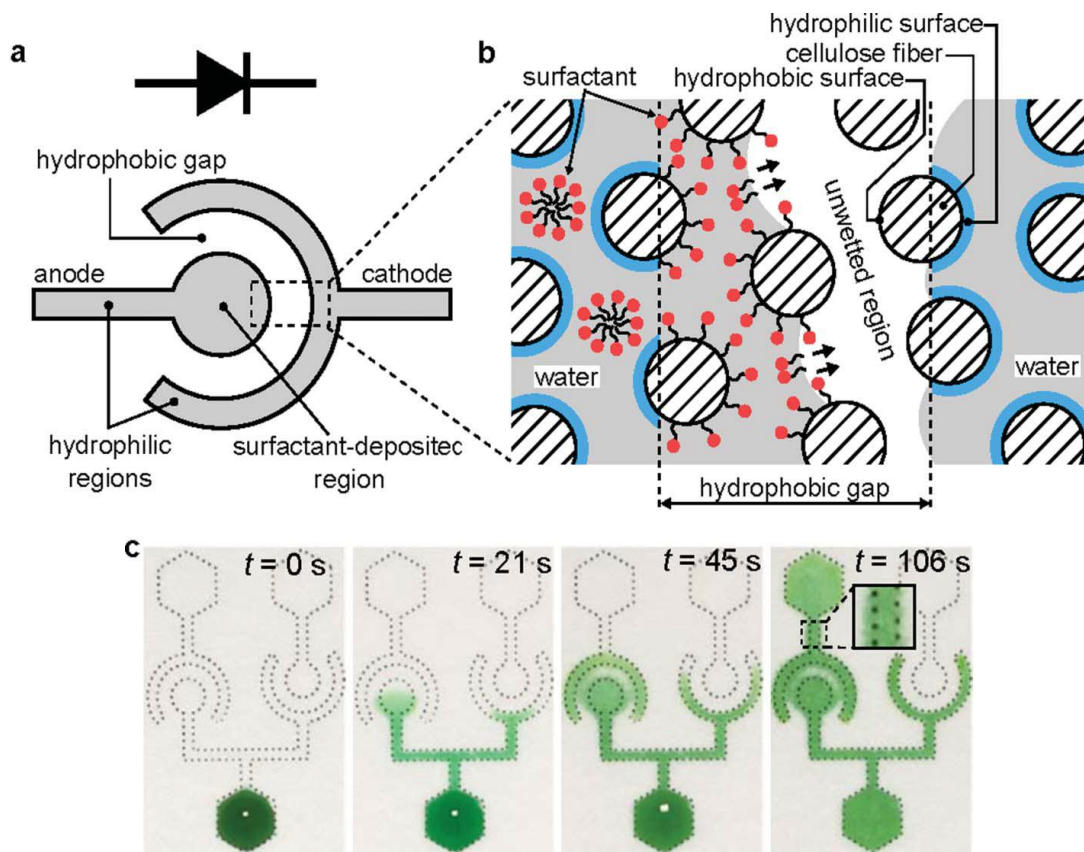


Figure 1.13 a) Schematic of a single-use fluidic diode. b) Enlarged schematic showing action of surfactant. c) Photographs indicating direction of flow through the diode. Dotted or solid lines were printed to indicate hydrophilic regions. Adapted from Ref. [68].

Adding a dissolvable barrier onto the paper channel allows the user to control the flow rate of the fluid. Barriers such as the sugar trehalose provide added resistance to flow and are able to delay movement through the channel (**Figure 1.14**). Increasing the thickness of this barrier leads to slower flow rates. [69]

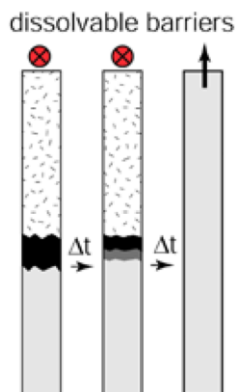


Figure 1.14 Dissolvable barrier used to vary transport time through the channel. Adapted from Ref. [69].

Paper Shaping

A fluid disconnect is a valve configuration that allows for multi-step processes. The paper is cut and shaped to have pathways which are removed from the solution sequentially to stop the flow within that channel (**Figure 1.15**). This method requires specific loading capabilities and cannot be used without a full well of the sample. [70, 71]

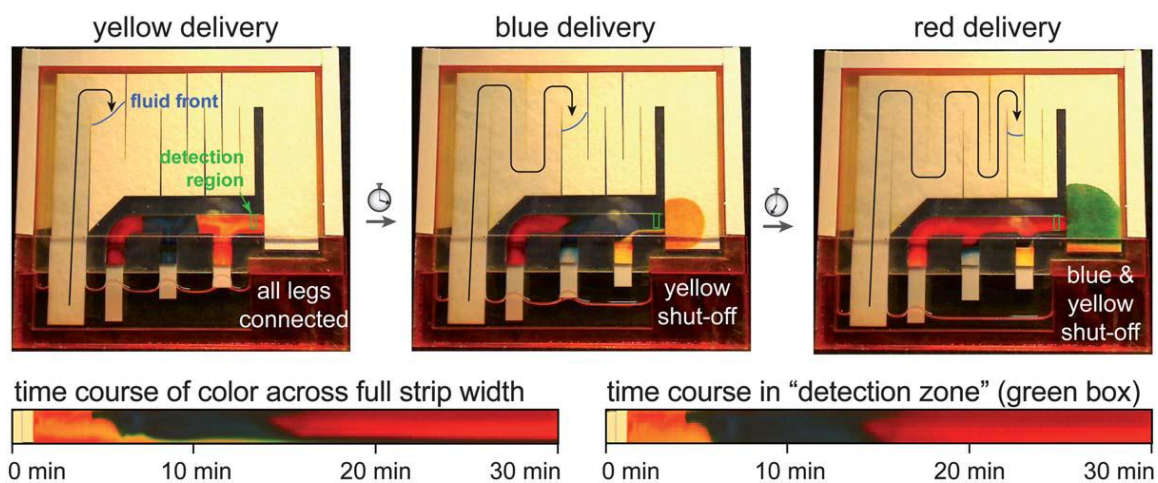


Figure 1.15 Depiction of a fluid disconnect with three legs having different shut-off times. Adapted from Ref. [70].

Varying the width and length of the channel can also affect fluid flow (**Figure 1.16**). A longer channel presents higher resistance to flow and slows the fluid front. Widening a section of the channel varies the time it takes for fluid to flow through that segment and leads to a slower fluid

advancement as well. [69, 72]

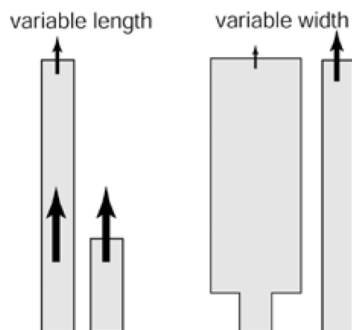


Figure 1.16 Varied length and width in a channel to alter fluid flow. Adapted from Ref. [69].

1.3.3 Paper-Based Bioassays for Detecting Pathogens and Toxins in Water

A very important application of bioactive papers (paper-based microfluidic devices) is in the area of pathogen and toxin detection in water and the environment. One of the very first series of functioning bioactive-paper detection assays had been demonstrated by Brennan's research team, working under SENTINEL Bioactive Paper Network at McMaster University in 2009. The issues of food and water contamination, spread of disease, and drug-resistant bacteria, which are concerns for the developing world as well as the developed world, are some of the major factors driving this research.[73]

For detection of organophosphate pesticides, Brennan's research group developed a bidirectional lateral flow paper-based biosensor using indophenyl acetate (IPA) and acetylcholinesterase (AChE). [10] In this work, Sol-Gel, bioreagents were printed using a piezoelectric inkjet printer onto filter Whatman #1 paper. They trapped enzyme and substrate within Sol-Gel derived silica for preservation purpose; the sensing zone was fabricated by entrapping PVAm/silica/AChE/silica layers while the substrate region was prepared by entrapping silica/IPA/silica layers. As is shown in **Figure 1.17**, to use this sensor, the dipsticks paper device

is first placed in the pesticide-containing sample from the end of the strip and is given 10 minutes for the sample solution to reach the sensing region by lateral flow. Following a 5 minute incubation period, the strip is then inverted and the bottom side of the paper strip is introduced to sample solution for about 10 minutes to let the substrate move to the sensing region and develop the color within 5 minutes. The developed color can easily be seen by the naked eye. This paper-based device shows excellent detection limits. To estimate the color intensity, which is inversely proportional to the pesticide concentrations, a digital camera and image-j software must be used.

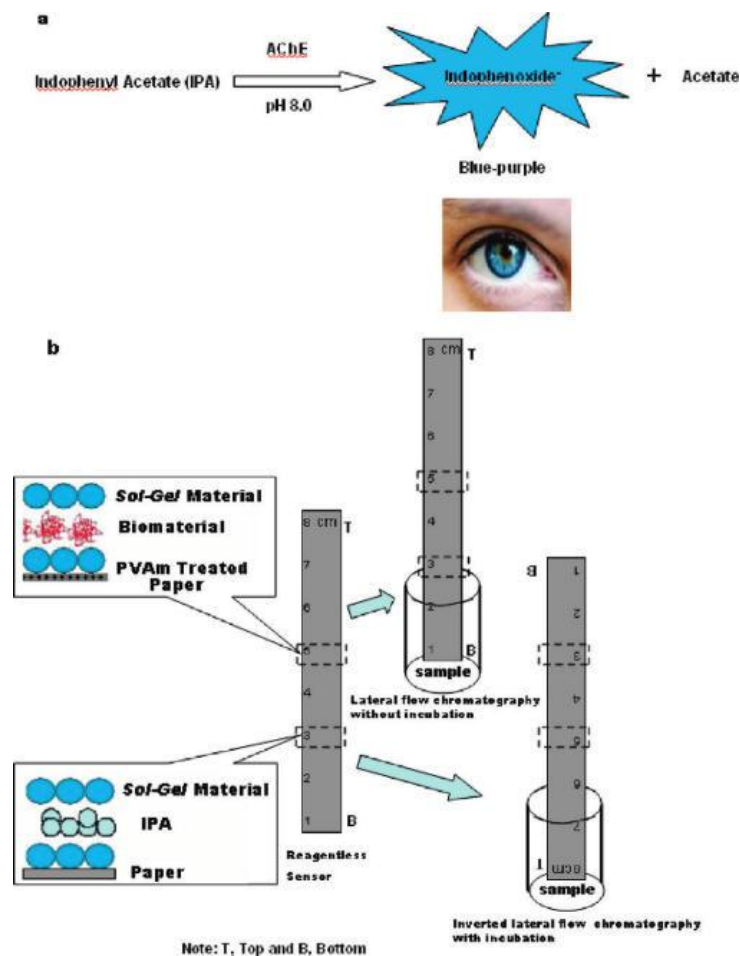


Figure 1.17 Detection of pesticide using paper based colorimetric biosensor. Adapted from Ref. [10].

In a later publication in 2011, a paper-based sensor was developed for quick and sensitive detection of heavy-metal ions based on inhibition of β -galactosidase (β -gal) and affecting the reaction rate between β -gal and Chlorophenol Red- β -D-galactopyranoside (CPRG). [9] β -

galactosidase is a metalloenzyme that cleaves lactose into glucose and galactose by hydrolyzing the terminal, non-reducing β -D-galactosidases. The reaction between CPRG and β -galactosidase is shown in **Figure 1.18**.

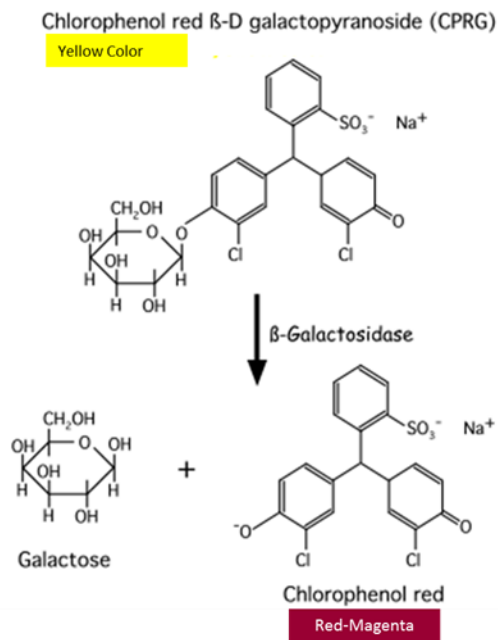


Figure 1.18 Reaction between CPRG and β -galactosidase

As shown in **Figure 1.19**, in this detection technique, the enzyme β -gal (sensing zone) and substrate CPRG (substrate zone) are printed with Sol-Gel onto paper in separate zones and lateral water flow causes a colour change in the presence of heavy metal. The vibrancy of colour can actually help estimate the concentration of heavy metal present. [9]

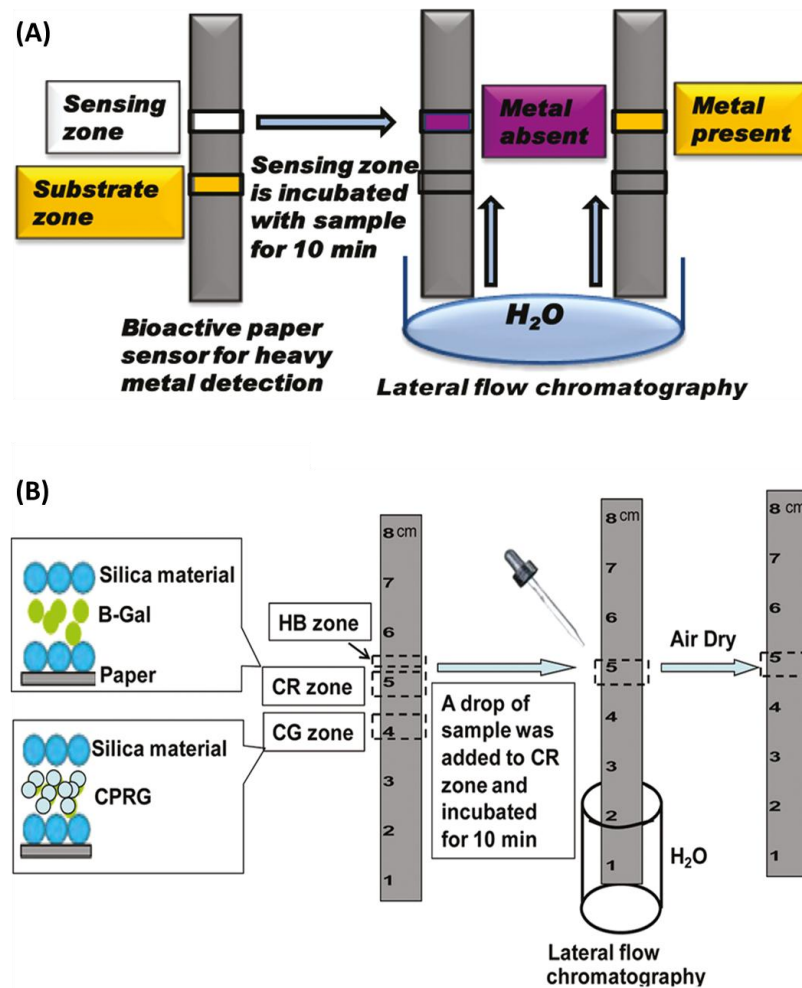


Figure 1.19 Detection of heavy metals using β -Galactosidase-based colorimetric paper sensor. In the absence of heavy metal, CPRG is hydrolyzed by the enzyme, β -gal, to produce red-magenta colored product. The presence of heavy metals causes a loss of the red-magenta color in a concentration-dependent manner. Adapted from Ref. [9].

Furthermore, determination of fecal coliform on paper test strips was demonstrated by Brennan's group in 2012. [74] In this work, detection of *E. coli* using bioactive paper based test strips was assessed based on the activity of intracellular enzyme β -galactosidase or β -glucuronidase. As shown **Figure 1.20**, the *E. coli* biosensor is composed of a paper strip onto which substrate was trapped within Sol-Gel-derived silica. To use this biosensor, the cell-containing sample is first lysed using Bacterial Protein Extraction Reagent (B-PER) with a volume ratio 9:1 of cell suspension to B-PER®, then the test strips is placed into the lysed cell sample and the liquid is allowed to flow up the paper strip via lateral flow to reach the substrate zone. When the solution

gets into the substrate zone, a color change occurs due to rapid enzyme hydrolysis of the substrate, and by measuring the color intensity (CI), the concentration of *E. coli* in the sample can be quantified.

As shown in **Figure 1-20c**, to improve the sensitivity and detection capacity of the system, a pre-concentration step, in which cells are first isolated from solution samples via antibody-derivatized magnetic beads (MB-Ab), is also suggested before the lysing step ,

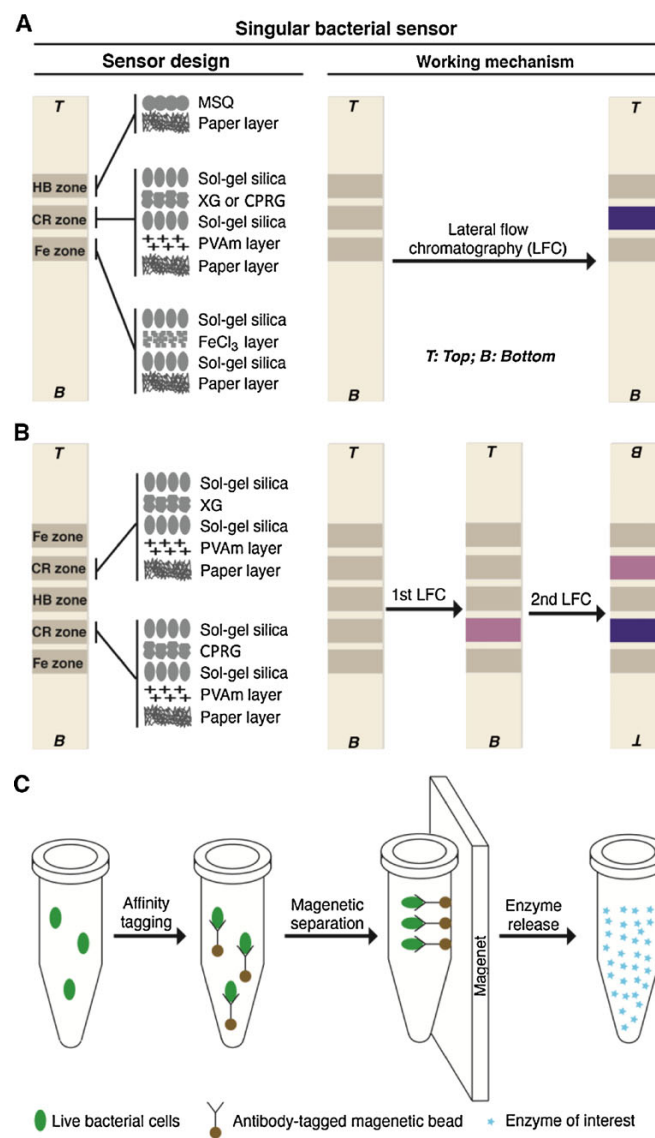


Figure 1.20 Detection of bacteria using paper-based sensor. Adapted from Ref. [74].

As mentioned in the abstract, in this thesis, pullulan is utilized for the creation of an automated shut-off valve/pipette on paper-based devices to control the flow of liquid within paper channels, thereby providing a method for having a “ready-to-use” pesticide paper-based biosensor which does not need any further manipulation from user (*Chapter 3*). In *Chapters 4* and *5*, using pullulan, a new generation of biosensors as “lab-on-pills” is introduced, which provide the possibility of having biosensors with longer shelf lives. In *Chapter 6*, the creation of paper-based biosensors that have been adapted for multi-step and more complex reactions is demonstrated by utilizing pullulan films. Using pullulan films allows for the development of multi-directional flow and time-dependent reagent delivery and sequential release within paper-based biosensors. *Section 1.4* a briefly describes pullulan and the important properties of this special polysaccharide.

1.4 Pullulan

Pullulan, a biopolymer with unique and interesting properties, is a water-soluble and biodegradable extracellular polysaccharide that is produced by the fungus *Aureobasidium pullulans* (*A. pullulans*). [75, 76] *A. pullulans* is an omnipresent fungus which is isolated from the environment (e.g. soil, water, rotting leaves, woods and other plant substance). Pullulan, which is developed through fermentation, is then purified by centrifugation and precipitation using organic solvents usually from the group of esters, alcohols, and ethers, and this step is followed by ultrafiltration and the introduction of ion-exchange resins for further purification as shown in **Figure 1.21**.

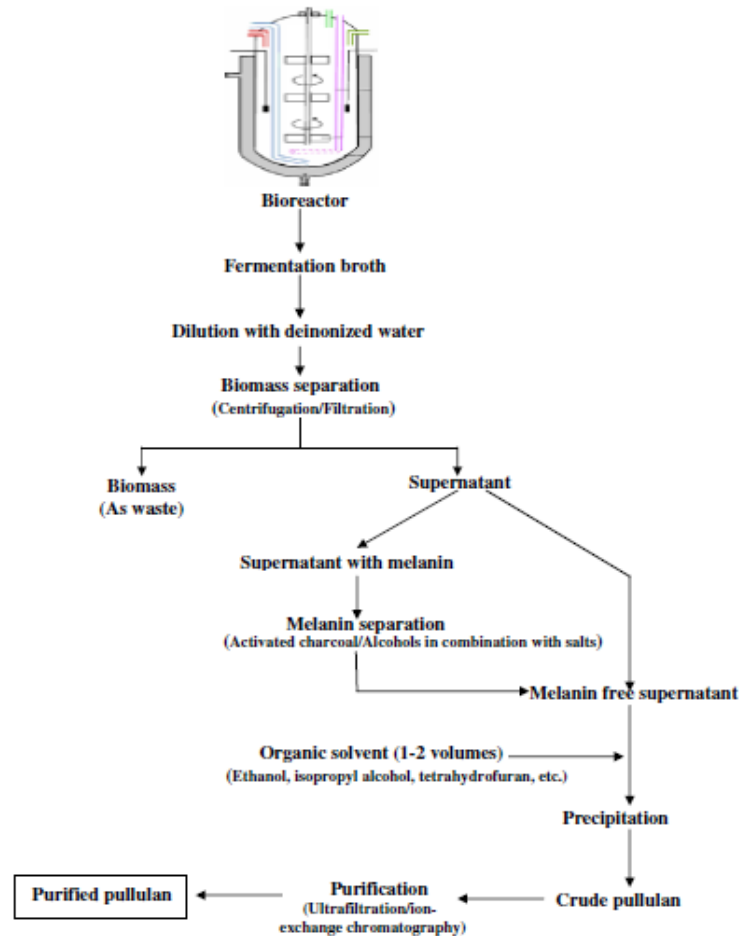


Figure 1.21 Flow diagram of pullulan processing and purification. Adapted from Ref. [75].

In the following sections, the important properties of pullulan are briefly discussed. However, in summary, the unique properties of pullulan which make this polysaccharide ideal for my work are:

- Rapidly water soluble, no need to increase temperature to dissolve
- Does not form gels
- Forms defect free, flexible films
- Easy to shape or punch as required
- Low oxygen permeability

1.4.1 Pullulan Properties

In term of appearance, pullulan is a white to offwhite powder, as shown in **Figure 1.22a**, and is tasteless, odourless, and extremely stable. Pullulan film-based oral care products are commercially available under the brand name Listerine, shown in **Figure 1.22c**.

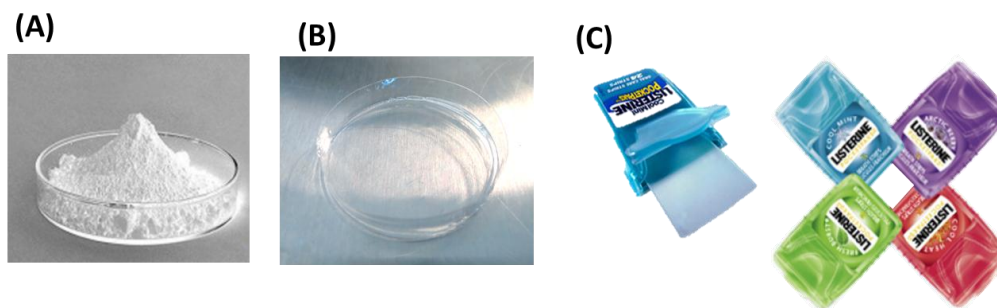


Figure 1.22 Pullulan (a) powder, (b) Highly transparent and defect-free pullulan film (C) Listerine strips: pullulan based oral care film

Pullulan with molecular formula of $(C_6H_{10}O_5)_n$, shown in **Figure 1.23**, is a polymer consisting of a repeating maltotriose trimer $\{\rightarrow 6\}\text{-}\alpha\text{-D-glucopyranosyl-(1}\rightarrow 4\text{)-}\alpha\text{-D-glucopyranosyl-(1}\rightarrow 4\text{)-}\alpha\text{-D-glucopyranosyl-(1}\rightarrow \}$, the alternation of (1 \rightarrow 4) and (1 \rightarrow 6) bonds gives pullulan enhanced solubility and structural flexibility.[75-77] The enzyme pullulanase which is also known as pullulan-6-glucanohydrolase (Debranching enzyme) specifically hydrolyzes and degrades the α -(1 \rightarrow 6) linkages in pullulan.

Recent studies have demonstrated that pullulan coatings applied to food packaging can act as oxygen barriers to increase the shelf-life of food stuffs. [77, 78] Other researchers have demonstrated the use of pullulan in the preservation of bacteria viability in various storage conditions. [79] Pullulan is only slightly depolymerized by digestive enzymes, such as pullulanase. [80] This low digestibility preserves this polysaccharide by preventing the growth of fungi and preventing the breakdown of the polymeric structure. Despite the increasing interest and studies on pullulan coatings, there are still many applications that have yet to be explored.

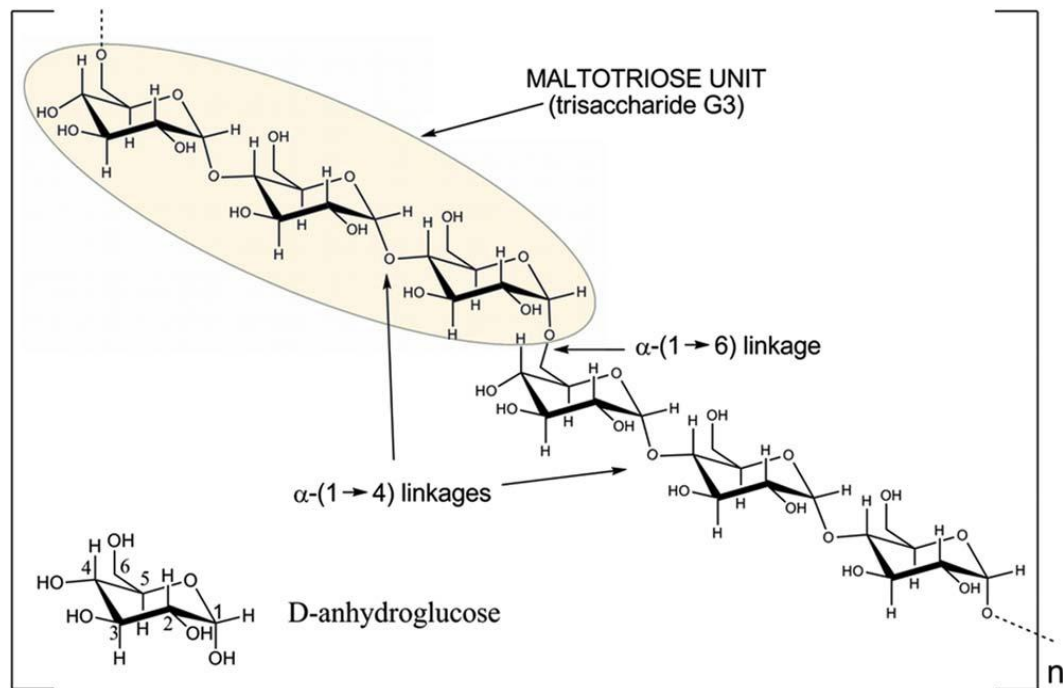


Figure 1.23 Chemical structure of pullulan with maltotriose as repeating unit. Adapted from Ref. [81].

The linear structure of pullulan is what causes the polymer to be so structurally flexible and can also be accounted for by its lack of crystalline regions. This property is the reason why pullulan possesses superior film-forming properties that are different from many other polysaccharides.[81] It was also determined that in water, pullulan has no electrical charge. [82] Furthermore, pullulan is known to have a completely amorphous organization. Lack of crystallinity in this biopolymer is also a parameter that makes it different from the other polysaccharides. [81]

Roughness and Hydrophilicity

Pullulan is a hydrophilic biopolymer with a surface tension value very similar to water, 74 dyne/cm². [80] Water contact angle on pullulan film in comparison to a few biopolymers is shown in **Figure 1.24**. [83] As exhibited in **Figure 1.24**, following drop deposition, the water drop profile began to change immediately for all demonstrated biocoatings. As evidenced further in **Figure 1.24**, among the studied biopolymer, pullulan exhibited the most hydrophilic properties, and the initial contact angle values (θ_0) for Pullulan, Pectin DE 72, Pectin DE 27 DA

20, Gelatin, and Chitosan are reported to be $\sim 30^\circ$, 56° , 60° , 66° , and 92° respectively.

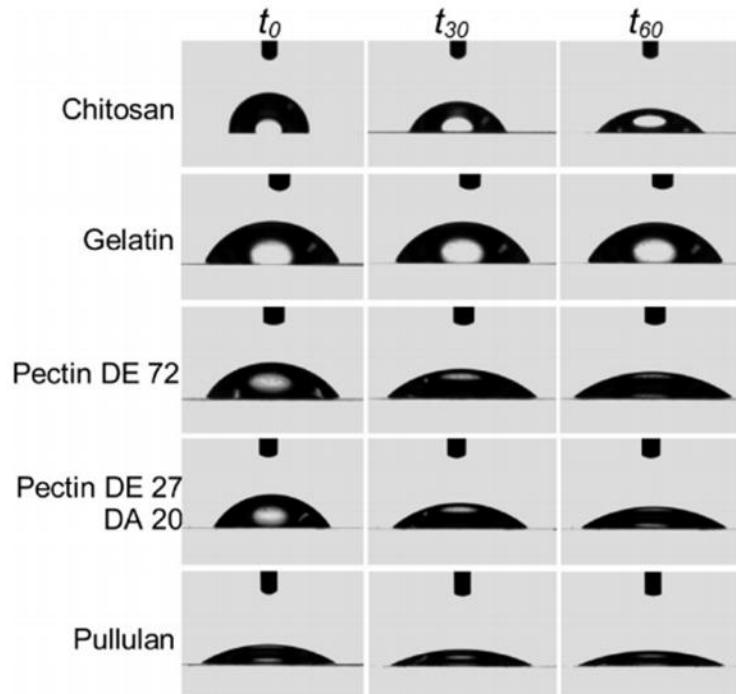


Figure 1.24 Water contact angle of pullulan coated on a plastic substrate of poly(ethylene terephthalate), in comparison to Chitosan, Gelatin, Pectin DE 72, and Pectin DE 27 DA 20 immediately after droplet deposition (t_0), after 30 s (t_{30}), and after 60 s (t_{60}) of analysis. Adapted from Ref. [83].

Furthermore, the AFM imaging of the mentioned biopolymers shown in **Figure 1.25** demonstrate that pullulan has the smoothest surface compared to the other demonstrated biopolymers, with no evidence of either molecular aggregation or discontinuities [83]. Related roughness values are also summarized in **Table 1-3**, which indicate the very low degree of roughness for pullulan.

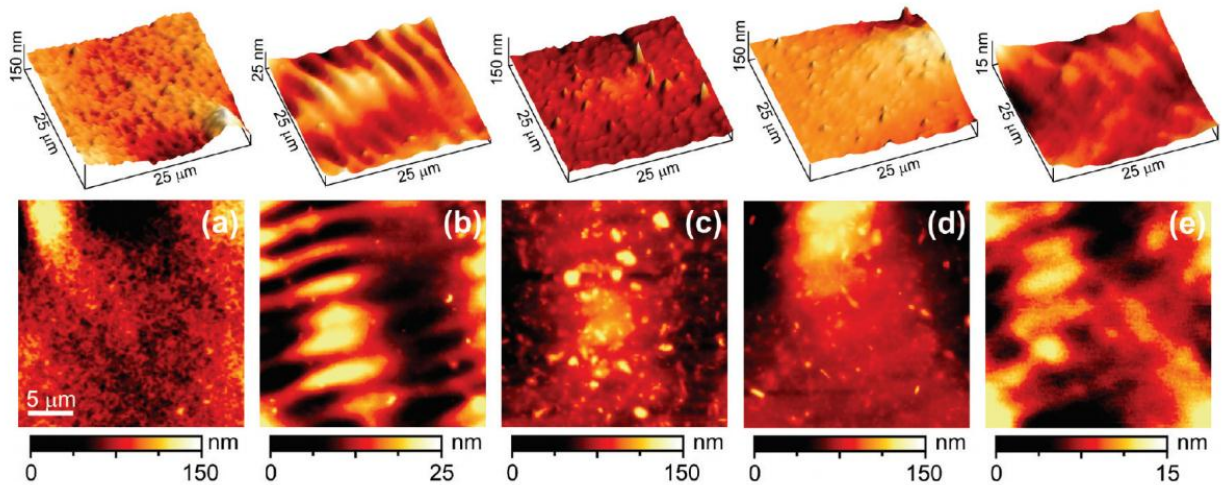


Figure 1.25 AFM 3D (upper) and height (lower) images ($25 \times 25 \mu\text{m}^2$) of (a) Chitosan, (b) Gelatin, (c) Pectin DE 72, (d) Pectin DE 27 DA 20, and (e) Pullulan-biocoated surfaces. Adapted from Ref. [83].

Table 1-3 Roughness Values of pullulan and other biocoating films [83]

Biocoating Film	Roughness (nm)
Chitosan	30
Gelatin	7
Pectin (DE 72)	30
Pectin (DE 27, DA 20)	36
Pullulan	3

Solution Properties

Since pullulan lacks branches, it readily dissolves in water and aqueous solutions. Pullulan has a low intrinsic viscosity ($[\eta]$) in comparison to other polysaccharides (0.38-0.70 dL/g for pullulan in comparison to 0.37 – 46 dL/g for other polysaccharides). [84]

The degree of chain flexibility in pullulan is relatively high due to the maltotriose repeating unit: – α -(1,6) linkages are more flexible and allow for a greater rotational freedom. [85]

Furthermore, pullulan has relatively high critical concentration (c^*) of 14-31 mg/ml, above which intermolecular interactions (chain entanglement) becomes significant. [84]

Viscosity as a Function of MW

The plot shown in **Figure 1.26**, shows the viscosity of aqueous pullulan solution made available from Hyashibara [86], the world's largest producer of food-grade pullulan, as well as the first to set up a commercial production facility for pullulan. Pullulan solution viscosity is not affected by pH values. [80] **Table 1-4** shows the viscosity of pullulan solution as compared to different polysaccharides. [80] Pullulan is similar to gum arabic in term of viscosity, (however, gum arabic does not form as flexible a film as pullulan does).

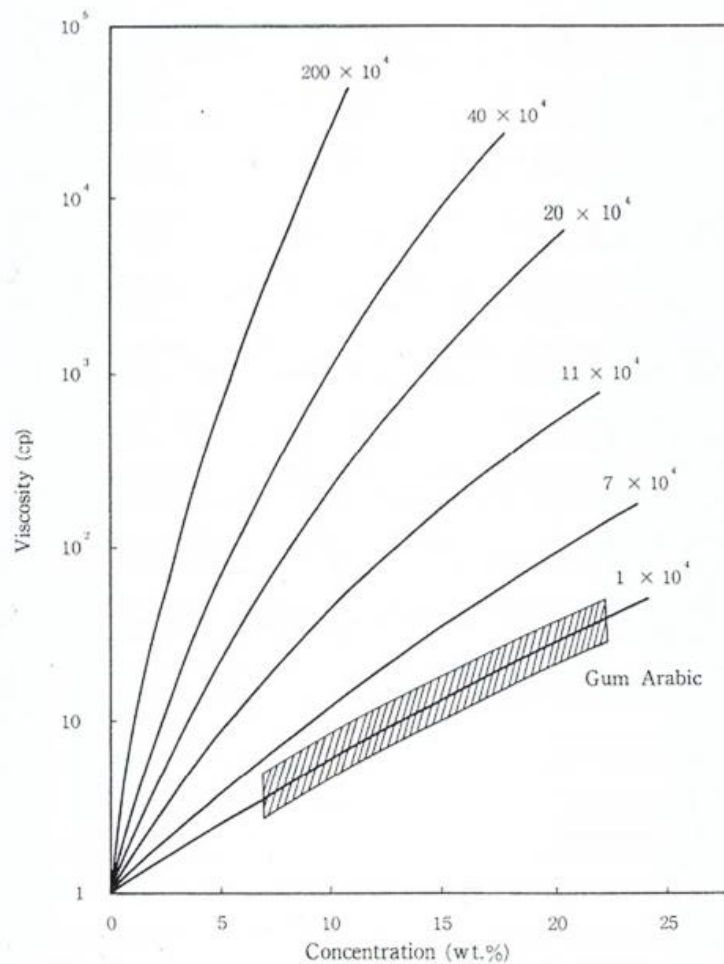


Figure 1.26 Viscosity of an aqueous pullulan solution at 23°C, as received from Hyashibara Co. [86]

Table 1-4 viscosity of 1% aqueous solution of different polysaccharide at 30°C [80]

Polysaccharide	Viscosity (<i>cp</i>)
Pullulan, PF-20	2
Gum arabic	1-5
Methylcellulose	200
Tamarind gum	100-200
Guar gum	2,000-3,000
Locust bean gum	2,000-3,000
Xanthan	2,000-3,000
Sodium alginate	200-700

Following equation relates intrinsic viscosity ($[\eta]$) to molecular weight (MW):

$$[\eta] = K \times MW^\alpha \quad (1)$$

Where K and α are the Mark–Houwink coefficients that are available for most water–soluble polymers. Mark Houwink coefficients for pullulan is determined by Sommermeyer et al. [87]

- $K = 1.79 \times 10^{-4}$ for $[\eta]$ in dL/g
- $\alpha = 0.69$

In comparison Mark–Houwink–Sakurada (MHS) relationship for guar [88], dextran [89], and acacia gum [90] is given below in **Table 1-5**.

Table 1-5 Mark–Houwink–Sakurada (MHS) parameters for different biopolymers for $[\eta]$ in dL/g.

Biopolymer	$K \times 10^4$ (dL/g)	α
Pullulan [87]	1.79	0.69
Guar [88]	3.04	0.75
Dextran [89]	8.52	0.52
acacia gum [90]	5.90	0.46

Chain Association in Solvent

Pullulan is a linear molecule; its interactions with other molecules, therefore, are primarily quantified by the interaction parameter (χ).

Polymer-polymer/polymer-solvent interactions are indicated by solubility parameters/Flory-Huggins coefficient. The solubility parameter (δ_1) can be predicted by a group contributions method (GCM), using molar attraction coefficients (F_i) for the polymer.

$\delta_1 = \frac{\sum F_i}{V}$, where F_i is obtained from tabulated values and V is the molar volume of the polymer (measured experimentally or tabulated).

The solubility parameter (δ_2) can be either for a solvent or another solute and is either calculated identically or obtained from a table (i.e. for solvents).

Then, the Flory-Huggins parameter (χ_{12}) can be calculated via:

$$\chi_{12} = \frac{V_1}{RT} (\delta_1 - \delta_2)^2 \quad (2)$$

And molar attraction constants for use with the Small & Hoy GCM method. [91]

Theoretically, the interaction parameter χ_{12} is a polymer property, independent of solution composition. However, Eckelt et al. [92] reported a dependence of this parameter on composition, as demonstrated in **Figure 1.27** below.

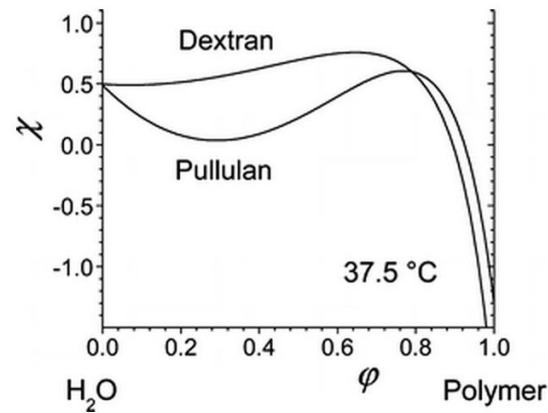


Figure 1.27 Composition dependence of the Flory–Huggins interaction parameter for aqueous solutions of pullulan and dextran. Adapted from Ref. [92].

This abnormal behavior of the interaction parameter for pullulan is then modeled as: [92]

$$\chi \approx \frac{\chi_0 + \xi\lambda}{1 - \nu\phi} - \xi\lambda(1 + 2\phi) + \varpi\phi(3\phi - 2) \quad (3)$$

Assumptions made for this derivation are:

- Ideal gas behavior of all gases considered
- Assume fixed bond rotations, and λ approaches 0.5 and ξ approaches zero (theta conditions – ideal solvent, where δ_1 is approximately equal to δ_2)
- Assume a constant, reference state χ_0 value (measured experimentally), simplifies expression as $\phi \rightarrow 0$
- Assume that the osmotic pressures can be measured with a high accuracy; the error in χ_0 is near zero, so the second virial coefficient of the expression is removed.
- Added a second term to the Gibbs energy of mixing to account for extra contributions due to polymer concentration changing the ξ and λ values (which were assumed constant at 0 and 0.5 respectively).

The Flory–Huggins interaction parameters obtained for pullulan and dextran show that water is a

better solvent for pullulan polysaccharide than for dextran.[92] **Table 1-6** below contains the measured parameters for pullulan solutions at different temperatures.

Table 1-6 Solubility and interaction parameters for an aqueous pullulan solution. Parameters fit Equation 3 listed in the text above. [92]

	$25^{\circ}C$	$37.5^{\circ}C$	$50^{\circ}C$
χ_0	0.491	0.488	0.491
ν	0.815 ± 0.032	0.753 ± 0.014	0.583 ± 0.04
$\xi\lambda$	-0.761 ± 0.057	-0.858 ± 0.05	-1.97 ± 0.891
ω	2.384 ± 0.393	2.183 ± 0.286	2.985 ± 0.919
α	-0.27	-0.37	-1.479

The hydrodynamic properties of pullulan are also reported on widely in published literature, as summarized by Shingel et al in 2004. [85]

- $R_g = 1.47 \times 10^{-2} MW^{0.58}$ (nm)
- $R_H = 2.25 \times 10^{-2} MW^{0.52}$ (nm)

Where R_g is the radius of gyration, R_H is the hydrodynamic radius, and MW is molecular weight. This verifies that pullulan in aqueous solution behaves as a random coil.

It is noted that while a polymer known to be a random coil is at a low concentration, the intrinsic viscosity increases linearly with concentration up to a certain point (critical concentration, c^*), above which the viscosity increases very quickly \rightarrow intermolecular entanglements begin \rightarrow total hydrodynamic volume of the individual chains exceeds the solution volume. The critical concentration for pullulan is known to be 14-31 mg/ml (1.4-3.1 wt%). [84] In comparison the critical concentration value for guar is~ 0.08-0.3 wt% . [93]

Solid Properties

Thermal Properties (T_g , T_d)

Glass transition temperature (T_g) of pullulan measured via Differential Scanning Calorimetry (DSC) and Dynamic Mechanical Thermal Analysis (DMTA) methods is reported to be 151~203 °C. [94]

Furthermore, the degradation temperature (T_d) of pullulan was determined using thermogravimetric analysis (TGA), and result in: [95]

- $T_{\text{onset, degradation}} = 290^\circ\text{C}$
- $T_{\text{max, degradation}} = 310^\circ\text{C}$

While for both amylose and dextran T_{onset} and T_{Max} occur at 315 and 340°C respectively, as shown in **Figure 1.28**. [95]

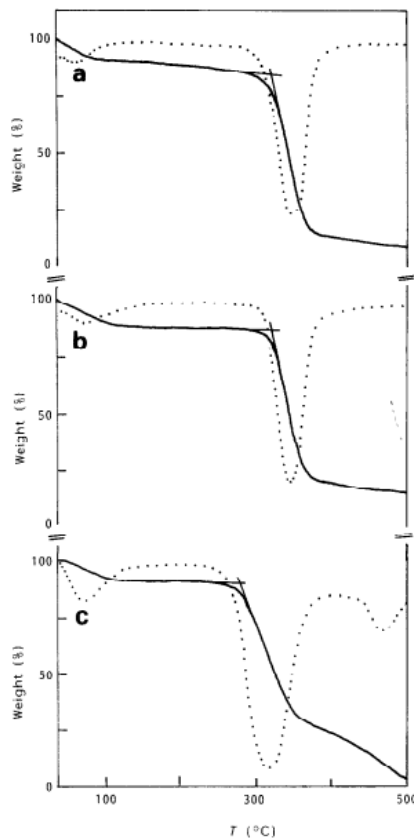


Figure 1.28 Thermogravimetric curves for: (a) amylose, (b) dextran, and (c) pullulan. Dotted line: derivative curve. Adapted from Ref. [95].

Mechanical Properties at Relative Humidity Levels

Experiments have been conducted by Teramoto et al. in 2001 to determine the visco-elasticity of pullulan across a range of temperatures, as evidenced in the **Figure 1.29** below. E' is the storage modulus and is plotted on the same axis as $\tan(\delta)$ to obtain a representation of how the visco-

elastic properties of pullulan change across different temperatures. It is noted that pullulan has a relatively constant E' value, slowly increasing with an increasing temperature. This trend is likely to change at the thermal degradation temperature, however.

The $\tan(\delta)$ values are also relatively constant for pullulan and are certainly considered constant given other sources of variation (experimental/measurement/random errors). As such, it can be stated that from the range of ~ 25 °C to 150 °C, pullulan is quite thermally stable.

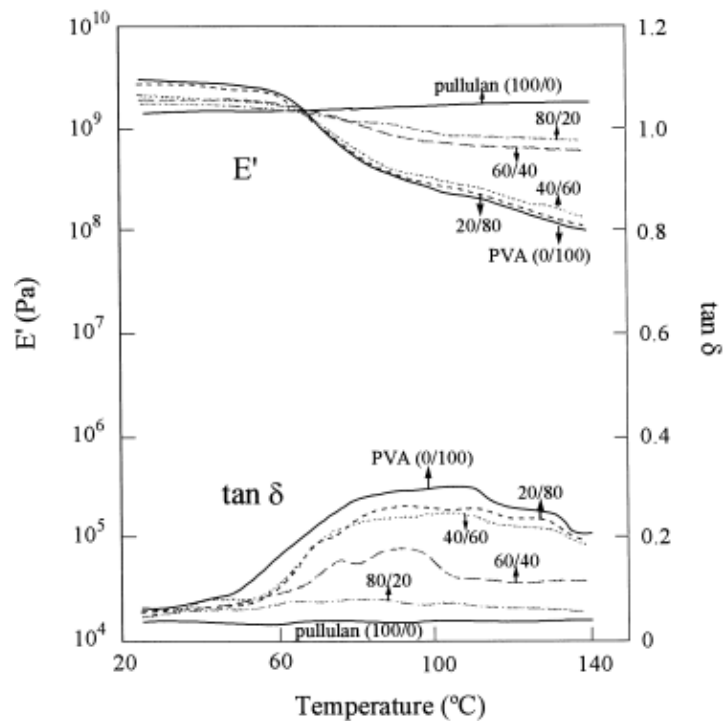


Figure 1.29 Dynamic visco-elastic curves of pullulan/PVA blend films. The storage modulus (E') and $\tan(\delta)$ as functions of temperature. Adapted from Ref. [96].

Further tests of mechanical properties (Young's modulus & maximum stress before yielding) was also tested by Diab et al. in 2001 across a range of humidity conditions as shown in **Figure 1.30**. [94]

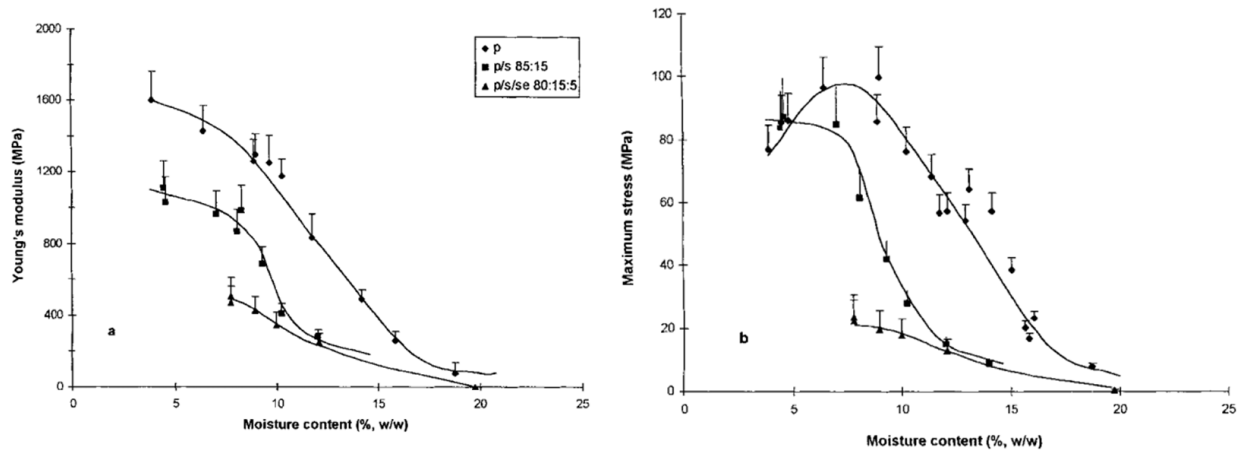


Figure 1.30 Effect of water content on (a) Young's modulus (E) and (b) maximum stress (σ_{max}) of pullulan films from tensile tests. Where: P = Pullulan, S = Sorbitol, SE = Sucrose fatty acid ester. Adapted from Ref. [94].

Water Content at Relative Humidity Levels

Pullulan has an equilibrium moisture content of 10-15% at relative humidity of less than 70%. [80] Water content is typically expressed in g H₂O per g dry matter, across a range of water activities (a_w), where:

$$a_w = \frac{p}{p_0} = \frac{ERH(\%)}{100} \quad (4)$$

The water content of pullulan is contained in **Figure 1.31** below. [94]

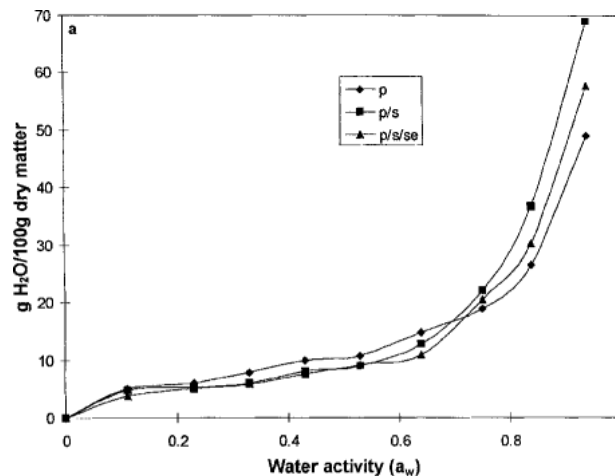


Figure 1.31 Water content of pullulan, pullulan/sorbitol, and pullulan/sorbitol/sucrose ester films at 25°C. Adapted from Ref. [94].

Water Vapour Permeability

Table 1-7 below, shows water vapour permeability of pullulan in comparison to a plasticized pullulan film (sorbitol (S) or sucrose fatty ester (SE) plasticizers). [94] As evidence from Table 1-7, pullulan shows lower water vapour permeability in comparison to a plasticized pullulan film.

Table 1-7 Apparent water vapour permeability ($\text{gm}^{-1}\text{s}^{-1}\text{Pa}^{-1}$) values of P, P/S, P/S/SE films at varying relative humidity gradients at 22°C. P = Pullulan, S = Sorbitol, SE = Sucrose fatty acid ester. [94]

a_w	P	P/S (85:15)	P/S/SE (80:15:5)
0.53	$1.67 (\pm 0.19) \times 10^{-10}$	$2.43 (\pm 0.19) \times 10^{-10}$	$5.14 (\pm 0.45) \times 10^{-11}$
0.75	$2.16 (\pm 0.09) \times 10^{-10}$	$3.66 (\pm 0.25) \times 10^{-10}$	$1.82 (\pm 0.08) \times 10^{-10}$

Oxygen/Air/Gas Permeability

The comparative rates at which different films allow gases (oxygen in particular) through is of key interest when discussing what allows a film to stabilize biological agents: good oxygen barrier properties are required in order to protect the encapsulated molecules from oxidation.

As an oxygen barrier, pullulan's performance is very comparable to PET/poly(vinylidene chloride) coating. Intermolecular hydrogen bonding is responsible for the network formed between pullulan and other biopolymers, which make it so flexible and "airtight." and encourages the formation of a tightly packed polymeric network. Furthermore, pullulan is a highly ordered (maltotriose repeat unit) linear polymer, which should allow for a close-packed structure upon film formation. The combination of pullulan with tetraethoxysilane had Oxygen Transmission Rate (OTR) was comparable to many of the current organic polymers on the market derived from petrol for the development of oxygen barrier coatings. [81]

Chemical Modification

Chemical modification of pullulan is usually based on the OH groups (9 OH groups present in each maltotriose repeating unit, available for substitution reactions). The reactivities of each of these OH groups varies widely, depending on sterics, etc. C-6 OH group appears to be the most active, unless alcohol-water solution is used, then C-2 OH group is more active (similar to

dextran). [85] The following are the chemical modifications commonly applied to pullulan:

- Carboxymethylation of pullulan (carboxymethylpullulan, CMP) is often carried out in an alcohol water solution, and is used as a drug carrier (negative charges in the CMP allows the polymer to be retained for longer in a biological environment).
- Sulfated derivatives commonly produced to investigate antithrombotic (clotting) agents.
- Chlorakyl groups on pullulan derivatives developed by reacting cross-linked pullulan micro/nano particles with chloralkyl chlorides in basic organic solvents, creating a drug carrier (slow release into plasma).
- Pullulan hydrogels are commonly produced by attaching cholesteryl groups, which then causes the pullulan to self-aggregate into stable, monodispersed nanoparticles which is easily complexed with proteins/enzymes. Nanoparticles and liposomes have been tested as drug delivery particles.
- Hydrophobically modified pullulan prepared by reacting alkylperfluorinated pullulan derived from pullulan and carboxymethylpullulan using perfluoroalkyl carboxylic acid and perfluoroalkylamines → compact nanoparticles for drug delivery or as a contrast agent.

1.5 Objectives, and Report Outline

The main objective of this work is to develop a variety of “unit process” and “bits and pieces” on bioassay systems and more specifically bioactive paper devices to serve as a toolbox to rapidly build ready-to-use biosensor devices.

To accomplish the goal, the first achievement is the development of a paper based pump/accelerator that can speed up or slow down the flow of liquid through the paper device (*Chapter 2*). This work has led to a publication in *Lab on a Chip* [97] and a U.S. Provisional Application. [98]

The second achievement is creating an automatic shut-off valve used in paper-supported microfluidics which has the potential to play the role of pipette/flow-meter on the paper device.

Using the developed accelerator and shut-off valve has led to the creation of a fully automated biosensor for the detection of organophosphate pesticide (*Chapter 3*). This work has led to a publication in *Lab on a Chip* [99] and a U.S. Provisional Application. [100]

The next accomplishment introduces “biolab-in-pills” and provides an immobilizer/stabilizer system for bio-devices to increase the storage time of biomaterials. Encapsulation of acetylcholinesterase (AChE) and indoxyl acetate (IDA) for the detection of pesticide (*Chapter 4*) and luciferase and luciferin for the detection of ATP (*Chapter 5*) are done using this technique. This work has led to one published paper in *Angewandte Chemie International Edition* [101] and a pending submission *Angewandte Chemie International Edition*, as well as a U.S. patent application. [102]

The final achievement deals with reagent delivery and multi-directional flow on paper-based microfluidic devices (*Chapter 6*). Using this method, ready-to-use assay kits for the detection of *E. coli* and secondary amines have been developed. This work is pending submission to *Nature Communications*, and two more provisional applications.

Finally, the main conclusions and contributions of this project, as well as suggestions for future research are given in *Chapter 7*.

The work presented in *Chapter 4* and the application of this idea for Thermal Stabilization of Vaccines has succeed and has won an award in the Grand Challenges Canada “Stars in Global Health” Program competition. The results presented in *Chapter 4* were also selected for the A. E. Hamielec Graduate Student Award in MUCEC 2014, and the Otto Maass Best Scientific Award at Fiber Conference 2014. Moreover, the results presented in *Chapter 3* were awarded for the Most Outstanding Student Presentation at PaperWeek Conference 2014.

Overall, the results reported in this thesis are projected to lead to 5 paper publications (3 currently published, and 2 pending submission) and 6 patent applications, as well as 9 conference presentations [103-111]. Also, two additional papers has been drafted based on work which is not directly presented in this thesis.

1.6 References

- [1] W. Van Zijl. Studies on diarrhoeal diseases in seven countries by the WHO Diarrhoeal Diseases Advisory Team. *Bulletin of the World Health Organisation*. 35 (1966) 249–61.
- [2] R. Lindskog, P. Lindskog. Bacteriological contamination of water in rural areas: an intervention study from Malawi. *Am J Trop Med Hyg*. 91 (1988) 1–7.
- [3] Public health implications of global ageing. World Health Organisation (WHO) 2011.
- [4] The World Health Report 2002. World Health Organisation (WHO) 2002.
- [5] Fact sheet, Ageing. World Health Organisation (WHO) 2014.
- [6] The World: Population 2014. *Geoba.se2014*.
- [7] World population to increase by 2.6 billion over next 45 years. Press Release POP/9182005.
- [8] R. Pelton. Bioactive paper provides a low-cost platform for diagnostics. *Trends Anal Chem*. 28 (2009) 925-42.
- [9] S.M.Z. Hossain, J.D. Brennan. β -Galactosidase-Based Colorimetric Paper Sensor for Determination of Heavy Metals. *Anal Chem*. 83 (2011) 8772–8.
- [10] S.M.Z. Hossain, R.E. Luckham, M.J. McFadden, J.D. Brennan. Reagentless Bidirectional Lateral Flow Bioactive Paper Sensors for Detection of Pesticides in Beverage and Food Samples. *Anal Chem*. 81 (2009) 9055–64.
- [11] S.M.Z. Hossain, R.E. Luckham, A.-M. Smith, J.M. Lebert, L.M. Davies, R.H. Pelton, et al. Development of a Bioactive Paper Sensor for Detection of Neurotoxins Using Piezoelectric Inkjet Printing of Sol-Gel-Derived Bioinks. *Anal Chem*. 81 (2009) 5474–83.
- [12] Y. Xu, Z. Zhang, M.M. Ali, J. Sauder, X. Deng, K. Giang, et al. Turning Tryptophanase into Odor-Generating Biosensors. *Angew Chem*. 126 (2014) 2658–60.
- [13] S.S. Rajinder. Transducer aspects of biosensors. *Biosens Bioelectron*. 9 (1994) 243–64.
- [14] L. John H.T., K.B. Male, J.D. Glennon. Biosensor technology: Technology push versus market pull. *Biotechnol Adv*. 26 (2008) 492–500.
- [15] Y. H. Lee. Biosensors. Engineering Biotechnology, Gateway Project, Drexel University.
- [16] Index of Watershed Indicators. Environmental Protection Agency (EPA) 1997.
- [17] A. Sassolas, L. J. Blum, B. D. Leca-Bouvier. Immobilization strategies to develop enzymatic biosensors. *Biotechnol Adv*. 30 (2012) 489-511.
- [18] B. Prieto-Simon, M. Campas, J.-L. Marty. Biomolecule Immobilization in Biosensor Development: Tailored Strategies Based on Affinity Interactions. *Protein Pept Lett* ;. 15 (2008) 757-63.
- [19] Contaminants in Your Drinking Water. *Fresh Water Systems*2013.
- [20] T.L. Pedersen. Tap Water Sources. EXTOXNET (The EXtension TOXicology NETwork)1997.
- [21] J. Wright, S. Gundry, R. Conroy. Household drinking water in developing countries:

- a systematic review of microbiological contamination between source and point-of-use. *Trop Med Int Health*. 9 (2004) 106-17.
- [22] Guidelines for Canadian Drinking Water Quality - Summary Table [Health Canada, 2012]. Health Canada, Government of Canada 2012.
- [23] L. Nash. Water quality and health." *Water in Crisis: A guide to the world's fresh water resources*. Oxford University Press, New York. (1993) 25-39.
- [24] S.W. Lagakos, Barbara J. Wessen, Z. Marvin. An analysis of contaminated well water and health effects in Woburn, Massachusetts. *J Am Statist Assoc*. 395 (1986) 583-96.
- [25] M. Berg, H.C. Tran, T.C. Nguyen, H.V. Pham, R. Schertenleib, W. Giger. Arsenic contamination of groundwater and drinking water in Vietnam: a human health threat. *Environ Sci Technol*. 35 (2001) 2621-6.
- [26] R. Vargas-Bernal, E. Rodríguez-Miranda, G. Herrera-Pérez. Evolution and Expectations of Enzymatic Biosensors for Pesticides. in: R.P. Soundararajan, (Ed.). *Pesticides - Advances in Chemical and Botanical Pesticides* 2012.
- [27] W. Aktar, D. Sengupta, A. Chowdhury. Impact of pesticides use in agriculture: their benefits and hazards. *Interdiscip Toxicol*. 2 (2009) 1-12.
- [28] S.M. Ross, I.C. McManus, V. Harrison, O. Mason. Neurobehavioral problems following low-level exposure to organophosphate pesticides: a systematic and meta-analytic review. *Crit Rev Toxicol*. 43 (2013) 21-44.
- [29] S. Giri, S.B. Prasad, A. Giri, G.D. Sharma. Genotoxic effects of malathion: an organophosphorus insecticide, using three mammalian bioassays in vivo. *Mutat Res*. 514 (2002) 223-31.
- [30] DailyNewsBlog. Organophosphate Poisoning Leads to the Death of School Children in India. *Beyond Pesticides* 2013.
- [31] B. Eskenazi, A.R. Marks, A. Bradman, K. Harley, D.B. Barr, C. Johnson, et al. Organophosphate Pesticide Exposure and Neurodevelopment in Young Mexican-American Children. *Environ Health Perspect*. 115 (2007).
- [32] S. Ciesielski, D.P. Loomis, S. Rupp Mims, A. Auer. Pesticide Exposures, Cholinesterase Depression, and Symptoms among North Carolina Migrant Farmworkers. *Am J Public Health* 84 (1994).
- [33] S. Koutros, L.E.B. Freeman, J.H. Lubin, S.L. Heltshe, G. Andreotti, K.H. Barry, et al. Risk of Total and Aggressive Prostate Cancer and Pesticide Use in the Agricultural Health Study. *Am J Epidemiol*. 177 (2013) 59-74.
- [34] R. Jeannot, H. Sabik, E. Sauvard, E. Genin. Application of liquid chromatography with mass spectrometry combined with photodiode array detection and tandem mass spectrometry for monitoring pesticides in surface waters. *J Chromatogr A*. (2000) 51-71.
- [35] V. Andreu, Y. Pico. Determination of pesticides and their degradation products in soil: critical review and comparison of methods. *Trends in Analytical Chemistry*, Vol , No , . 23 (2004) 772-89.
- [36] A. Corcia, M. Marchetti. Multiresidue Method for Pesticides in Drinking Water Using a Graphitized Carbon Black Cartridge Extraction and Liquid

- Chromatographic Analysis. *Anal Chem.* (1991) 580-5.
- [37] G. Wang, C.G. Clark, F.G. Rodgers. Detection in *Escherichia coli* of the Genes Encoding the Major Virulence Factors, the Genes Defining the O157:H7 Serotype, and Components of the Type 2 Shiga Toxin Family by Multiplex PCR. *J Clin Microbiol.* 40 (2002) 3613–9.
- [38] K.J. Vicente, K. Christoffersen. The Walkerton *E. coli* outbreak: a test of Rasmussen's framework for risk management in a dynamic society. *Theor Issues Ergon Sci.* 7 (2006) 93–112.
- [39] R.Y.C. Kong, S.K.Y. Lee, T.W.F. Law, S.H.W. Law, R.S.S. Wu. Rapid detection of six types of bacterial pathogens in marine waters by multiplex PCR. *Water Res.* (2002) 2802-12.
- [40] P. Held. Luminescent Determination of ATP Concentrations Using the Clarity™ Luminescence Microplate Reader. *Nat Methods Appl Notes.* (2006).
- [41] S. Falzoni, G. Donvito, F.D. Virgilio. Detecting adenosine triphosphate in the pericellular space. *Interface Focus.* 3 (2013) 201-10.
- [42] R. Beigi, E. Kobatake, M. Aizawa, G.R. Dubyak. Detection of local ATP release from activated platelets using cell surface-attached firefly luciferase. *Am J Physiol.* 276 (1999) C267–78.
- [43] A.R.S. Riberio, R M; Rosario, L M; Gill, M H. Immobilization of luciferase from a firefly lantern extract on glass strips as an alternative strategy for luminescent detection of ATP. *J Biolumin Chemilumin.* (1998) 371-8.
- [44] C.S. Lee, X.L. W. Shi, S.C. Cheung, I. Thornton. Metal contamination in urban, suburban, and country park soils of Hong Kong: A study based on GIS and multivariate statistics. *Sci Total Environ.* 356 (2006) 45–61.
- [45] S.A. Mansour, M.M. Sidky. *Ecotoxicological Studies.* 3. Heavy metals contaminating water and fish from Fayoum Governorate, Egypt. *Food Chem.* 78 (2002) 15–22.
- [46] J.M. Matés, J.A. Segura, F.J. Alonso, J. Márquez. Roles of dioxins and heavy metals in cancer and neurological diseases using ROS-mediated mechanisms. *Free Radic Biol Med.* 49 (2010) 1328–41.
- [47] Water-related Diseases. World Health Organisation (WHO)2014.
- [48] M. Harada. Minamata Disease: Methylmercury Poisoning in Japan Caused by Environmental Pollution. *Crit Rev Toxicol.* 25 (1995) 1–24.
- [49] M.R. Aceves-Mijares, J M; Pedraza, J; Roman-Lopez, S; Chavez, C. Determination of heavy metals contamination using a silicon sensor with extended responsive to the UV. *J Phys Conf Ser.* (2013) 1-6.
- [50] D. Kar, P. Sur, S.K. Mandal, R.K. Kole. Assessment of heavy metal pollution in surface water. *IJEST.* (2008) 119-24.
- [51] M. Jung. Heavy metal contamination of soils and waters in and around the Imcheon Au–Ag mine, Korea. *Appl Geochem.* (2001) 1369-75.
- [52] D. Erickson, D. Li, C.B. Park. Numerical Simulations of Capillary-Driven Flows in Nonuniform Cross-Sectional Capillaries. *J Colloid Interface Sci.* 250 (2002) 422–30.
- [53] X. Li, J. Tian, W. Shen. Paper as a low-cost base material for diagnostic and

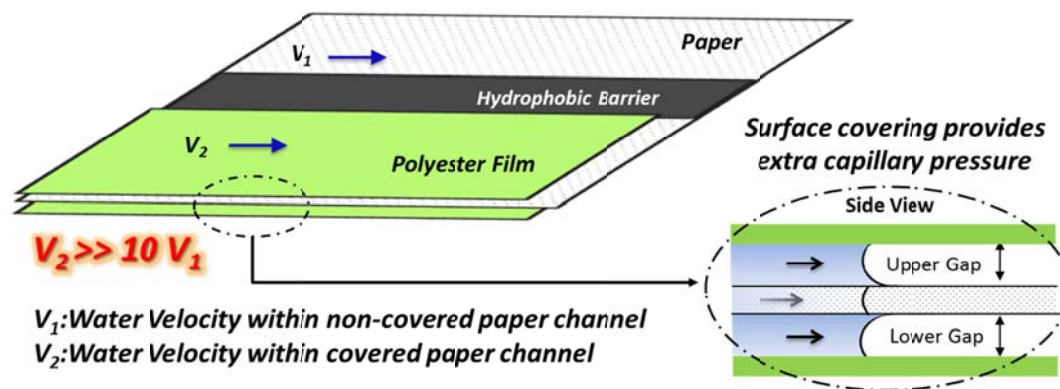
- environmental sensing applications. 63rd Appita Annual Conference and Exhibition, Melbourne 2009. pp. 19-22.
- [54] R. Pelton. Bioactive paper provides a low-cost platform for diagnostics. *Trends Anal Chem.* 28 (2009) 925-42.
- [55] X. Li, D.R. Ballerini, W. Shen. A perspective on paper-based microfluidics: Current status and future trends. *Biomicrofluidics.* 6 (2012) 011301-13.
- [56] X. Li, J. Tian, W. Shen. Progress in patterned paper sizing for fabrication of paper-based microfluidic sensors. *Cellulose.* 17 (2010) 649–59.
- [57] A. Martinez, S. Phillips, G. Whitesides. Diagnostics for the Developing World: Microfluidic Paper-Based Analytical Devices. *Anal Chem.* 82 (2010) 3-10.
- [58] A.W. Martinez, S.T. Phillips, M.J. Butte, G.M. Whitesides. Patterned Paper as a Platform for Inexpensive, Low-Volume, Portable Bioassays. *Angew Chem Int Ed.* 46 (2007) 1318 –20.
- [59] K. Abe, K. Suzuki, D. Citterio. Inkjet-Printed Microfluidic Multianalyte Chemical Sensing Paper. *Anal Chem.* 80 (2008) 6928–34.
- [60] J. Wang, M.R.N. Monton, X. Zhang, C.D.M. Filipe, R. Pelton, J.D. Brennan. Hydrophobic sol-gel channel patterning strategies for paper-based microfluidics. *Lab Chip.* 14 (2014) 691-5.
- [61] F. Deiss, W.L. Matochko, N. Govindasamy, E.Y. Lin, R. Derda. Flow-Through Synthesis on Teflon-Patterned Paper To Produce Peptide Arrays for Cell-Based Assays. *Angew Chem Int Ed.* 53 (2014) 6374–7.
- [62] M. Altstein, G. Segev, N. Aharonson, O. Ben-Aziz, A. Turniansky, D. Avnir. Sol-gel-entrapped cholinesterases: a microtiter plate method for monitoring anti-cholinesterase compounds. *J Agric Food Chem.* 46 (1998) 3318-24.
- [63] M. Hitzbleck, L. Avrain, V. Smekens, R. Lovchik, P. Mertens, E. Delamarche. Capillary soft valves for microfluidics. *Lab on a Chip.* (2012).
- [64] McAvoy, e. al. Mechanically-actuated microfluidic pinch valve. US, 2011.
- [65] X. Li, J. Tian, W. Shen. Progress in patterned paper sizing for fabrication of paper-based microfluidic sensors. *Cellulose.* 17 (2010) 649-59.
- [66] W. Shen, X. Li, J. Tian, T.H. Nguyen, G. Garnier. *Switches for microfluidic Systems.* International, 2010.
- [67] A. Siegel, S. Phillips, M. Dickey, D. Rozkiewicz, B. Wiley, G. Whitesides, et al. *Paper-based microfluidic systems.* United States, 2009.
- [68] H. Chen, J. Cogswell, C. Anagnostopoulos, M. Faghri. A fluidic diode, valves, and a sequential-loading circuit fabricated on layered paper. *Lab on a Chip.* 12 (2012) 2909-13.
- [69] E. Fu, B. Lutz, P. Kauffman, P. Yager. Controlled reagent transport in disposable 2D paper networks. *Lab on a Chip.* 10 (2010) 918-20.
- [70] B. Lutz, P. Trinh, C. Ball, E. Fu, P. Yager. Two-dimensional paper networks: programmable fluidic disconnects for multi-step processes in shaped paper. *Lab on a Chip.* 11 (2011) 4274-8.
- [71] E. Fu, T. Liang, P. Spicar-Mihalic, J. Houghtaling, S. Ramachandran, P. Yager. Two-Dimensional Paper Network Format That Enables Simple Multistep Assays for Use

- in Low-Resource Settings in the Context of Malaria Antigen Detection. *Anal Chem.* 84 (2012) 4574-9.
- [72] E. Fu, S. Ramsey, P. Kauffman, B. Lutz, P. Yager. Transport in two-dimensional paper networks. *Microfluid Nanofluid.* 10 (2011) 29-35.
- [73] M.M. Ali, S.D. Aguirre, Y. Xu, C.D.M. Filipe, R. Pelton, Y. Li. Detection of DNA using bioactive paper strips. *Chem Commun.* (2009) 6640-2.
- [74] S.M.Z. Hossain, C. Ozimok, C. Sicard, S.D. Aguirre, M.M. Ali, Y. Li, et al. Multiplexed paper test strip for quantitative bacterial detection *Anal Bioanal Chem.* 403 (2012) 1567-76.
- [75] R.S. Singh, G.K. Saini, J.F. Kennedy. Pullulan: Microbial sources, production and applications. *Carbohydr Polym.* 73 (2008) 515-31.
- [76] M. Shibata, M. Asahina, N. Teramoto, R. Yosomiya. Chemical modification of pullulan by isocyanate compounds. *Polymer.* 42 (2001) 59-64.
- [77] S. Farris, L. Introzzi, J.M. Fuentes-Alventosa, N. Santo, R. Rocca, L. Piergiovanni. Self-Assembled Pullulan-Silica Oxygen Barrier Hybrid Coatings for Food Packaging Applications. *J Agric Food Chem.* 3 (2012) 782-90.
- [78] S. Wu, J. Chen. Using pullulan-based edible coatings to extend shelf-life of fresh-cut 'Fuji' apples. *Int J Biol Macromol.* 55 (2013) 254- 7.
- [79] A.A. Krumnow, I.B. Sorokulova, E. Olsen, L. Globa, J.M. Barbaree, V.J. Vodyanoy. Preservation of bacteria in natural polymers. *J Microbiol Methods.* 78 (2009) 189-94.
- [80] R.E. Whistler. *Industrial Gums: Polysaccharides and Their Derivatives* 2012.
- [81] S. Farris, I.U. Unalan, L. Introzzi, J.M. Fuentes-Alventosa, C.A. Cozzolino. Pullulan-Based Films and Coatings for Food Packaging: Present Applications, Emerging Opportunities, and Future Challenges. *J APPL POLYM SCI* (2014) 40539 (1-12).
- [82] K. Kawahara, K. Ohta, H. Miyamoto, S. Nakamura. Preparation and solution properties of pullulan fractions as standard samples for water-soluble polymers. *Carbohydr Polym.* 4 (1984) 335-56.
- [83] S. Farris, L. Introzzi, P. Biagioni, T. Holz, A. Schiraldi, L. Piergiovanni. Wetting of Biopolymer Coatings: Contact Angle Kinetics and Image Analysis Investigation. *Langmuir.* 27 (2011) 7563-74.
- [84] A. Lazaridou, C.G. Biliaderis, V. Kontogiorgos. Molecular weight effects on solution rheology of pullulan and mechanical properties of its films. *Carbohydr Polym.* 52 (2003) 151-66.
- [85] K.I. Shingel. Current knowledge on biosynthesis, biological activity and chemical modification of the exopolysaccharide, pullulan. *Carbohydr Res.* 333 (2004) 447-60.
- [86] Hyashibara. *Viscosity of Aqueous Pullulan.* Hyashiabara Co. 2013.
- [87] K. Sommermeyer, K. Cech, E. Pfitzer. Characterization of Polymers by Size Exclusion Chromatography Using Multiple Detection Determination of the Mark-Houwink Constant for Pullulan 100. *Friedr Vieweg & Sohn Verlagsgesellschaft mbH.* (1988).
- [88] Y. Cheng, K.M. Brown, R.K. Prud'homme. Preparation and characterization of

- molecular weight fractions of guar galactomannans using acid and enzymatic hydrolysis. *Int J Biol Macromol.* 31 (2002) 29-35.
- [89] E. Antoniou, M. Tsianou. Solution properties of dextran in water and in formamide. *J Appl Polym Sci.* 125 (2012) 1681–92.
- [90] C. Sanchez, C. Schmitt, E. Kolodziejczyk, A. Lapp, C. Gaillard, R. D. The Acacia Gum Arabinogalactan Fraction Is a Thin Oblate Ellipsoid: A New Model Based on Small-Angle Neutron Scattering and Ab Initio Calculation. 94 (2008) 629-40.
- [91] E. Cranston. Chemical Engineering 3Q03. Polymer Solubility, McMaster University, Hamilton ON, 2014.
- [92] J. Eckelt, R. Sugaya, B.A. Wolf. Pullulan and Dextran: Uncommon Composition Dependence of Flory-Huggins Interaction Parameters of their Aqueous Solutions. *Biomacromolecules.* 9 (2008) 1691-7.
- [93] R. Mafi, C. Gray, R. Pelton, H. Ketelson, J. Davis. On formulating ophthalmic emulsions. *Colloids and Surfaces B: Biointerfaces.* 122 (2014) 7–11.
- [94] T. Diab, C. Biliaderis, D. Gerasopolous, E. Sfakiotakis. Physicochemical properties and application of pullulan edible films and coatings in fruit preservation. *Journal of the Science of Food and Agriculture.* 81 (2001) 988-1000.
- [95] M. Scandola, G. Ceccorulli, M. Pizzoli. Molecular motions of polysaccharides in the solid state: dextran, pullulan and amylose. *Int J Biol Macromol.* 13 (1991) 254-60.
- [96] N. Teramoto, M. Saitoh, J. Kuroiwa, M. Shibata, R. Yosomiya. Morphology and Mechanical Properties of Pullulan/Poly(vinyl alcohol) Blends Crosslinked with Glyoxa. *J Appl Polym Sci.* 82 (2001) 2273–80.
- [97] S. Jahanshahi-Anbuhi, P. Chavan, C. Sicard, V. Leung, S.M.Z. Hossain, R. Pelton, et al. Creating fast flow channels in paper fluidic devices to control timing of sequential reactions. *Lab Chip.* 12 (2012) 5079-85.
- [98] S. Jahanshahi-Anbuhi, C.D.M. Filipe, R. Pelton, J.D. Brennan, K. Dalnoki-Veress. *Methods of Controlling Flow in Paper-Based Microfluidic Devices.* 2012.
- [99] S. Jahanshahi-Anbuhi, A. Henry, V. Leung, C. Sicard, K. Pennings, R. Pelton, et al. Paper-based microfluidics with an erodible polymeric bridge giving controlled release and timed flow shutoff. *Lab Chip.* 14 (2014) 229-36.
- [100] S. Jahanshahi-Anbuhi, C.D.M. Filipe, R. Pelton, J.D. Brennan. *Automatic Flow Shutoff System for Paper-Based Microfluidics Formed through Dissolving Polymers.* 2013.
- [101] S. Jahanshahi-Anbuhi, K. Pennings, V. Leung, M. Liu, C. Carrasquilla, B. Kannan, et al. Pullulan Encapsulation of Labile Biomolecules to Give Stable Bioassay Tablets. *Angew Chem Int Ed.* 126 (2014) 6269–72.
- [102] S. Jahanshahi-Anbuhi, C.D.M. Filipe, R. Pelton, J.D. Brennan, Y. Li. *Method for stabilizing various molecules without refrigeration using water soluble polymers – demonstration using pullulan.* 2013.
- [103] S. Jahanshahi-Anbuhi, P. Chavan, C. Sicard, V. Leung, S.M.Z. Hossain, R. Pelton, et al. *Pump on paper-based microfluidic devices.* SENTINEL2012.
- [104] S. Jahanshahi-Anbuhi, P. Chavan, C. Sicard, V. Leung, S.M.Z. Hossain, R. Pelton, et al. *Speeding up the Capillary Flow in Paper-Based Fluidic Devices for Rapid*

- Diagnostics and Environmental Sensing Applications. CSCHE, Vancouver, Canada, 2012.
- [105] S. Jahanshahi-Anbuhi, A. Henry, V. Leung, C. Sicard, K. Pennings, R. Pelton, et al. Development of an Automatic Time Dependent Flow Cut-Off System Using Rapid Dissolvable Polymer. Fiber Conf, Cornwall, Canada, 2013.
- [106] S. Jahanshahi-Anbuhi, A. Henry, V. Leung, C. Sicard, K. Pennings, R. Pelton, et al. Automatic Time-Dependent Flow Cut-Off System for Paper-Based Microfluidic Devices Using Erodible Polymeric Bridge. AIChE2013.
- [107] S. Jahanshahi-Anbuhi, A. Henry, V. Leung, C. Sicard, K. Pennings, R. Pelton, et al. Fully Automated Bioactive Paper-Based Sensor for Detection of Organophosphate Pesticides. PaperWeek Conf, Montreal, Canada, 2014.
- [108] S. Jahanshahi-Anbuhi, A. Henry, V. Leung, C. Sicard, K. Pennings, R. Pelton, et al. Paper-based microfluidics with erodible polymeric bridge giving controlled release and timed flow shutoff. 247th ACS National Meeting and Exposition, Dallas, Texas, 2014.
- [109] S. Jahanshahi-Anbuhi, K. Pennings, V. Leung, M. Liu, C. Carrasquilla, B. Kannan, et al. Lab on Pills. MUCEC, Hamilton, Canada, 2014.
- [110] S. Jahanshahi-Anbuhi, K. Pennings, V. Leung, M. Liu, C. Carrasquilla, B. Kannan, et al. Immobilized BioLab in Pills. Fiber Conf, Vancouver, Canada, 2014.
- [111] S. Jahanshahi-Anbuhi, K. Pennings, V. Leung, M. Liu, C. Carrasquilla, B. Kannan, et al. Simple Method for Long-term Preservation of Labile Enzymes at Room Temperature. CSCHE, Niagara Falls, Canada, 2014.

Chapter 2 Flow Speeding-Up System for Paper- Based Microfluidics Devises



20 Word Summary:

Accelerating the flow of water through paper by over 10-fold, by placing a flexible film on top of the paper.

In Chapter 2, all experiments were conducted by myself and Puneet Chavan with assistance from Vincent Leung and Dr. Clemence Sicard. Puneet Chavan and Clemence Sicard assisted in the development of the dose-dependent inhibition of acetylcholinesterase. And Vincent Leung worked with me to complete most of the experiments. Prof. Filipe aided in the modeling section to describe the capillary flow between flexible walls. Dr. Filipe and Dr. Pelton gave many helpful suggestions on both experiments and data analysis. I initiated the first draft of the paper. Prof. Filipe, Prof. Pelton, and Prof. Brennan helped in revising the draft to final version. This work has been published in Lab Chip, 2012, 12, 5079-5085, 2012. DOI: 10.1039/C2LC41005B. It is produced by permission of The Royal Society of Chemistry.
 URL: <http://pubs.rsc.org/en/content/articlelanding/2012/lc/c2lc41005b#!divAbstract>

Creating fast flow channels in paper fluidic devices to control timing of sequential reactions

Sana Jahanshahi-Anbuhi,^a Puneet Chavan,^b Clémence Sicard,^b Vincent Leung,^a S. M. Zakir Hossain,^b Robert Pelton,^a John D. Brennan^{*b} and Carlos D.M. Filipe^{*a}

Received 2nd September 2012, Accepted 2nd October 2012

DOI: 10.1039/c2lc41005b

This paper reports the development of a method to control the flow rate of fluids within paper-based microfluidic analytical devices. We demonstrate that by simply sandwiching paper channels between two flexible films, it is possible to accelerate the flow of water through paper by over 10-fold. The dynamics of this process are such that the height of the liquid is dependent on time to the power of 1/3. This dependence was validated using three different flexible films (with markedly different contact angles) and three different fluids (water and two silicon oils with different viscosities). These covered channels provide a low-cost method for controlling the flow rate of fluid in paper channels, and can be added following printing of reagents to control fluid flow in selected fluidic channels. Using this method, we redesigned a previously published bidirectional lateral flow pesticide sensor to allow more rapid detection of pesticides while eliminating the need to run the assay in two stages. The sensor is fabricated with sol-gel entrapped reagents (indoxyl acetate in a substrate zone and acetylcholinesterase, AChE, in a sensing zone) present in an uncovered “slow” flow channel, with a second, covered “fast” channel used to transport pesticide samples to the sensing region through a simple paper-flap valve. In this manner, pesticides reach the sensing region first to allow preincubation, followed by delivery of the substrate to generate a colorimetric signal. This format results in a uni-directional device that detects the presence of pesticides two times faster than the original bidirectional sensors.

Introduction

The development of paper-based devices for diagnostics and biosensing has attracted a great deal of interest as they provide portable, low-cost, low-volume, disposable, and simple analytical devices for bioassays and environmental analysis^{1,2} in areas such as point-of-care diagnostics, food and water testing, and military applications.^{3–5} Several groups are now active in this area, including Canada’s Sentinel Bioactive Paper Network, as well as groups in the United States, Japan, Australia and Scandinavia.^{6–9} This technology is already having an impact in low-cost diagnostics, and is expected to be used globally and in particular in resource-limited settings, in the near future.

Paper-based microfluidic devices generally contain hydrophilic (unmodified paper) channels surrounded by hydrophobic barriers composed of wax or other materials. There are several methods to create the channels on paper, from relatively complex

methods such as photolithography⁹ to very simple methods such as wax printing.¹⁰ Alternatively, a hydrophobically modified paper can have hydrophilic channels generated by inkjet printing of reagents that dissolve the hydrophobic material.⁸

While several microfluidic paper-based analytical devices (μ PADs) have been demonstrated for a range of analytes (*e.g.* pesticides, heavy metals, neurotoxins, coliform bacteria, DNA, pH, glucose, liver proteins, blood typing)^{1,3,6,8,11–15} such devices still do not have the range of capabilities of conventional microfluidic devices (*i.e.*, control over flow rates, mixing, timing of sequential reactions, *etc.*). Yager’s group has perhaps done the most to address these issues, having reported on a simple method to perform mixing on paper,¹⁶ and a method to control reaction sequences by using strips combining a long and short arm to delay the lateral flow of one reagent to a reaction zone relative to a second reagent.^{17,18} Simple valves have also been reported to control when specific reagents are added to a reaction to generate a paper based assay.¹⁹ However, much remains to be done to fully develop μ PADs for use in more complex, multi-step assays.

In this report, we introduce a method to not only control, but also accelerate liquid flow through paper, which provides both a means to perform multi-step assays using channels with different flow velocities, and to shorten the total time needed for such

^aDepartment of Chemical Engineering, McMaster University, 1280 Main Street West, Hamilton, ON, L8S 4M1, Canada.

E-mail: filipec@mcmaster.ca; Fax: +1 905 521-1350;

Tel: +1 905 525-9140 (ext. 27278)

^bDepartment of Chemistry & Chemical Biology, McMaster University, 1280 Main Street West, Hamilton, ON, L8S 4M1, Canada.

E-mail: brennanj@mcmaster.ca; Fax: +1 905 527-9950;

Tel: +1 905 525-9140 (ext. 27033)

assays. The method is based on placing flexible films on both sides of the paper strip, whereby a capillary channel, with collapsible walls, is formed in between the film and the paper. As the water rises in this capillary, the negative capillary pressure in the liquid causes the surface of the flexible film to become closer to the paper surface. This deformation “pushes” the liquid in the front, as recently demonstrated²⁰ using a vertical glass plate covered by a flexible polypropylene film, with spacers placed on the side borders of the glass plate, to allow flow of liquid from the reservoir to the rising front of liquid. Two aspects of this work inspired us to use flexible films in paper-based devices: (1) the fluid rose much faster when a flexible surface was used to cover the glass support, as compared to using a rigid surface. Using a flexible film, the front moved in proportion to time elevated to power of 1/3, a dependence predicted theoretically²¹ and experimentally observed for capillary flow between wedges²² of various geometries;²³ (2) when the surface of the glass support was modified to increase its roughness, the liquid moving up the space between the flexible film and the support was being continuously drained into the interstices associated with the presence of roughness. These two observations led us to the idea of using flexible covers to accelerate liquid flow in μ PADs, since paper is a porous medium. We also wanted to determine how the physical–chemical characteristics of the flexible film and the fluid to be transported affect the rate at which the liquid moves in these devices, capturing these effects with a simple mathematical model.

In this study, we developed a μ PAD for organophosphate pesticides based on a previously reported design.¹ As shown in Fig. 1a, the original design had indophenyl acetate (IPA) printed in a substrate zone (Subs.) and acetylcholinesterase (AChE) printed in a sensing zone (ENZ.). The sample was first introduced to the sensing zone by lateral flow from the end of the strip distal to the substrate zone. Following incubation, the

proximal end was placed in the sample to bring the substrate to the sensing zone and elicit a color change. The entire assay required ~ 30 min, including 10 min for the sample to reach the sensing zone by lateral flow, followed by a 5 min incubation period, a further 10 min for the reagents to reach the sensing zone by lateral flow after inversion and 5 min incubation to let the color develop.

The new sensor, shown in Fig. 1b, is fabricated with sol–gel entrapped reagents (indoxyl acetate, an improved indicator in a substrate zone and AChE in a sensing zone) present in a “slow” flow channel, with a second “fast” channel used to transport pesticide samples to the sensing region through a flap valve. In this manner, pesticides reach the sensing region rapidly (~ 2 min) to allow preincubation, instead of the 15 min required with the previous design. This is then followed by delivery of the substrate to this region (~ 8 min) and an extra 5 min incubation to let the color develop. This format results in a simplified assay that detects the presence of pesticides two times faster than the previous bidirectional sensors.

Experimental section

Materials

Sodium silicate solution ($\sim 14\%$ NaOH, $\sim 29\%$ SiO₂) was purchased from Fisher Scientific. Dowex 50WX8-100 ion-exchange resin, acetylcholinesterase (AChE, from *Electrophorus electricus*, EC 3.1.1.7), malathion (an organophosphate), and indoxyl acetate (IDA) were obtained from Sigma-Aldrich (Oakville, ON, Canada). Poly(vinylamine) (PVAm; 1.5 MDa) was obtained from BASF (Mississauga, ON, Canada), as a gift. Whatman #1 filter paper was used for all assays. Distilled deionized water was obtained from a Milli-Q Synthesis A10 water purification system. PET slide (polyester film, 0.004'' thick, clear, Part # 8567k44) was purchased from McMaster-CARR (Hamilton, ON, Canada). Parafilm® M roll size 4 in. \times 250 ft was obtained from Sigma-Aldrich (Oakville, ON, Canada). Clear Tape (premium packaging tape, 48 mm \times 50 m, #99842) from GRAND & TOY.

Solution preparation

Stock solutions of indoxyl acetate (3 mM) and malathion (1 nM to 100 μ M) were made up daily and were not used for more than 3 h after preparation to minimize the potential for hydrolysis (CAUTION: malathion is extremely toxic. This material should be handled with appropriate personal protective equipment). A mixture of Tris buffer (100 mM, pH 8.0) with 3% methanol (Sigma) was used for dilution of indoxyl acetate solutions. Distilled deionized water (ddH₂O) was used to dissolve PVAm (0.5 wt%). AChE (500 U mL⁻¹) and malathion were prepared in Tris buffer (100 mM, pH 8.0). SS sols were prepared by mixing 10 mL of ddH₂O with 2.59 g of sodium silicate solution (pH ~ 13) followed by addition of 5.5 g of Dowex cation exchange resin to replace Na⁺ with H⁺. The mixture was stirred for 2 min to reach a final pH of ~ 4 , and then vacuum filtered through a Büchner funnel. The filtrate was then further filtered through a 0.45 μ m membrane syringe filter. These sols were used to prepare silica-containing inks as described below.

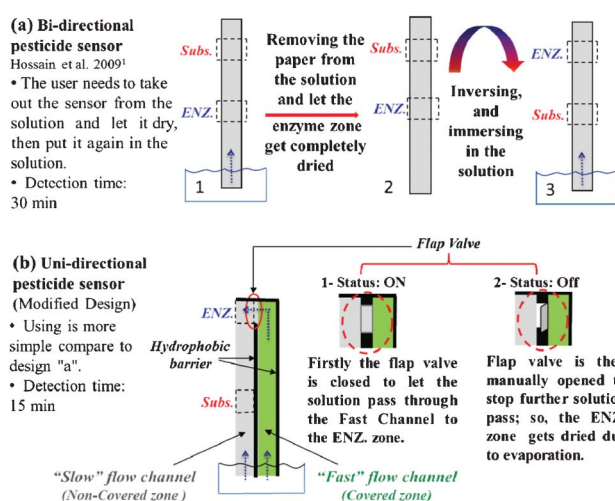


Fig. 1 Modification of bioactive paper for pesticide detection. (a) Bidirectional pesticide detection sensor. (b) Modified, uni-directional, pesticide detection sensor. The green zone is covered by PET cover slips creating a faster flow zone. A manual valve is constructed at the top of the paper strip. This modification allows for a simpler uni-directional pesticide sensor.

Fabrication of reagentless bioactive paper-based lateral flow sensor

The bidirectional sensor was prepared as previously reported.¹ However, in the previously reported method indophenyl acetate (IPA) was used as a chromogenic substrate; herein it was replaced by using indoxyl acetate and all layers were deposited by hand using a microliter volume pipette. After depositing the reagents, the sensor was allowed to dry for at least 1 h in air at room temperature. The microfluidic pattern for the uni-directional sensor was created using Microsoft PowerPoint and printed onto Whatman #1 paper using a wax printer (Xerox Phaser 6580), followed by melting of the wax in an oven at 120 °C. The pattern consisted of a wax line (3.5 pt, producing a 0.5 cm wide line 4.3 cm in length) separating two channels (0.7 cm in width and 5.0 cm in length). A manual valve was introduced between the two channels directly above this wax barrier by cutting the paper, creating a flap that was 0.3 cm in width and 0.9 cm in length. This valve was supported by an additional wax barrier, placed above the two channels, which was used to stop the flow. The channel on the right ("fast" channel) was covered with a PET slide (polyester film) on both sides of the paper and to make the handling of the sensors easier, and an extra wax line was printed at the right of the "fast" channel, onto which the PET films were taped to ensure that the PET films stayed in position. The PET contact angle (θ) was 42.7°, as measured using a Kruss DSA 10 drop shape analyzer system. The channel on the left ("slow" channel) had AChE and indoxyl acetate entrapped in two different regions (enzyme and substrate zones) and had no PET covering. The enzyme zone was prepared by depositing PVAm (0.5 wt%)/silica/AChE/silica layers in the order described, while the substrate zone was prepared by depositing silica/indoxyl acetate/silica layers. All layers were deposited by hand using a microliter volume pipette. After depositing the reagents, the sensor was allowed to dry for at least 1 h in air at room temperature.

Measurement of pesticides using reagentless paper-based lateral flow assays

The bidirectional sensor assay was carried out as previously reported.¹ The uni-directional assay involved placing the sensor into the sample (0.5 cm in depth in a 10 mL Falcon tube cap) at an angle of 15° with respect to the solution surface with the valve in the "open" position. The solution reached the enzyme zone *via* the "fast" channel much sooner than the solution in the "slow" channel. This allowed for the wetting of the enzyme zone with pesticide prior to the substrate reaching the enzyme zone, allowing preincubation of the enzyme. Once the enzyme zone was fully wetted (~2 min), the valve was moved to the "closed" position (pushing the flap valve back) stopping the flow of solution from the "fast" channel to the enzyme zone. Solution flow continues in the "slow" channel, through the substrate zone and into the pre-wetted enzyme zone for detection (~8 min). Once the substrate had reached the enzyme zone, the sensor was removed from solution and allowed to dry for 5 min before being analyzed.

Data analysis

The inhibitory effect of malathion was evaluated on the sensor by measuring the decrease in the intensity of the blue color

produced by AChE catalyzed hydrolysis of indoxyl acetate. Images were obtained using a Canon A630, 8.0 MegaPixel camera operated in automatic mode with no flash and using the macroimaging setting. Images were analyzed using ImageJ software. Images were first inverted and then color intensity was split into a 256 bit color scale, with white corresponding to a color intensity of zero and black corresponding to 256. Using this scale, increases in the amount of blue color cause an increase in color intensity. To account for variations in color intensity owing to differences in environmental illumination, a background subtraction (color intensity of the paper surface closest to the sensing area) was done for each data point.

Monitoring the weight of paper strips

Whatman filter paper was cut into 12 cm × 2.5 cm strips. Cover slips of the same dimensions were prepared. The device was assembled by sandwiching a filter paper strip between two cover slips and clipping it on top using a paper clip. The test liquid, *i.e.* water or silicone oil, was poured into a Petri dish and placed on a scale (Mettler Toledo PB303-S). The balance was then zeroed and the paper device was suspended above the Petri dish and dipped vertically into the liquid. Each experiment was captured by a video camera and the time and the reading of the scale were recorded. From the data retrieved, the weight of liquid taken up by the device as a function of time and distance was determined, and corrected for any changes in weight obtained over the same time interval without the uptake of the liquid by the paper strip.

Results and discussion

Dynamics of fluid rise: experimental behaviour and modelling

The application of non-porous surface covers on paper not only prevents the evaporation of liquid but also provides extra capillary driving force for the liquid to quickly wick along the paper without the need for an external pump. Fig. 2 shows the arrangement of a paper strip and two PET (polyethylene terephthalate) films to produce a "fast" channel, and the method by which the paper is introduced to the sample solution. The "fast" channel had PET films on the top and bottom surfaces of the paper. The covered paper strip was then dipped into the water at an angle α ; 0.5 cm of the paper strip was submerged in water. To perform the experiments over a wide range of slip angles we made a simple device, as shown in Fig. 2(b). The side screws allow for easy adjustment of the angle of the plastic plate on which the paper strip was laid.

A side view of a paper strip sandwiched between two PET film covers is shown in Fig. 3. The picture was captured using the camera on the contact angle measurement instrument. The gap between the PET film slides and paper (grey area) was measured. The gap between the paper surface and the PET film was 0.9 mm for the film at the top and 0.7 mm for the film at the bottom.

A comparison of the rate of water flow on paper strips with and without the PET film covers is shown in Fig. 4. The results shown for each case are the average of four experiments. Paper strips with film cover slips demonstrated significantly faster flow (7 cm in <150 s) when compared with paper strips with no cover (7 cm in >2000 s), as shown in Fig. 4.

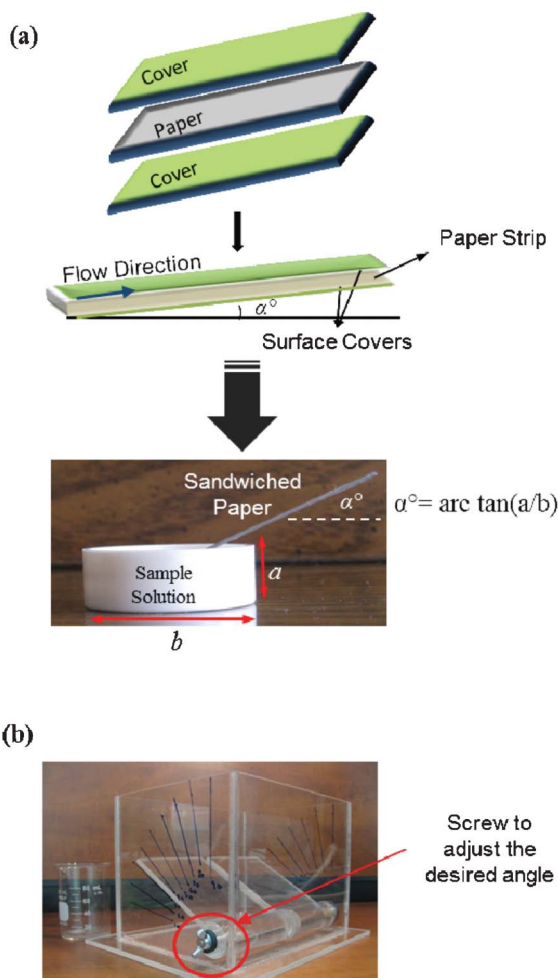


Fig. 2 Diagram of experimental setup. (a) The paper strip was placed between two surface covers (PET film slides). The paper with the covers was then dipped in water at a slip angle of α . (b) The simple device we made to control the slip angle; the screw in the side is used to adjust the exact desired slip angle.

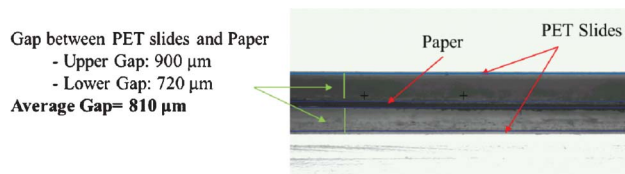


Fig. 3 Side view of the paper strip with PET film surface covers. The dark band in the middle of the picture is the paper strip. The grey bands are the gaps between the paper strip and the PET film slide.

Fig. 4 also reveals that for the uncovered paper, the height of the liquid changes with time (t) according to $t^{1/2}$, as predicted by the Lucas–Washburn equation^{24,25} for a fully wettable surface:

$$h(t) = \left(\frac{\gamma D t}{4\eta} \right)^{\frac{1}{2}} \quad (1)$$

where γ is the surface tension of the fluid, D is the effective pore diameter of the medium where flow is taking place and η is the dynamic viscosity of the fluid.

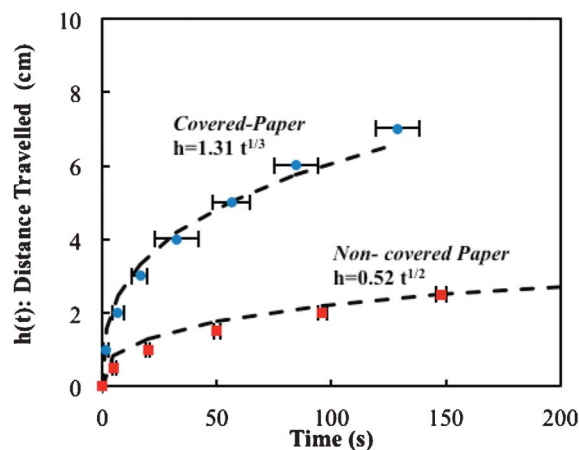


Fig. 4 Comparison of water penetration distance in the paper strip as a function of time for paper strips with no cover (■), paper strips with PET film covers (●). All of a size of 8 cm × 2.5 cm in a vertical position. Four repeats were conducted for each case and the figure shows the average of the repeats. Error bars represent the standard deviation of four measurements. Dashed lines represent the best fitted curves to the experimental data, and equations beside them show the relation of h (cm) to t (s) of the best fitted curves for each case.

For the covered paper, the height of the liquid changes with $t^{1/3}$, a dependence associated with capillary flow in wedges of various geometries,²³ and observed in an experimental system consisting of a glass plate covered with a flexible polypropylene film.²⁰ In that study, it was found that the height of the liquid scales with time according to:

$$h(t) \sim \left(\frac{\gamma^2 t}{\eta \rho g} \right)^{\frac{1}{3}} \quad (2)$$

where ρ is the density of the fluid and g is the acceleration of gravity. To test this relationship with our system, Whatman #1 paper was covered with three different flexible films, each with different water contact angles (θ): PET film with $\theta = 42.7^\circ$; tape-backside (consists of sticking two pieces of adhesive Clear Tape together and using the non-sticking surface to cover the paper) with $\theta = 84.6^\circ$; and Parafilm® M with $\theta = 104^\circ$. The device was assembled by sandwiching a filter paper strip between two cover slips, clipped on top using a paper clip, and hung vertically above the liquid container. We tested each of the three paper strips–flexible film combinations with three different fluids, to cover a range of surface tensions and viscosities: water ($\gamma = 0.072 \text{ N m}^{-1}$, $\eta = 0.849 \text{ mPa s}$) and two silicon oils with the same surface tension ($\gamma = 0.021 \text{ N m}^{-1}$) but different viscosities ($\eta = 5 \text{ mPa s}$ and $\eta = 20 \text{ mPa s}$). Fig. 5a shows the evolution of the height of the liquid as a function of time, for every combination of flexible film and fluid. Fig. 5b shows the experimental data plotted according to the relationship given by eqn (2). The results show that: (1) for a particular fluid, the contact angle of the film used to cover the paper strip has a negligible effect on the rate at which the liquid rises. This is consistent with the scaling law (eqn (2))—note that all surfaces used were fully wettable; (2) for all experiments, the height of the liquid scales with $t^{1/3}$, as shown by the linearity of all data sets in Fig. 5b; (3) the dependence of the rise rate on the viscosity of the fluid is well captured by the

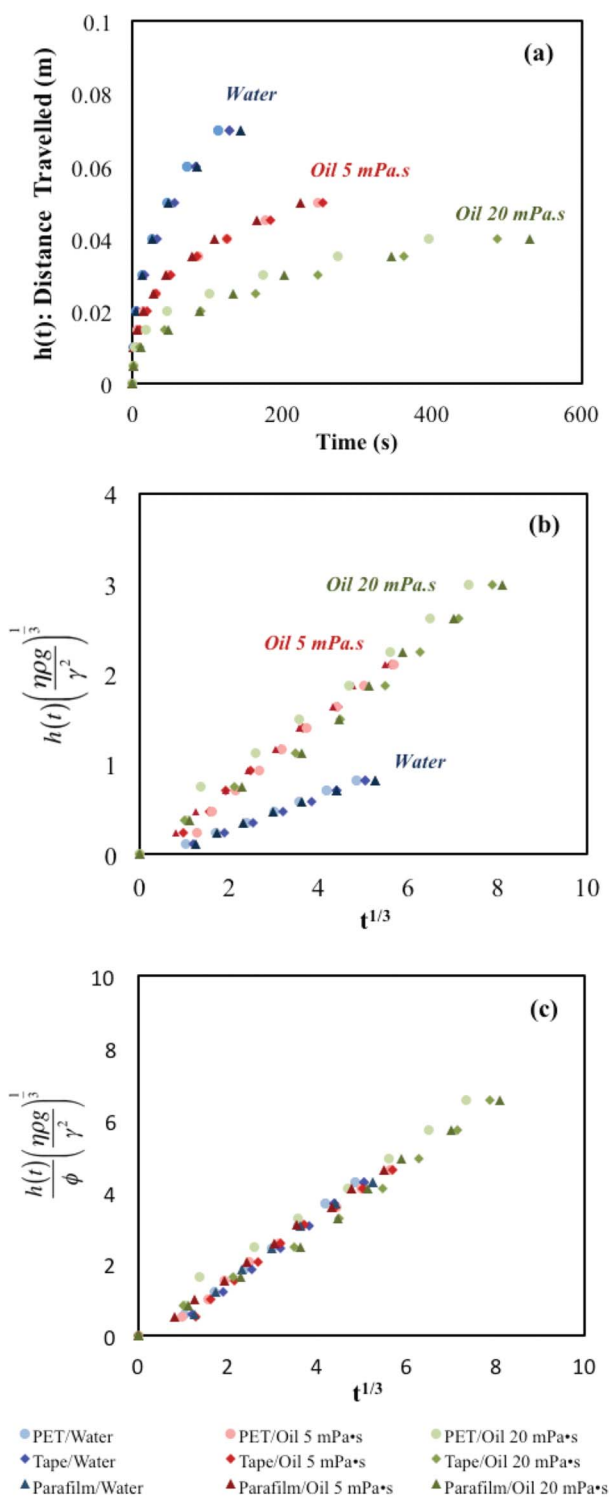


Fig. 5 Evaluation of the scaling law using multiple flexible films and multiple fluids. (a) Height of the liquid as a function of time. (b) Plotting the data using the scaling law given by eqn (2). (c) Introducing the effect of drainage (ϕ) into the scaling law, as given by eqn (4) (ρ , γ and η are density, surface tension and viscosity of the fluid, and g is the acceleration of gravity).

scaling law, since the scaled data sets for the two different silicon oils fall virtually identically (Fig. 5b); (4) The scaling law does not capture the differences observed in the experiments with water and oil. We hypothesized that this was due to a different

split between the volume of fluid in the gap between the paper surface and the flexible film (we define this gap as having a length δ) and the total volume of fluid imbibed in the paper. Liquids with different surface tensions, such as water and oil, should result in gaps of different sizes and thus a different total volume of liquid should be associated with a given height for these different liquids. The split in volume can be determined using a simple material balance that relates how a similar volume of liquid results in a different observed liquid height, as the liquid distributes between the gap (of length δ), and the paper (with a thickness L and paper porosity ε). The result of the material balance (noting that the paper is covered on both faces) can be expressed in terms of a drainage coefficient ϕ :

$$\phi = \frac{2\delta}{2\delta + \varepsilon L} \quad (3)$$

If glass is used as the support,^{20,23} then $\varepsilon = 0$ and the drainage coefficient is equal to 1. This means that the totality of the volume of liquid taken up is associated with the gap of length δ . If paper is used, (for Whatman #1 $\varepsilon = 0.74$, measured using standard porosimetry), part of the liquid taken up will be imbibed in the paper and this will result in an observed height lower than for a non-porous support. In fact, it will be lower by a factor equal to ϕ . The key assumption in this approach is that the time scale associated with full penetration of the fluid into the paper is much smaller than the time scale associated with liquid rise (*i.e.* the paper gets fully wet at a particular height, as soon as the liquid in the gap reaches that height). This assumption was tested using eqn (1) and calculating the time (t) that it takes a fluid to fully penetrate half of the thickness of the paper (the paper is covered on both sides, also the reason why the factors of 2 appear in eqn (3)). For Whatman #1 paper, half of thickness = $90 \mu\text{m}$ and the average pore size (D) is $1 \mu\text{m}$. For water, this time is 9.5×10^{-5} s and for the oils used in this work, this time is less than 0.04 s. The time scale for penetration is thus much lower than the time scale associated with liquid rise (tens of seconds, Fig. 5a). The drainage coefficient can be incorporated into the scaling law, leading to:

$$h(t) \sim \phi \left(\frac{\gamma^2 t}{\eta \rho g} \right)^{1/3} \quad (4)$$

The drainage coefficient can be experimentally determined by monitoring the weight of a paper strip as a function of time with and without flexible film covers, as described in the experimental section. For water and using the different films, $\phi = 0.19 \pm 0.02$ ($n = 20$), with very small variations in this parameter with time and type of film, as indicated by the small standard deviation. For the two different oils and different films, $\phi = 0.46 \pm 0.02$ ($n = 10$), again with small variations with time and type of film. The lower value for the drainage coefficient associated with water was expected, as water has a higher surface tension leading to a smaller gap, hence a smaller total volume of liquid will be associated with a given height of liquid. The length of the gap can be estimated using the drainage coefficients and eqn (3), resulting in $\delta = 82 \pm 1.6 \mu\text{m}$ for water and $\delta = 123 \pm 5 \mu\text{m}$ for oil. Note that these values are smaller than those shown in Fig. 3,

since in the figure the paper was dry and the values above were calculated with the gap filled with liquid in contact with wet paper. In Fig. 5c, we plot the experimental data scaled with eqn (4), where the entire data set (all possible combinations of three different flexible films with three different fluids) can be explained with a single relationship.

In the next section, we use the PET flexible films as part of a sensor and the effect of the inclination of the paper (slip angle) on the rise rate of the liquid is evaluated (Fig. 6), since a high dependence of the behaviour of the system on the angle would make it practically unusable. The dipping angle affects the contribution of gravity to the overall force balance that drives the flow of water. Lower slip angles produced faster flow (7 cm with slip angle of 10° in <50 s) when compared with paper strips operated at higher slip angles (7 cm with slip angle of 45° in >100 s); Working with a slip angle less than 15° reduced the simplicity of handling the device; thus $\alpha = 15^\circ$ is the suggested slip angle for having both the advantage of high velocity and simplicity of operation. However, during the initial stage of the lateral flow experiment (first ~ 20 s), the acceleration is only very weakly dependent on the angle, hence inclination has only a small effect for reasonably small travel distances (less than 4 cm).

In addition, based on the proposed model, another way to control the flow in the sensor could be to either increase the thickness of the paper, which will slow down the fluid due to a smaller value for the drainage coefficient; or decrease the thickness of the paper or the depth of the porous region, which will accelerate the fluid and increase flow because the drainage coefficient will increase.

Application to paper based sensors

Use of flexible films is easily applicable to any paper-based sensor where flow acceleration is required. Since PET is easily available, easy to manipulate and inexpensive (Canadian \$37.45 for a $40'' \times 25'$ roll), we used it as a part of a paper based sensor for pesticide detection.

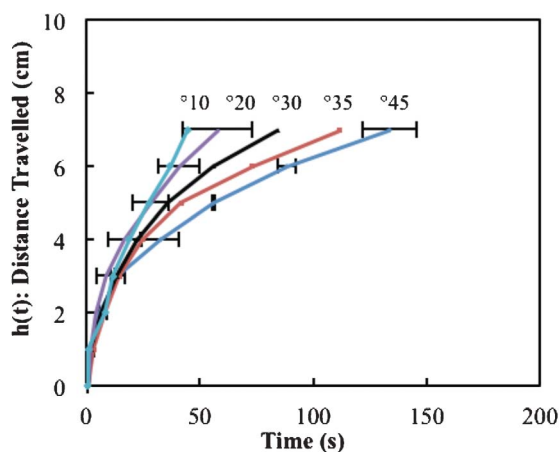


Fig. 6 Water flow distance as a function of time for PET film-covered paper strips at different slip angles of 10° , 20° , 30° , 35° and 45° . Four repeats were conducted for each case and the figure shows the average of the repeats. The plot includes the standard deviation for two experiments, to improve readability.

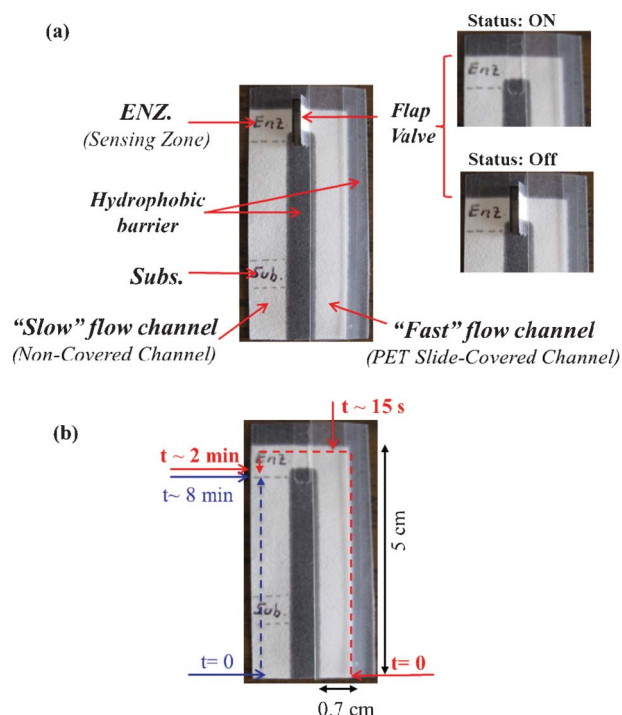


Fig. 7 Paper sensor for detection of pesticides with cover slip modification. (a) Sensor components: two channels were separated by a hydrophobic barrier. The right channel was covered by PET films, creating a “fast” channel. A valve was created to control the flow from the covered area to the uncovered area. Substrate and enzyme were applied on the uncovered side. (b) Time profile (t): initially the liquid diffuses to both covered and non-covered channels; after 15 s it passes through the covered channel and reaches the valve position; after 2 min the enzyme zone would be fully wet and the valve is moved to the “closed” position. On the other hand, the solution is passing slowly through the non-covered channel and substrate zone, and arrives in the pre-wetted enzyme zone around 8 min from the starting time.

Fig. 7 shows a top-view image of the pesticide sensor modified with wax separator and the PET cover slip on the right side of the paper channel providing the “fast” channel, so that, the detection of pesticides can be achieved in a shorter period of time and without the need to invert the sensor.

Fig. 8 shows a semi log plot of the dose-dependent inhibition response of malathion. The insets show images of the paper strips at each inhibitor concentration and clearly show a decrease in blue color intensity with increasing inhibitor concentration. Our data as previously reported suggest that an increasing concentration of malathion progressively inhibits the activity of AChE. The IC_{50} value for malathion (50% inhibition), calculated by fitting the data to the Hill equation (SigmaPlot 2011), was found to be 276 nM and 289 nM for the original and modified sensor, respectively. In addition, the limit of detection (concentration corresponding to the signal that was 3 standard deviations below the mean signal from the blank) of malathion was found to be 75 nM and 78 nM for the original and modified sensor, respectively. The results obtained from the modified sensor were comparable with the original sensor. Thus, the addition of the cover slip accelerator did not affect the sensitivity of the sensor, while decreasing the time needed for detection by two-fold.

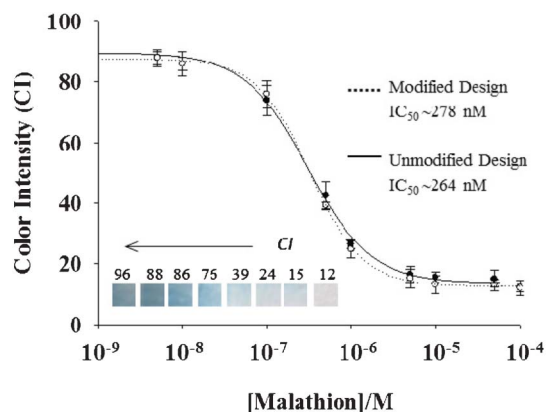


Fig. 8 Plot of dose-dependent inhibition of acetylcholinesterase (AChE 500 U mL⁻¹) by various concentrations of malathion. Insets are the color intensity (CI) at each malathion concentration. All points are means (\pm the standard deviation) of three measurements for each concentration. The solid line represents the bidirectional lateral flow sensor, whereas the dotted line represents the uni-directional lateral flow sensor.

Conclusions

Cover slips have been used to fabricate an accelerator for paper-based microfluidic analytical devices. Sandwiching the paper channel between two polyester films increases the elution distance and accelerates the capillary wicking process more than ten times compared to capillary flow through non-covered paper. The basis for this behaviour is deformation of the flexible film by capillary forces and formation of a wedge at the front of the liquid, where the height of the liquid increases with $t^{1/3}$. This dependence was demonstrated using three different flexible films (PET, Clear Tape back-side and Parafilm® M) and with three different fluids (water and two silicon oils). An advantage of using covered paper as the accelerator is that it provides a way to control and increase the flow rate and also the possibility of having different flow velocities in paper-based devices without the use of external energy. Another advantage of using PET films is that these devices can be fabricated with basic tools without compromising the simplicity, low cost, or ease-of-use that are characteristic of paper-based devices. This accelerator technology allows the user to prioritize tests based on the required incubation time of the reaction and could also be used to control a time sensitive sequence of fluid movements for an assay.

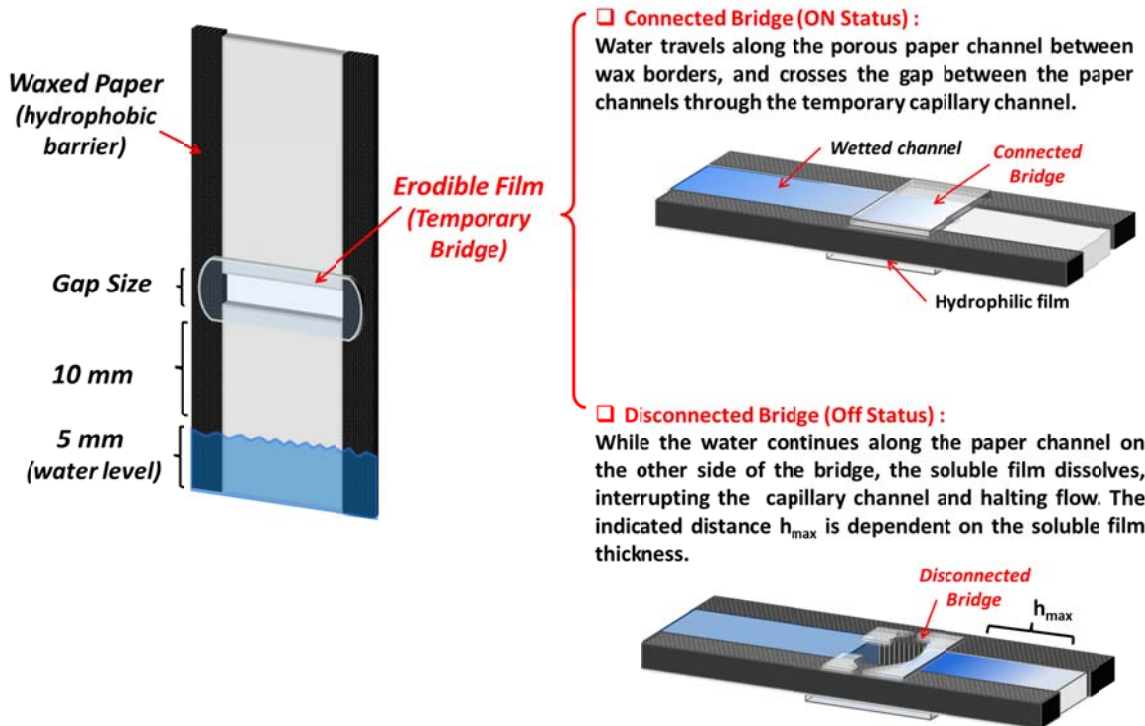
Acknowledgements

The authors thank the Natural Sciences and Engineering Research Council of Canada for funding this work through a Network Grant - SENTINEL Canadian Network for the Development and Use of Bioactive Paper. The authors wish to thank Dr Kari Dalnoki-Veress for valuable discussions on this work. The authors also thank the Canada Foundation for Innovation and the Ontario Innovation Trust for support of this work. R.P. holds the Canada Research Chair in Interfacial Technologies. J.D.B. holds the Canada Research Chair in Bioanalytical Chemistry and Bionterfaces.

References

- S. M. Z. Hossain, R. E. Luckham, M. J. McFadden and J. D. Brennan, *Anal. Bioanal. Chem.*, 2009, **81**, 9055–9064.
- X. Li, J. Tian and W. Shen, in *63rd Appita Annual Conference and Exhibition*, Melbourne, 2009, pp. 19–22.
- S. M. Z. Hossain and J. D. Brennan, *Anal. Chem.*, 2011, **83**, 8772–8778.
- W. Lewis, E. Keshavarz-Moore, J. Windust, D. Bushell and N. Parry, *Biotechnol. Bioeng.*, 2006, **94**, 625–632.
- S. Su, R. Nutiu, C. D. M. Filipe, Y. Li and R. Pelton, *Langmuir*, 2007, **23**, 1300–1302.
- R. Pelton, *TrAC, Trends Anal. Chem.*, 2009, **28**, 925–942.
- X. Li, J. Tian and W. Shen, *Anal. Bioanal. Chem.*, 2010, **396**, 495–501.
- K. Abe, K. Suzuki and D. Citterio, *Anal. Chem.*, 2008, **80**, 6928–6934.
- A. W. Martinez, S. T. Phillips, M. J. Butte and G. M. Whitesides, *Angew. Chem., Int. Ed.*, 2007, **46**, 1318–1320.
- E. Carrilho, A. W. Martinez and G. M. Whitesides, *Anal. Chem.*, 2009, **81**, 7091–7095.
- A. W. Martinez, S. T. Phillips, G. M. Whitesides and E. Carrilho, *Anal. Chem.*, 2009, **82**, 3–10.
- M. Al-Tamimi, W. Shen, R. Zeineddine, H. Tran and G. Garnier, *Anal. Chem.*, 2011, **84**, 1661–1668.
- M. M. Ali, S. D. Aguirre, Y. Xu, C. D. M. Filipe, R. Pelton and Y. Li, *Chem. Commun.*, 2009, 6640–6642.
- S. M. Z. Hossain, R. E. Luckham, A.-M. Smith, J. M. Lebert, L. M. Davies, R. H. Pelton, C. D. M. Filipe and J. D. Brennan, *Anal. Chem.*, 2009, **81**, 5474–5483.
- S. M. Z. Hossain, C. Ozimok, C. Sicard, S. D. Aguirre, M. M. Ali, Y. Li and J. D. Brennan, *Anal. Bioanal. Chem.*, 2012, **403**, 1567–1576.
- J. L. Osborn, B. Lutz, E. Fu, P. Kauffman, D. Y. Stevens and P. Yager, *Lab Chip*, 2010, **10**, 2659–2665.
- E. Fu, B. Lutz, P. Kauffman and P. Yager, *Lab Chip*, 2010, **10**, 918–920.
- E. Fu, S. A. Ramsey, P. Kauffman, B. Lutz and P. Yager, *Microfluid. Nanofluid.*, 2011, **10**, 29–35.
- X. Li, J. Tian, T. Nguyen and W. Shen, *Anal. Chem.*, 2008, **80**, 9131–9134.
- T. Cambau, J. Bico and E. Reyssat, *Europhys. Lett.*, 2011, **96**, 24001.
- L. H. Tang and Y. Tang, *J. Phys. II*, 1994, **4**, 881–890.
- F. J. Higuera, A. Medina and A. Linan, *Phys. Fluids*, 2008, **20**, 102102.
- A. Ponomarenko, D. Quere and C. Clanet, *J. Fluid Mech.*, 2011, **666**, 146–154.
- R. Lucas, *Kolloid-Z.*, 1918, **23**, 15–22.
- E. Washburn, *Phys. Rev.*, 1921, **17**, 273–283.

Chapter 3 Automatic Flow Shut-Off Valve for Paper-Based Microfluidics Devices



20 Word Summary:

Water-soluble pullulan films as time dependent valves in paper-based microfluidics and their use in enzymatic assays for pesticide detection.

In Chapter 3, all experiments were performed by myself with the help of Aleah Henry and Kevin Pennings who worked with me as undergraduate students, and Vincent Leung. Dr. Clemence Sicard a postdoc fellow of Prof. Brennan gave many helpful assistance in sol-gel preparation. Prof. Filipe and Prof. Pelton gave many helpful suggestions on both experiments and data analysis. I initiated the first draft of the paper. Prof. Filipe, Prof. Pelton, and Prof. Brennan helped in revising the draft to final version. This work has been published in Lab Chip, 2014, 14, 229–236. DOI: 10.1039/c3lc50762a. . It is produced by permission of The Royal Society of Chemistry.

URL: <http://pubs.rsc.org/en/content/articlelanding/2014/lc/c3lc50762a#!divAbstract>

Paper-based microfluidics with an erodible polymeric bridge giving controlled release and timed flow shutoff†

 Cite this: *Lab Chip*, 2014, 14, 229

 Sana Jahanshahi-Anbuhi,^a Aleah Henry,^a Vincent Leung,^a Clémence Sicard,^b Kevin Pennings,^a Robert Pelton,^a John D. Brennan^{*b} and Carlos D. M. Filipe^{*a}

Water soluble pullulan films were formatted into paper-based microfluidic devices, serving as a controlled time shutoff valve. The utility of the valve was demonstrated by a one-step, fully automatic implementation of a complex pesticide assay requiring timed, sequential exposure of an immobilized enzyme layer to separate liquid streams. Pullulan film dissolution and the capillary wicking of aqueous solutions through the device were measured and modeled providing valve design criteria. The films dissolve mainly by surface erosion, meaning the film thickness mainly controls the shutoff time. This method can also provide time-dependent sequential release of reagents without compromising the simplicity and low cost of paper-based devices.

 Received 25th June 2013,
Accepted 3rd October 2013

DOI: 10.1039/c3lc50762a

www.rsc.org/loc

Introduction

The recent literature describes many paper-based microfluidic devices for point-of-care diagnostics,^{1,2} food safety^{3,4} and water quality monitoring.^{5,6} The most compelling examples function without instrumental or electronic support – ideal for emergency and resource limited situations.⁷ Like the classic glucose sensor⁸ and some current home pregnancy test kits, many tests involve simple lateral-flow assays that include sequential reactions. However, potentially interesting paper-based assays, such as ELISA assays,⁹ involve more complex sequences that are not easily implemented as one-step dip and read operations on paper. For example, we recently described a sensitive pesticide sensor that functions by exposing an immobilized enzyme, acetylcholinesterase (AChE), to the test solution for a fixed time. In a second step, the immobilized enzyme is treated with indophenyl acetate solution, a color producing substrate for the enzyme.³ Pesticides present in the test sample bind to and deactivate AChE, preventing color generation.

The first prototype of our pesticide sensor was clumsy, labour intensive and required some user skill. The paper sensor strip was first exposed to the test liquid for a fixed time, after which it was dried. In the second step, lateral flow

was used to carry the substrate³ to the enzyme layer. In this assay, enzyme deactivation by pesticides in the test liquid and the subsequent generation of color (or lack of it) are time dependent, requiring careful control. On the other hand, the ideal implementation of the pesticide sensor would simply involve dipping one end of a paper strip in the test liquid. After a fixed time the user would then read the color output either qualitatively or possibly more accurately with a scanner or cell phone camera.

Two innovations were required to achieve a more useful format for our pesticide sensor. First we needed a way to sequentially bring two separate liquid streams to the enzyme test zone on the paper sensor. For this, two separate channels were employed – a fast channel that brings test liquid to the enzyme zone first, followed by a slow channel that carried the color producing substrate to the enzyme after a set incubation time.

The second innovation required, and the subject of this paper, was a shutoff valve that stopped the fast channel flow after a fixed time, giving the enzyme zone a chance to dry and accept substrate solution from the slow channel. The fast channel design was described previously and consists of a paper channel sandwiched between hydrophilic films.¹⁰ The shutoff valve was a flap valve that needed to be manually actuated. However, this required that a user intervene in the assay at an appropriate time, making the assay less user-friendly and more prone to human error.

Several valve types have been proposed for paper-based microfluidics. Chen *et al.*¹¹ described a non-return valve (fluidic diode valve), created by strategically patterning hydrophilic regions with and without surfactants, and separating these

^a Department of Chemical Engineering, McMaster University, 1280 Main Street West, Hamilton, ON L8S 4M1, Canada. E-mail: filipec@mcmaster.ca; Fax: +1 905 521 1350; Tel: +1 905 525 9140 (ext. 27278)

^b Department of Chemistry & Chemical Biology, McMaster University, 1280 Main Street West, Hamilton, ON L8S 4M1, Canada. E-mail: brennanj@mcmaster.ca; Tel: +1 905 525 9140 (ext. 20682)

† Electronic supplementary information (ESI) available. See DOI: 10.1039/c3lc50762a

regions with hydrophobic areas. Fluid flow occurs only from the region containing surfactant (the anode) to the region not containing surfactant. The effect of the surfactant on the surface tension is the driving force directing the flow. This design is capable of forming complex circuits within paper, but it does not function as a shutoff valve. Li *et al.*¹² described a magnetic timing valve using a resistor and an electromagnet that triggers a cantilever valve. However, the incorporation of a resistor and an electromagnet increases the complexity of the device. A number of authors have described timed-opening valves based on filling the paper pores with hydrophobic material^{13,14,17} such as paraffin wax or with a water-soluble barrier^{15,16} such as sucrose or trehalose, to provide additional resistance to flow. These temporary barriers delay fluid movement through the channel and allow the user to control the flow rate of the fluid. The flow rate is determined mainly by the barrier thickness, and increasing this factor leads to a reduction in flow rate. While this method of flow control works well for delaying flow, it is insufficient for cases in which different fluids must be delivered to the same space sequentially, as the first sample will not dry and consequently blocks the next fluid from entering the space. Yager and coworkers¹⁶ recently reported a barrier composed of sucrose which delays the flow through a paper channel. The timing of the delay is tuneable based on the amount of sucrose that is added. This flow control method allows for sequential reactions, however, the essential flow shut-off system is only provided by a limited sample supply (*via* source pads). While this is a viable method of metering, it requires more materials to construct each sensor and also increases the possibility of user error, such as an incompletely wetted source pad. A fluid disconnect is yet another type of valve based on the shape of the paper channels. The paper is shaped to have pathways/legs that are sequentially removed from the fluid to stop flow in that channel. These channels allow for multi-step processes, but require specific loading capabilities and cannot be used without a full well of sample.^{17,18} Although automated sequential delivery has been demonstrated in non-paper-based microfluidic devices,¹⁹ we have found very few examples of flow shutoff valves in paper-based devices that do not require electrical power or human intervention.^{20,21}

The essence of our shutoff valve is a pullulan film that dissolves as water flows past it. Pullulan is also the supporting film material used for commercial breath freshening strips; the good film forming properties and rapid dissolution characteristics required for breath strips are also ideal for microfluidic shutoff valves. Pullulan is produced from the fungus *Aureobasidium pullulans*, and is a non-ionic polysaccharide comprised of three linked maltose residues.²² The molecular weight of pullulan can be as high as 10^6 – 10^7 Da.²³ Pullulan is non-hygroscopic, thermally stable and biodegradable.²² In addition, pullulan has good oxygen barrier properties, providing a good encapsulation environment for oxygen sensitive reagents.

The following sections present experiments and models leading to design rules for the pullulan shutoff valves. Finally, we successfully demonstrate the use of the valve to

fully automate a previously reported paper-based organophosphate pesticide sensor.^{3,10}

Experimental section

Materials

Pullulan (MW ~100 000) was obtained from Sigma-Aldrich (Oakville, ON, Canada), citric acid was obtained from Caledon Laboratories Ltd. (Georgetown, ON, Canada), methoxy PEG 350 was obtained from Union Carbide Chemicals and Plastics Company (Danbury, CT, USA), ethyl alcohol (95%) was obtained from Commercial Alcohols (Brampton, ON, Canada), Brilliant Blue dye, Allura Red, Tartrazine and Methyl Orange were obtained from Sigma-Aldrich (Oakville, ON, Canada). Whatman #1 filter paper was used for all assays. Distilled deionized water with a resistance of 18.2 m Ω cm and <5 ppm total organic content was used in all assays. PET films (polyester film, 0.004" thick, clear, part # 8567k44) were purchased from McMaster-CARR (Hamilton, ON, Canada). Clear Tape (premium packaging tape, 48 mm \times 50 m, #99842) was purchased from GRAND & TOY. The wax printer used was a Xerox Phaser 8560. Acetylcholinesterase (AChE, from *Electrophorus electricus*, EC 3.1.1.7), indoxyl acetate (IDA), malathion, tris(hydroxymethyl)aminomethane, methanol (LC/MS grade), and Dowex 50WX8 cation exchange resin were obtained from Sigma-Aldrich. Sodium silicate solution was purchased from Fisher Scientific. Poly(vinylamine) (45 kDa) was obtained as a gift from BASF.

Solution preparation

500 mg of pullulan was dissolved in 10 mL of distilled water using a magnetic stirrer. Once fully dissolved, 120 mg of citric acid, 0.328 mL of methoxy PEG 350, and 0.15 mL of ethyl alcohol were added to the solution.²⁴ The solution was mixed until all components were dissolved. Films were created through a casting method. The solution was poured into a 3.5 cm diameter Falcon petri dish, and allowed to air dry for 24–48 hours. Different amounts of the pullulan solution, ranging from 1 mL to 7 mL, were cast into petri dishes to create different thicknesses in the resultant films.

Shutoff system assembly

Fig. 1 depicts the steps for assembling a shutoff system. A 2 mm \times 10 mm gap was cut in a 7.5 mm channel, ensuring that the gap width exceeded that of the channel. Following this, a strip of hydrophilic flexible film (can be: a PET transparency slide, or the non-sticky side of normal clear tape, *etc.*) was cut to the channel width or slightly wider. This was taped to one side of the channel so that the hydrophobic area and gap were completely covered by the flexible film. The entire device was then flipped over, and glue was applied on the section of the gap between the edge of the device and the hydrophobic channel as shown in Fig. 1. The pullulan film was then cut to an appropriate size, slightly larger than the

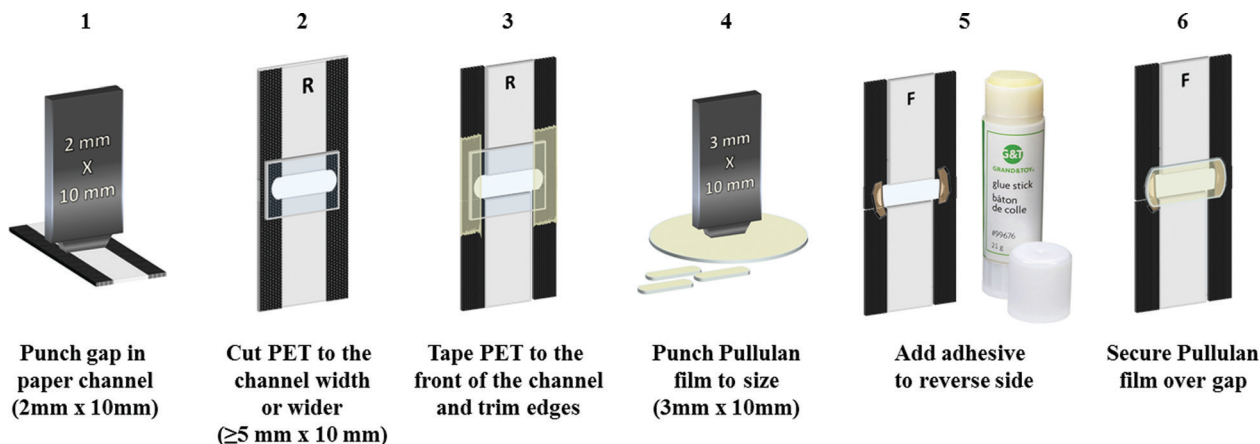


Fig. 1 Schematic of the flow shutoff system assembly. Letters “F” and “R” refer to front and rear side of the device, respectively.

gap,[‡] and placed over the gap. It was then pressed down to secure it to the paper channel.

For ease of cutting, two similarly shaped hole-punchers were made. The smaller hole-punch (~2 mm × 10 mm) was used for cutting the gap in the paper channel, and the larger hole-punch (~3 mm × 10 mm) was used to punch the pullulan films. The main advantage of the hole-punch is its ability to create reproducible and uniform samples. The construction process for the pullulan bridge device demonstrated here is performed at the lab scale. However, the process can be scaled up to produce greater quantities of the device (see the ESI[†] for a proposed scale-up process).

Dynamic viscosity measurement

The dynamic viscosity of the pullulan solutions was measured using a Fisherbrand uncalibrated glass Ubbelohde tube (#50). The experiments were conducted at 23 °C. 10 mL of water was added to the Ubbelohde tube and the time taken for the water to pass through the tube was recorded. This was used to determine the viscometer constant. Different concentrations of pullulan solutions: 41.6 g L⁻¹, 20.8 g L⁻¹, 8.3 g L⁻¹, and 4.2 g L⁻¹, were added to the Ubbelohde tube and the times for the solutions to pass through the tube were recorded and the viscosities were calculated.

Pesticide sensor construction

The sensing device was prepared as previously reported,³ with the flow shutoff system described in this paper constructed in place of the flap valve originally used, following the process illustrated in Fig. 1. Briefly, the sensors consisted of two channels of 0.7 × 0.5 cm linked by the flow shutoff system (using a 0.15 mm thick pullulan film). The channel on the right (fast flow) was covered on both sides of the filter paper with polyester film in order to increase the flow speed. The channel on the left (slow flow) was

constructed with a sensing zone and a substrate zone. The sensing zone was prepared by manually depositing PVAm (0.25% wt% in ddH₂O)/silica sol precursor (prepared as previously described^{3,25})/acetylcholinesterase (500 U ml⁻¹ in 100 mM Tris buffer pH 8)/silica sol precursor, while the substrate zone was prepared by manually depositing silica sol precursor/indoxyl acetate (3 mM in 100 mM Tris buffer pH 8 with 3% v/v methanol)/silica sol precursor.

Pesticide sensor testing

The assembled pesticide sensors were tested by exposing the bottom 5 mm of each channel to the sample solution (0–100 μM malathion in 100 mM Tris buffer pH 8). Similarly to the uni-directional design sensor previously described,³ the sample solution reaches the sensing zone first (in approximately two minutes) allowing incubation of the enzyme. Previously at that point users had to open the flap valve, whereas now the soluble pullulan film automatically dissolves and cuts off the flow to the sensing zone. The sample solution flow in the left channel continues, allowing the substrate to flow to the sensing zone. Once the sensing zone is fully wetted the sensor is removed from the solution and allowed to air dry. The test strips were then imaged using a handheld scanner (Flip Pal 100C mobile scanner). The color intensity of the sensing zone was quantified using ImageJ software. Images were inverted so that in the 256 bit color scale white corresponds to a color intensity of 0 and black corresponds to 256.

Results and discussion

Flow system

Pullulan films can be used in paper-based microfluidic devices as a flow shutoff system as shown in Fig. 2. The pullulan film acts as a dissolvable bridge, which is able to control the amount of liquid flowing past the gap. Before dipping the device in water, there is an air gap between the pullulan and PET films (see panel for time = 0). As the device is dipped in water, the capillary formed between these two films becomes filled with water, which initiates dissolution

[‡] The film needs to be long enough to slightly overlap the channel, and wider than the gap for gluing purposes.

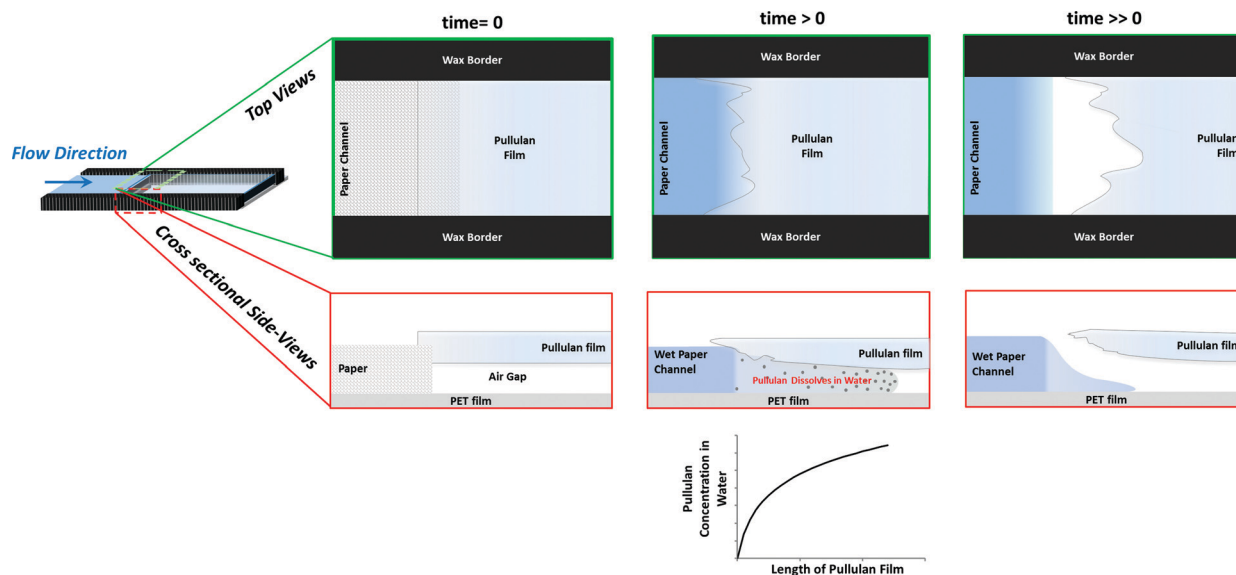


Fig. 2 Working principle of the pullulan dissolvable bridge showing the top and cross sectional side views. Initially, there is an air gap between the pullulan and PET films. As the water fills the gap, the pullulan dissolves with a faster rate in the initial part of the bridge since the pullulan concentration in the liquid is the lowest in this portion of the bridge. After some time, the pullulan film in the initial part of the bridge dissolves and the capillary gap between the pullulan and PET films is destroyed, stopping the flow.

of the pullulan film. According to the Noyes–Whitney equation,²⁶ the rate of dissolution is highest when the bulk solute (pullulan in this case) concentration is lowest, giving maximum driving force for dissolution. For our device, this happens when the water first meets the pullulan film (see panel for time > 0). The flow in the device stops when the capillary formed between the pullulan and PET films is destroyed due to complete dissolution of the pullulan bridge in the *z*-direction in the initial section of the pullulan bridge. Note that not all the pullulan in the bridge needs to be dissolved to stop the flow – just enough dissolution has to occur to destroy the capillary gap in the initial section of the bridge. Sequential dye release from the pullulan bridge, shown in Fig. III in the ESI† confirms that the bridge dissolves from the bottom upwards.

Fig. 3 shows the relationship between the thickness of the pullulan film and the distance of the liquid flow past the gap. In the pullulan shutoff system, due to the dissolution of the pullulan bridge the upper section of the paper channel is disconnected from the water source; and there is a linear relationship between the thickness of the film and the maximum distance travelled by the liquid. These results are in good agreement with the working principle depicted in Fig. 2. In the ESI† we describe how to cast films with well-defined thicknesses.

We also performed experiments (data not shown) to determine the effect of the widths of the paper channel and pullulan bridge on the behaviour of the device. The effect was found to be negligible, in agreement with the working principle depicted in Fig. 2, where flow switch off is solely dependent on the thickness of the pullulan bridge. No attempts were made to accurately control the size of the gap existing between the pullulan and PET films, since it has been shown by us¹⁰ and others²⁷ that the rate at which water moves between two fully wettable flexible surfaces does not depend on the distance

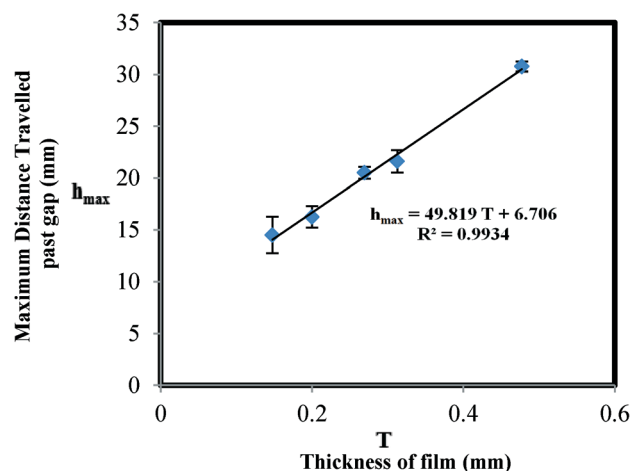


Fig. 3 Thickness of pullulan film vs. maximum distance water travelled past the gap. All experiments were performed at 21 °C and 48% RH. Four repeats were conducted for each case and the figure shows the average of the repeats. Error bars represent the standard deviation of the four measurements.

between the films at time zero. As the water moves due to capillary action, the films are deformed in response to the capillary force, resulting in the formation of a wedge at the front of the water, *i.e.* the capillary formed is self-controlled through a balance of capillary forces and the forces associated with the mechanical deformation of the films.

Data analysis and parameter extraction

Flow regime through the pullulan shutoff system considering evaporation, gravitational, and paper fibre water content effects. In this section, an appropriate model for predicting the meniscus height vs. time for water

passing through the pullulan-paper based shutoff system is considered.

The shutoff system can be divided into three separate sections: the *lower section*, the *bridge section*, and the *upper section*. The *lower section* starts from the very bottom of the paper strip and ends at the point just before the pullulan film. The *bridge section* refers to the gap in the channel where a capillary is formed between the PET film and the pullulan film. Finally, the *upper section* begins at the top edge of the pullulan film and continues to the top of the paper strip.

In the lower section, the water flow in the paper strip is the same as water flow through plain filter paper. This is expected since the lower section is made up of unmodified filter paper. Therefore, the water flow in the lower section follows a modified version of the Lucas–Washburn equation.²⁸

Fig. 4 depicts the experimental data of the water flow on Whatman #1 filter paper strips and shows the comparison between the traditional Lucas–Washburn model and the modified models adapted from N. Fries *et al.* 2008²⁹ and A. Rogacs *et al.* 2010.³⁰ The two modified models were further altered by taking into account the effect of the water content of the paper fibres.³¹ Cellulose fibres have a “fibre saturation point” that describes the water content in the pores of the fibre wall. The water in the pores is more difficult to evaporate because of capillary condensation. Due to this, the effect of evaporation cannot be viewed as binary, *i.e.* the paper is fully dry or the paper is fully wet. Depending on the relative humidity, paper can hold almost 10 w/w% water.³² The models proposed by N. Fries *et al.* in 2008²⁹ assumed the system to be binary, *i.e.* either wet or dry. This assumption leads to over-prediction of the capillary height rise rate.³¹ The adjusted model takes into account the water content of the paper fibres and is shown in Fig. 4.

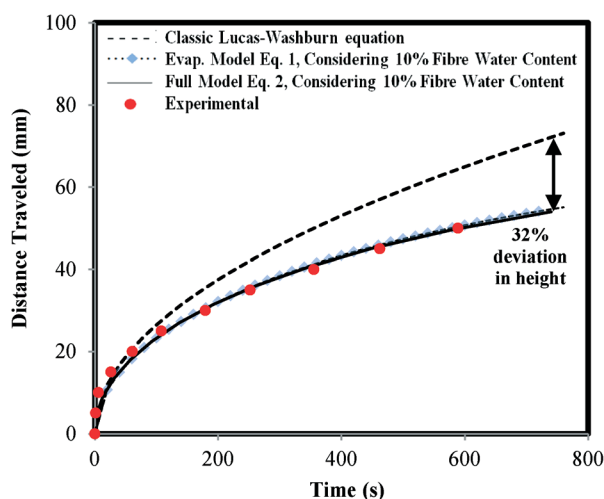


Fig. 4 Water flow distance in plain Whatman #1 paper strips as a function of time. Strip size was 8 cm (length) \times 2.5 cm (width). Experimental data (●), Lucas–Washburn equation (---), evaporation model considering 10% fibre water content (⋯◆⋯), and full model considering 10% fibre water content (—).

In the full model prediction,^{29,31} the effects of gravity, evaporation, and water content of the paper fibres have been incorporated into the traditional Lucas–Washburn equation:

$$t = (1 - w\%) \frac{1}{2B} \ln \left(\frac{Bh^2 + Dh + A}{A} \right) - \frac{D}{2B\sqrt{D^2 - 4BA}} \ln \left(\frac{(2Bh + D - \sqrt{D^2 - 4BA})(D - \sqrt{D^2 - 4BA})}{(2Bh + D + \sqrt{D^2 - 4BA})(D + \sqrt{D^2 - 4BA})} \right) \quad (1)$$

While in the evaporation model,^{30,31} the gravitational effect is neglected:

$$h(t) = (1 - w\%) \sqrt{\frac{A}{B} \exp(2Bt) - \frac{A}{B}} \quad (2)$$

Where:

$$A = \frac{2K\delta_{lv}\cos\theta}{R\mu\phi}, B = \frac{-\dot{m}_{\text{cvp}}}{2d\rho\phi}, D = \frac{-g\rho K}{\mu\phi}$$

where, h : distance travelled, t : time, $w\%$: fibre water content, K : permeability, θ : contact angle, R : average capillary radius, ϕ : porosity, μ : viscosity, δ : average paper thickness, ρ : density, g : gravitational constant, and δ_{lv} : surface tension. The evaporation rate of water at each relative humidity (RH) can be calculated by a correlation from the ASHRAE handbook, edition 2003,³³ as:

$$\dot{m}_{\text{cvp}} = (P_w - P_{\text{RH}}) \times (0.089 + 0.0782V_{\text{air}}) / Y \quad (3)$$

where, P_w : water saturated pressure, P_{RH} : partial pressure of water vapor, Y : heat of vaporization of water, and V_{air} : air flow velocity in the environment (zero in all cases we studied).

From Fig. 4, it can be seen that for paper strips shorter than 10 cm the gravitational effect can be neglected since the deviation of the evaporation model from the full model prediction is less than 0.5%. Thus, the evaporation model was chosen due to its simplicity in comparison to the full model. Furthermore, the evaporation model fits well with the data when the water content of the paper fibre is taken into account.

In the pullulan shutoff system, the water flow in the *upper section* is much slower than that in the *lower section*. This is due to the increase in viscosity as the pullulan is dissolved into the solution. Nevertheless, the evaporation model that was applied to the *lower section* can still be used to describe the flow in the *upper section*. The main difference between the two sections is the viscosity of the travelling liquid.

To estimate the pullulan concentration in the water after it passes over the pullulan bridge, a series of pullulan solutions of different concentrations were made. The viscosities of these solutions were measured using an Ubbelohde viscometer. The rate of capillary rise of these solutions on Whatman #1 filter paper was measured. As shown in Fig. 5, an increase in concentration leads to slower capillary rise. This is due to the increase in viscosity as the concentration of

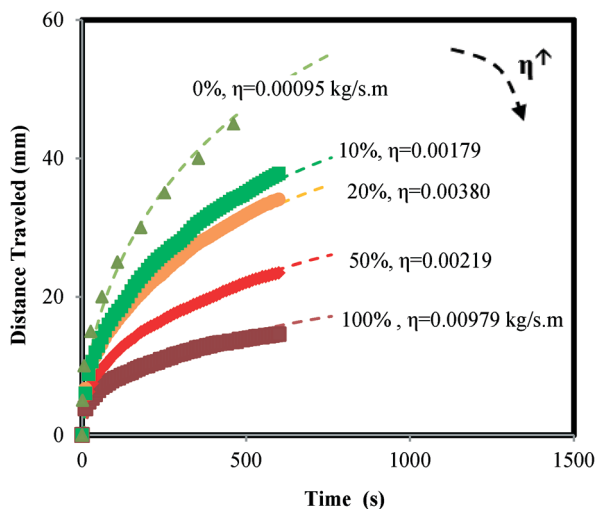


Fig. 5 Capillary rise flow rate through plain Whatman #1 filter paper, with a fluid sample of distilled water containing 0% (\blacktriangle), 10% (\blacksquare), 20% (\bullet), 50% (\blacklozenge), and 100% (\blacksquare) pullulan solution (the 100% solution contains 41.2 g L^{-1} pullulan as explained in the experimental section). In all cases, the dashed lines (---) represent the evaporation model prediction, and the solid markers are experimental data.

pullulan increases. Using the viscosities measured for each of the solutions, the evaporation model is fitted to the data. As shown in Fig. 5, the evaporation model adequately describes the data.

Additionally, the rate of water capillary rise through the pullulan shutoff system (Fig. 6) was compared with the

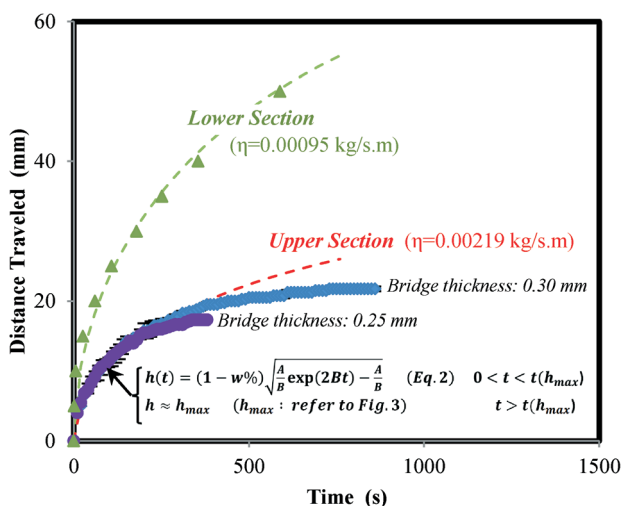


Fig. 6 Rate of water capillary rise through the pullulan shutoff system at $21 \text{ }^\circ\text{C}$ and $48\% \text{ RH}$. Dashed lines represent the evaporation model prediction in the lower (green) and upper (red) sections of the device, and the solid markers show experimental data in the lower section (\blacktriangle), and in the upper section while the film thickness of the pullulan bridge is 0.30 mm (\blacklozenge) and 0.25 mm (\bullet). Water flow through the upper section of the device behaves similarly to the rate of capillary rise of the 50% diluted pullulan solution through plain filter paper; this analogy lasts until the flow approaches to its maximum possible height when the upper section is severed from the water source as the pullulan bridge connection is dissolved.

results of Fig. 5. It can be seen that the rate of capillary rise for the 50% diluted pullulan solution (20.8 g L^{-1} pullulan) fits well with the data from water capillary rise through the upper section of the pullulan shutoff system. Therefore, it may be inferred that the solution in the upper section has a similar viscosity to that of the 50% diluted pullulan solution.

Fig. 6 compares rate of capillary rise of the lower and upper sections of the pullulan shutoff device. It also shows the evaporation model for both sections. In the upper section, it should be noted that the deviation which is observed after a specific height (dependent on pullulan film thickness) is due to the full dissolution of the pullulan bridge (refer to Fig. 3) which severs the upper section from the water source.

Application in a paper based sensor

Pesticide sensor with automatic flow shut-off. As with traditional 'lab-on-a-chip' devices, paper-based sensors can be viewed as a lab or a factory but on a paper network. The porous structure of the paper serves as pipes/pumps which supply reactants to the reaction area. Given this analogy, the pullulan shutoff system can be considered as a *pipette/meter on a chip*, which allows analytes to be loaded into the reaction media in controlled amounts. The pullulan shutoff system can be easily applied to any paper-based sensor where flow severing is required in order to program multi-step reactions. Since cast pullulan films are stable over a wide range of ambient temperature and humidity values ($\leq 45 \text{ }^\circ\text{C}$ and $99\% \text{ RH}$) and are fairly inexpensive (\sim Canadian $\$0.001 \text{ mm}^{-3}$ cast film), the system was evaluated as a part of a paper-based sensor for pesticide detection.

The pesticide sensor previously reported^{1,3} is based on the colorimetric detection of acetylcholinesterase (AChE) activity, which is known to be inhibited in the presence of organophosphate pesticides. The sensor exhibits a blue color change in the sensing region in the absence of inhibitors (organophosphate pesticides) in the sample solution, while in the presence of organophosphate pesticides the AChE activity is inhibited, and a dose-dependent decrease in the blue color intensity is observed. The intensity of the color change can be quantitatively analysed, correlating the concentration of pesticide in the sample to the intensity of the color generated.

To detect organophosphate pesticides the sensing (enzyme) zone first needs to be pre-incubated with the sample for at least 2 min prior to the addition of the substrate, as inhibition is time-dependent. The substrate is then introduced to the reaction area after the delay time to elicit a color change. In both of the previous designs the exact moment of when the sensing zone is fully wetted is determined by the user either (a) removing the sensor from the solution in the originally developed bi-directional design (so-called inverted lateral flow),³ or (b) manually switching off the flap valve in the uni-directional design.¹ These two previous designs relied on the user's ability to determine the moment when the enzyme zone was fully wetted, which may lead to inconsistent amounts of analyte loaded into the sensing zone and thus

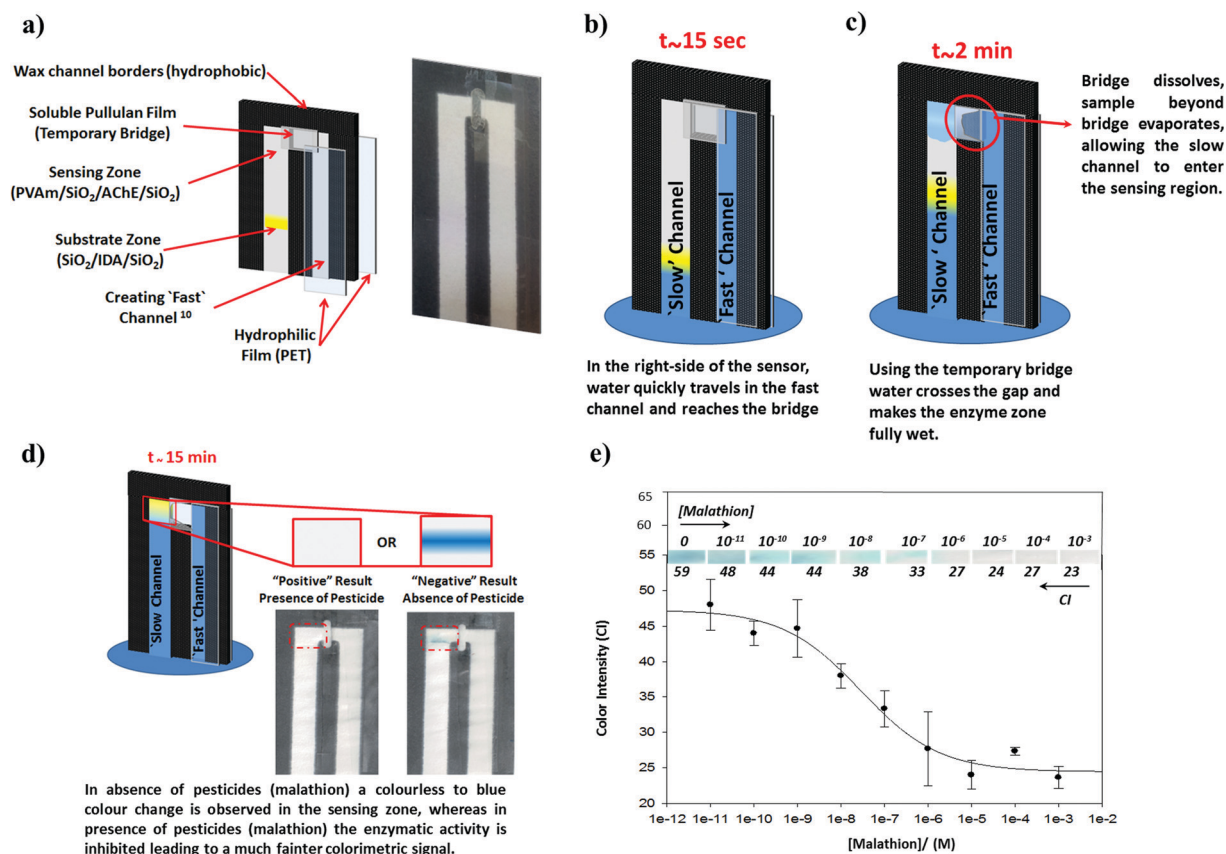


Fig. 7 A fully automated bioactive paper sensor for organophosphate pesticide detection. (a) Schematic illustration of the sensor construction (on the left), and an image of the actual device (on the right). The right side of the sensor is covered by PET film to create a 'fast' channel.¹⁰ An automatic shut-off system (temporary bridge) was created using a soluble pullulan film to control the flow from the covered "fast" channel to the uncovered "slow" channel on the left. A sensing zone (PVAm/SiO₂/AChE/SiO₂) and a substrate zone (SiO₂/IDA/SiO₂) were deposited on the uncovered "slow" channel. Following sample introduction, time-sequential schematics are shown as: (b) at around 15 s the sample passes through the "fast" channel and reaches the bridge position; (c) after 2 min the enzyme zone is fully wetted, and due to the dissolution of the soluble pullulan film the bridge automatically disconnects, enabling the sensing zone to dry, and (d) at around 15 min the solution moves through the non-covered "slow" channel and arrives in the pre-wetted enzyme zone and the color change is elicited after 5 min; the intense blue color on the right images was obtained with a Tris buffer solution which did not contain any pesticide, while the left image was obtained for a 10⁻⁵ M malathion sample. (e) Plot of dose-dependent inhibition of acetylcholinesterase (AChE) by various concentrations of malathion; three repeats were conducted for each concentration and all points are average of the repeats.

irreproducible quantitative results. In order to improve both the reproducibility and ease of use of the sensor, in the present design, the automatic shutoff bridge replaces the manual flap valve as demonstrated in Fig. 7.

In this new format, the pullulan temporary bridge-system severs the flow stream from the fast channel automatically and provides a consistent incubation time while allowing the sensing (enzyme) zone to be dried before the substrate arrives. This new format results in a simplified assay that detects the presence of pesticides automatically without any further manipulation from the user.

Fig. 7d illustrates both a positive and a negative test result for the pesticide sensor and Fig. 7e shows a semi logarithmic plot of the dose-dependent inhibition by malathion. As previously reported,^{3,10} an increasing concentration of malathion progressively inhibits the activity of AChE. The IC₅₀ value for malathion (*i.e.*, 50% inhibition) was 29 nM (calculated by fitting the four parameter Hill equation with SigmaPlot 10.0)

and the limit of detection (concentration corresponding to 3 standard deviations below the mean signal from the blank) was 6 nM. The obtained results were comparable with the original sensor. The reliable operation of the pesticide sensor indicates that the functionality of the previously reported sensor³ is not affected by the addition of an automatic flow shut-off system or the presence of the pullulan.

Conclusions

Pullulan, a rapidly dissolving polymer, has been used to fabricate an automatic flow shutoff system for paper-based microfluidic analytical devices. Replacing part of the paper channel with an interruptible capillary channel formed by a dissolvable film allows for automatic flow control through paper-based devices. This time dependent flow shutoff technology allows the user to manipulate fluid movement to cater to time sensitive or multi-step reactions and assays.

The construction of a modified organophosphate pesticide detector demonstrates that with an automatic flow shut-off system as presented, paper-based microfluidic devices are more useful for multi-process systems and timed reactions due to enhanced flow control, while remaining inexpensive, reliable and equipment-free to operate. In addition to serving as a flow shutoff system and possessing the ability to control fluid flow in the system, pullulan films can also be used for the delivery of reagents; reagents can be added to the pullulan films to provide time dependent reagent release. Not only the release of multiple reagents, but also the sequential release of reagents is possible using pullulan. These results will be reported in a separate manuscript.

Acknowledgements

The authors thank the Natural Sciences and Engineering Research Council of Canada for funding this work through a Network Grant-SENTINEL Canadian Network for the Development and Use of Bioactive Paper. The authors also thank the Canada Foundation for Innovation and the Ontario Innovation Trust for support of this work. R. P. holds the Canada Research Chair in Interfacial Technologies. J. D. B. holds the Canada Research Chair in Bioanalytical Chemistry and Biointerfaces.

Notes and references

- M. Hitzbleck, L. Avrain, V. Smekens, R. Lovchik, P. Mertens and E. Delamarche, *Lab Chip*, 2012, **12**, 1972–1978.
- P. Von Lode, *Clin. Biochem.*, 2005, **38**, 591–606.
- S. M. Z. Hossain, R. E. Luckham, M. J. McFadden and J. D. Brennan, *Anal. Chem.*, 2009, **81**, 9055–9064.
- J. Lankelma, Z. Nie, E. Carrilho and G. M. Whitesides, *Anal. Chem.*, 2012, **84**, 4147–4152.
- S. M. Z. Hossain, C. Ozimok, C. Sicard, S. D. Aguirre, M. M. Ali, Y. Li and J. D. Brennan, *Anal. Bioanal. Chem.*, 2012, **403**(6), 1567–1576.
- D. D. Liana, B. Raguse, J. J. Gooding and E. Chow, *Sensors*, 2012, **12**, 11505–11526.
- G. G. Lewis, M. J. DiTucci and S. T. Phillips, *Angew. Chem., Int. Ed.*, 2012, **51**, 12707–12710.
- J. Comer, *Anal. Chem.*, 1956, **28**, 1748–1750.
- A. Apilux, Y. Ukita, M. Chikae, O. Chailapakul and Y. Takamura, *Lab Chip*, 2013, **13**, 126–135.
- S. Jahanshahi-Anbuhi, P. Chavan, C. Sicard, V. Leung, S. M. Z. Hossain, R. Pelton, J. D. Brennan and C. D. M. Filipe, *Lab Chip*, 2012, **12**(23), 5079–5085.
- H. Chen, C. Jeremy, C. Anagnostopoulos and M. Faghri, *Lab Chip*, 2012, **12**, 2909–2913.
- X. Li, P. Zwanenburg and X. Liu, *Lab Chip*, 2013, **13**, 2609–2614.
- H. Noh and S. T. Phillips, *Anal. Chem.*, 2010, **82**, 4181–4187.
- H. Noh and S. T. Phillips, *Anal. Chem.*, 2010, **82**, 8071–8078.
- E. Fu, B. Lutz, P. Kauffman and P. Yager, *Lab Chip*, 2010, **10**, 918–920.
- B. Lutz, T. Liang, E. Fu, S. Ramachandran, P. Kauffman and P. Yager, *Lab Chip*, 2013, **13**, 2840–2847.
- B. Lutz, P. Trinh, C. Ball, E. Fu and P. Yager, *Lab Chip*, 2011, **11**, 4274–4278.
- E. L. T. Fu, P. Spicar-Mihalic, J. Houghtaling, S. Ramachandran and P. Yager, *Anal. Chem.*, 2012, **84**, 4574–4579.
- P. Novo, F. Volpetti, V. Chu and J. O. P. Conde, *Lab Chip*, 2013, **13**, 641–645.
- A. W. Martinez, S. T. Phillips, Z. Nie, C. M. Cheng, E. Carrilho, B. J. Wiley and G. M. Whitesides, *Lab Chip*, 2010, **10**, 2499–2504.
- H. Liu, X. Li and R. M. Crooks, *Anal. Chem.*, 2013, **85**, 4263–4267.
- M. R. Rekha and C. P. Sharma, *Trends Biomater. Artif. Organs*, 2007, **20**, 116–121.
- T. D. Leathers, *Biopolymers Online*, 2005, pp. 1–11.
- R. Mishra and A. Amin, *Indian J. Pharm. Educ. Res.*, 2010, **45**(1), 71–77.
- S. M. Z. Hossain, R. E. Luckham, A.-M. Smith, J. M. Lebert, L. M. Davies, R. H. Pelton, C. D. M. Filipe and J. D. Brennan, *Anal. Chem.*, 2009, **81**, 5474–5483.
- A. Noyes and W. R. Whitney, *J. Am. Chem. Soc.*, 1897, **19**(12), 930–934.
- T. Cambau, J. Bico and E. Reyssat, *Europhys. Lett.*, 2011, **96**, 24001.
- J. Hyväluoma, P. Raiskinmäki, A. Jäsberg, A. Koponen, M. Kataja and J. Timonen, *Phys. Rev. E: Stat., Nonlinear, Soft Matter Phys.*, 2006, **3**(73), 036705-1-8.
- N. Fries, K. Odic, M. Conrath and M. Dreyer, *J. Colloid Interface Sci.*, 2008, **321**, 118–129.
- A. Rogacs, J. E. Steinbrenner, J. A. Rowlette, J. M. Weisse, X. L. Zheng and K. E. Goodson, *J. Colloid Interface Sci.*, 2010, **349**, 354–360.
- D. A. Barry, J. Y. Parlange, D. A. Lockington and L. Wissmeier, *J. Colloid Interface Sci.*, 2009, **336**, 374–375.
- S. A. Reardon, M. R. Davis and P. E. Doe, *Tappi J.*, 2000, **83**(9), 58–79.
- American Society of Heating, Ashrae handbook. Heating, ventilating, and air-conditioning applications, in *Refrigerating and Air Conditioning Engineers*, Atlanta, GA, 2003.

Paper-based microfluidics with an erodible polymeric bridge giving controlled release and timed flow shutoff

Sana Jahanshahi-Anbuhi,^a Aleah Henry,^a Vincent Leung,^a Clémence Sicard,^b Kevin Pennings,^a Robert Pelton,^a John D. Brennan*,^b and Carlos D.M. Filipe*^a.

5

^aDepartment of Chemical Engineering, McMaster University, 1280 Main Street West, Hamilton, ON, L8S 4M1, Canada. Fax: (905) 521-1350; Tel: (905) 525 9140 (ext. 27278); E-mail: filipec@mcmaster.ca

^b Department of Chemistry & Chemical Biology, McMaster University, 1280 Main Street West, Hamilton, ON L8S 4M1, Canada. Fax: (905) 527-9950; Tel: 10 (905) 525-9140 (ext. 27033); E-mail: brennanj@mcmaster.ca

Supplementary Information

15 1. Proposed process to scale-up production of the pullulan shutoff system

In order to scale this process, it is necessary to have simple steps through which the channels can be created. Here a simple approach is proposed to create tens of pullulan shutoff systems quickly and easily. This process is illustrated step-by-step in Figure I as:

Step 1- Cut paper (Figure I-A): The initial step is to create holes in the paper (using a customized hole-punch). This can be done by hole punching a strip across each channel width.

20

Step 2 – Apply adhesive (Figure I-B): Using a stencil cover to reveal only the area around the holes in each channel, an adhesive can be applied. The process of spraying on the adhesive is then to be repeated on the other side.

Step 3- Place PET Film (Figure I-C): Next, the PET film is cut to strips that allows coverage of the channel holes across the entire paper sheet.

25

Step 4- Place pullulan film (Figure I-D): The pullulan solution can be casted onto trays to produce letter-sized films. Then, the pullulan film is cut to a size slightly larger than the holes; following this, these strips are placed onto the paper with the already applied adhesive securing them.

Step 5- Cut Paper (Figure I-E): Finally, the paper with the pullulan and PET are cut; and 48 strips come out of a letter size paper sheet.

30

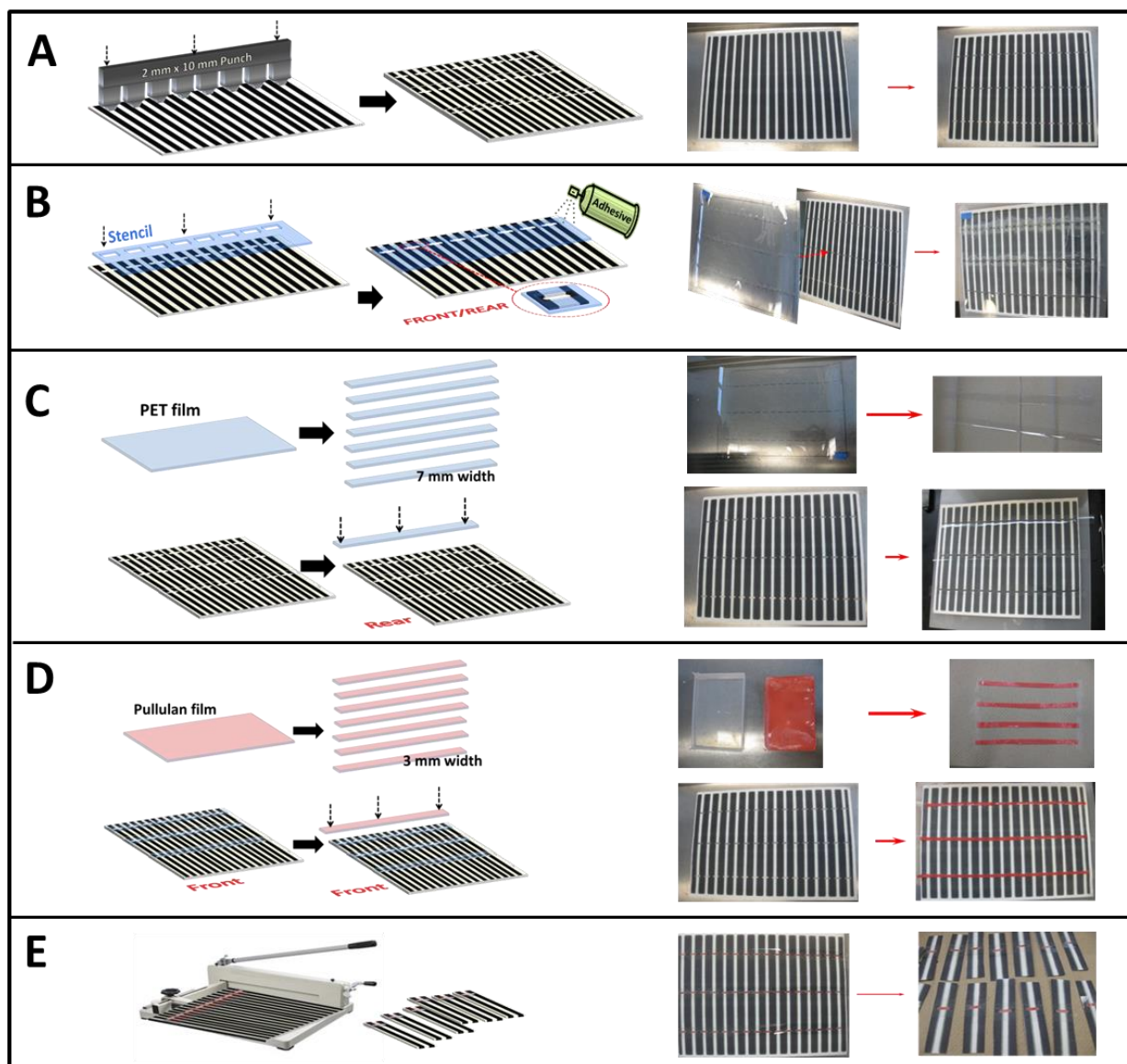


Fig. I Step-by-step demonstration of the proposed approach for scaling-up the pullulan shutoff system. Schematic cartoons of these proposed steps are depicted in the left column, and the related real images are shown in the right side.

2. Preparing pullulan films with well-defined thicknesses

The relationship between the volume of pullulan solution cast and the thickness of the resulting films is shown in Figure II. It is evident from this Figure that there is a linear relationship between the volume of pullulan solution added and the thickness of the film. Thus, the film thickness can be easily controlled by adjusting the amount of pullulan solution used.

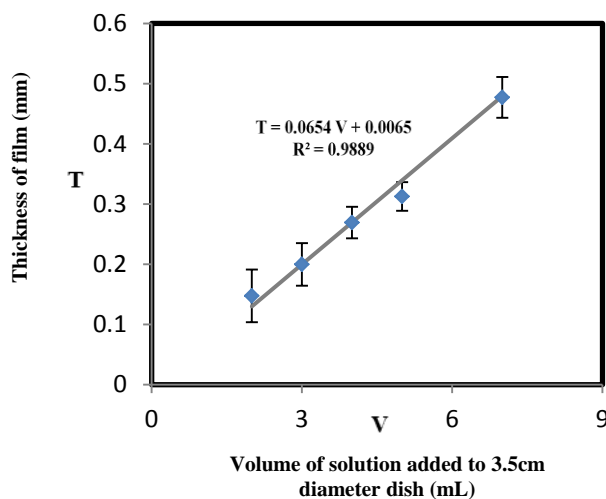


Fig.II Amount of pullulan solution cast vs. thickness of resulting film.

3. Multidirectional Flow and Sequential Release

Apart from serving as a flow shutoff system, the pullulan bridge can also facilitate multidirectional flow and sequential release of reagents. Figure III depicts colored pullulan films layered and adhered with a thin layer of water to form a layered bridge. Figure III also shows water flow through the layered bridge, which results in the bottom dye (yellow) being delivered farther than the top dye (red). These results are expected, as the bridge dissolves from the bottom upwards, releasing the dyes in order. This demonstrates the possibility of not only the release of multiple reagents but the sequential release of reagents using pullulan films.

In addition, this pattern shows flow in both a lateral direction through the paper and vertical direction through the pullulan film simultaneously. Controlled multidirectional flow is a unique capability of the pullulan bridges.

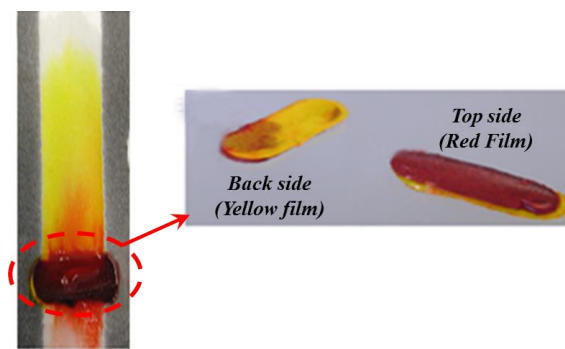
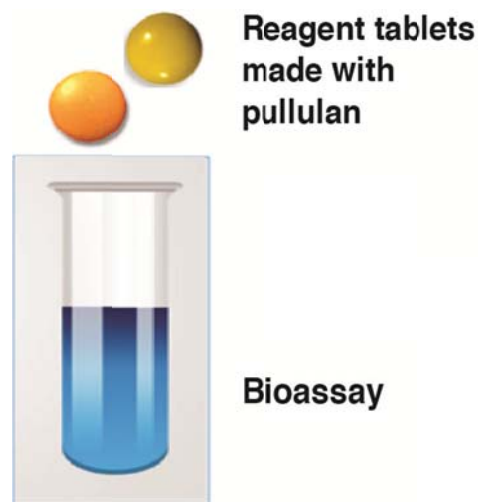


Fig.III Multidirectional flow, a unique capability of the pullulan bridges, is demonstrated by showing a two-tone layered red and yellow bridge, and the flow through this dissolvable bridge.

Chapter 4 Biolab-on-Pills

Highly Stable Premeasured Pullulan Pills for Detection of Organophosphate Pesticides



20 Word Summary:

Ready to go Pre-made pullulan tablets allow long-term storage of unstable biomolecules (such as enzymes and their substrates), but dissolve quickly in aqueous solution to allow easy execution of diagnostic tests.

In Chapter 4, I initiated this project, and all experiments regarding pullulan tablet/pill preparation and the pesticide assay kit creation were performed by myself with assistance from Kevin Pennings who worked with me as undergraduate students, and Vincent Leung. I made TaqDP pullulan tablets, with assistance of Dr. Meng Liu a postdoc fellow of Prof Li, and Meng Liu performed the PCR tests over time. I prepared the HSA-pullulan films, and Carmen Carrasquilla conducted the thermal stability tests on HSA which is reported in the supplementary information of Chapter 4. Prof Filipe and Prof. Brennan, and Prof. Li gave many helpful suggestions on both experiments and data analysis. I initiated the first draft of the paper. Balamurali Kannan gave helpful suggestion on draft format of paper, and Prof. Filipe, Prof. Brennan, and Prof. Li and Prof. Pelton helped in revising the draft to final version. This work has been published in *Angew. Chem.*, 2014, 126, 6269–6272. DOI: 10.1002/ange.201403222. It is produced by permission of John Wiley and Sons. License Number 3496060440055.

URL: <http://onlinelibrary.wiley.com/doi/10.1002/ange.201403222/abstract>

Pullulan Encapsulation of Labile Biomolecules to Give Stable Bioassay Tablets**

Sana Jahanshahi-Anbuhi, Kevin Pennings, Vincent Leung, Meng Liu, Carmen Carrasquilla, Balamurali Kannan, Yingfu Li, Robert Pelton, John D. Brennan,* and Carlos D. M. Filipe*

Abstract: A simple and inexpensive method is reported for the long-term stabilization of enzymes and other unstable reagents in premeasured quantities in water-soluble tablets (cast, not compressed) made with pullulan, a nonionic polysaccharide that forms an oxygen impermeable solid upon drying. The pullulan tablets dissolve in aqueous solutions in seconds, thereby facilitating the easy execution of bioassays at remote sites with no need for special reagent handling and liquid pipetting. This approach is modular in nature, thus allowing the creation of individual tablets for enzymes and their substrates. Proof-of-principle demonstrations include a Taq polymerase tablet for DNA amplification through PCR and a pesticide assay kit consisting of separate tablets for acetylcholinesterase and its chromogenic substrate, indoxyl acetate, both of which are highly unstable. The encapsulated reagents remain stable at room temperature for months, thus enabling the room-temperature shipping and storage of bioassay components.

Almost all bioassays make use of bioreagents (such as enzymes and small-molecule substrates) that are labile to various degrees and require special shipping and storage. The instability of these molecules can arise from either thermal denaturation or chemical modification,^[1] such as oxidation or hydrolysis.^[2] Because of these issues, they often have to be shipped on dry ice with special packaging, which is costly. These reagents also have to be stored in bulk in refrigerators or freezers to minimize loss of activity, but they must be retrieved, thawed, and aliquoted for intended tests that are often performed at room temperature. Repeated freezing and

thawing can result in significant loss of activity, which often leads to less reliable test results. These problems make running such assays in resource-limited settings a significant challenge.

One approach to address this problem is to place the assay reagents into a tablet or capsule, which both provides premeasured quantities of reagents and allows the addition of preservatives that can prolong the shelf life of the reagents. Such an approach is used in several commercial assay kits that use nonbiological reagents but has thus far not been extended to biological agents like enzymes, which are often the key components of bioassays.^[3] This is in part due to a lack of a suitable material that can meet the following three conditions: 1) it allows the encapsulation of biomolecules in a form suitable for shipping; 2) it provides outstanding protection for entrapped biomolecules against thermal denaturation and chemical modification during shipping and storage;^[4] and 3) it is readily soluble in aqueous solution, allows the release of the encapsulated molecules, and does not interfere with the assay itself.^[5] In this work we report on the use of pullulan to create bioassay tablets (cast, not compressed) that meet these three conditions.

Pullulan is a natural polysaccharide produced by the fungus *Aureobasidium pullulans*.^[6] It readily dissolves in water but resolidifies into films upon drying.^[6a,b,7] The film-forming property of pullulan has been utilized in some unique applications in the pharmaceutical and food industries, such as breath fresheners and food additives.^[6b,8] Recent studies have found that pullulan coatings applied to food packaging can act as oxygen barriers to prolong the shelf life of various foods.^[7,9] In addition, pullulan has been shown to preserve the viability of bacteria under various storage conditions.^[8]

Given the above findings, we hypothesized that pullulan might be suitable for producing assay tablets with encapsulated enzymes or other labile molecules, and more importantly, that these tablets may not only allow the long-term storage of unstable molecules at room temperature but may also provide a simplified platform for carrying out bioassays in resource-limited settings. Herein, we demonstrate the use of pullulan to create tablets to facilitate two different enzymatic reactions: a single-tablet system for DNA amplification through the polymerase chain reaction (PCR) with Taq DNA polymerase (TaqDP); and a two-tablet system for pesticide detection, where one tablet contains acetylcholinesterase (AChE) and the other contains indoxyl acetate (IDA, a chromogenic substrate for AChE).

Our first case study involves using AChE and IDA for the detection of malathion, a widely used organophosphate pesticide that has been implicated in causing reduced neuro-

[*] S. Jahanshahi-Anbuhi, K. Pennings, V. Leung, Dr. M. Liu, C. Carrasquilla, Dr. B. Kannan, Prof. Dr. Y. Li, Prof. Dr. R. Pelton, Prof. Dr. J. D. Brennan, Prof. Dr. C. D. M. Filipe
Departments of Chemical Engineering, Chemistry & Chemical Biology, and Biochemistry and Biomedical Sciences
McMaster University
1280 Main Street West, Hamilton, ON, L8S 4M1 (Canada)
E-mail: brennanj@mcmaster.ca
filipe@mcmaster.ca

[**] We thank the Natural Sciences and Engineering Research Council of Canada and Sentinel Bioactive Paper Network for funding. The authors also thank the Canada Foundation for Innovation and the Ontario Innovation Trust for support of this work. R.P. holds the Canada Research Chair in Interfacial Technologies. J.D.B. holds the Canada Research Chair in Bioanalytical Chemistry and Biointerfaces. We would also like to thank Dr. Clemence Sicard for her useful consultation. We also acknowledge the McMaster Biointerfaces Institute (BI) where part of the experiments was performed.

Supporting information for this article is available on the WWW under <http://dx.doi.org/10.1002/anie.201403222>.

logical function, eventually leading to Alzheimer's, ADHD, reduced IQ, or even death.^[10] IDA can be hydrolyzed by AChE into hydroxyindole and acetic acid: in the presence of oxygen, hydroxyindole spontaneously changes into blue-colored indigo (Figure 1a).^[11] Malathion is known to be an inhibitor of AChE^[12] and the AChE–IDA combination has been shown to be an excellent system for the colorimetric detection of malathion.^[13] However, the main challenge for

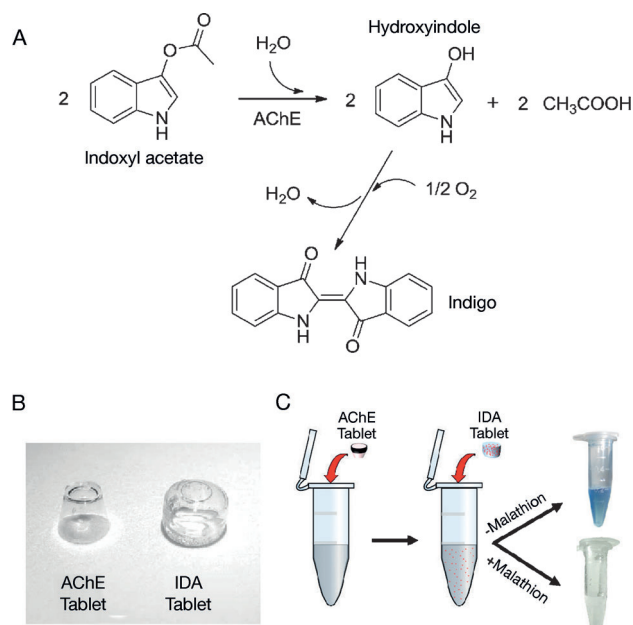


Figure 1. Tablet assay kit for malathion. a) Hydrolysis of IDA by AChE. b) A photograph of the AChE and IDA pullulan tablets. c) Operational principle of the assay kit.

this assay is the instability of both AChE and IDA.^[14] When stored at room temperature, AChE loses its enzymatic activity and IDA becomes oxidized within a few hours.^[14b,15] After being left in air, unprotected IDA turns slightly pink as a result of indirubin formation. There are two competing oxidative reactions involved in the hydrolysis of IDA. One results in the formation of the indigo dimer (the desired product of the assay), while the other produces isatin, which then dimerizes with indoxyl to give indirubin (pinkish).^[16] Therefore, fresh solutions must be prepared prior to each test, thus making this test unsuitable for on-site applications. Given these issues, the AChE–IDA system offers an excellent case study for examining the utility of pullulan tablets.

We produced individual AChE–pullulan tablets and IDA–pullulan tablets (Figure 1b) by using a simple process that involves 1) the mixing of a pullulan solution with either an AChE or IDA solution, 2) the casting of each mixture into a polypropylene mold with small wells (3 mm in diameter \times 3 mm in depth), and 3) air-drying. Note that defined concentrations of AChE and IDA were chosen to achieve a maximum rate of color formation (see Figure S1 in the Supporting Information). To conduct the assay, an AChE tablet is added to the sample to allow preincubation with the pesticide,

followed by the addition of an IDA tablet (Figure 1c). If malathion is present, the sample remains colorless or turns faint blue (dependent on the concentration of malathion, as discussed below). In the absence of malathion, IDA is fully hydrolyzed by AChE and the test sample turns deep blue (Figure 1c). Experimental details are provided in the Supporting Information.

The tablet system can not only be used to achieve qualitative detection of malathion by eye, it can also provide quantitative analysis of the pesticide concentration in a test sample when using a smartphone and image-processing software (such as ImageJ).^[13b,c,17] Figure 2 shows a plot of the dose-dependent inhibition of AChE by malathion, with data obtained using a smartphone. This simple method can be used to detect malathion at levels as low as 64 nM (S/N = 3).

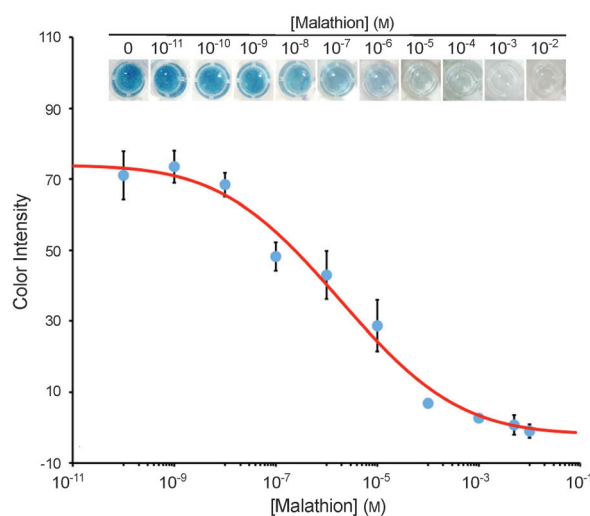


Figure 2. Dose-dependent inhibition of AChE at varying concentrations of malathion.

We next evaluated the long-term stability of both the AChE and IDA tablets. As shown in Figure 3, AChE stored in solution at room temperature became completely inactive within 3 days. Similarly, IDA in solution at room temperature lost 70% of its activity within one day and became completely inactive within a week. In sharp contrast, both AChE and IDA in tablet form remained fully active for at least 2 months when stored at room temperature. In the case of IDA, the loss in performance was related to oxidation.^[16] Our data suggests that pullulan acts as a strong barrier to oxygen, an effect that is consistent with previous findings.^[7,9] In theory, an antioxidant could be used to prevent the oxidation of IDA during storage at room temperature. However, the antioxidant would also inhibit the formation of indigo during the assay.

The loss of AChE activity, however, is attributed to thermal denaturation. To further examine the role of pullulan in stabilizing AChE, we monitored the activity of AChE as a function of temperature. For this experiment, native (unencapsulated) AChE and the corresponding pullulan tablet were treated at a given temperature for 30 min, followed by activity assessment at room temperature. Figure 4 shows that the free AChE became completely

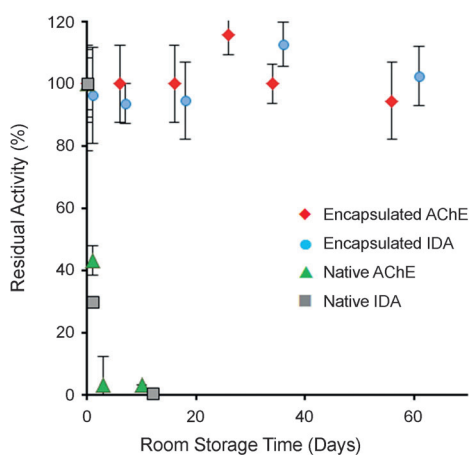


Figure 3. Evaluation of the long-term stability of AChE and IDA tablets stored at room temperature. Normalized activity of encapsulated AChE in reaction with fresh IDA, encapsulated IDA in reaction with fresh AChE, unencapsulated (native) AChE in reaction with fresh substrate, and unencapsulated IDA in reaction with fresh AChE.

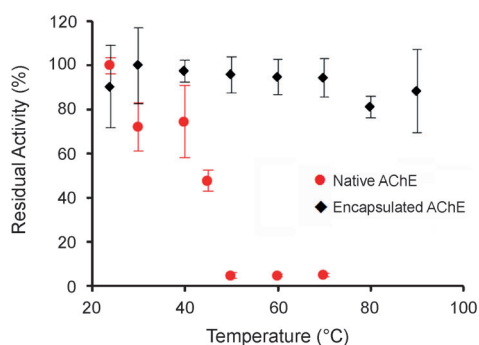


Figure 4. Loss of AChE activity as a function of temperature. Both encapsulated AChE and native enzyme were assessed.

inactive following a 30-minute heat treatment at 50°C or above. In stark contrast, AChE tablets retained ca. 90% of their initial activity even after a 30-minute incubation at 90°C.

Significant thermal stabilization was also observed for human serum albumin (HSA; Figure S2), where the unfolding temperature of the protein, as determined by tryptophan emission intensity, increased by 20°C, thus demonstrating that the stabilizing effects of pullulan are generic.

To show that pullulan encapsulation is a general strategy for increasing the long-term stability of enzymes, we carried out a second case study with TaqDP, which has been widely used in molecular biology laboratories around the world to achieve DNA amplification and has been increasingly explored for disease diagnosis and pathogen detection.^[18] Even though TaqDP is a much more stable enzyme than AChE, it still can lose significant activity when stored at room temperature. As shown in Figure 5 (see also Figure S3), the encapsulation of TaqDP in pullulan tablets resulted in the retention of 90% of initial activity after storage at room temperature for 50 days versus only 40% for native TaqDP. Once again, the data indicate that the pullulan tablet strategy offers a general method for enzyme stabilization. It is

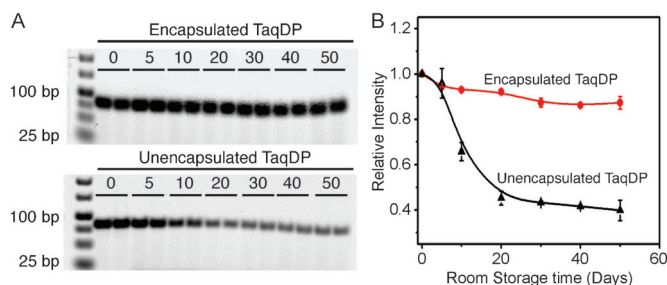


Figure 5. TaqDP activity loss during room-temperature storage with and without pullulan encapsulation.

noteworthy that when combined with portable PCR systems, TaqDP–pullulan tablets should facilitate the on-site detection of DNA.

In summary, we demonstrate that pullulan is an excellent material for producing water-soluble bioassay tablets containing labile enzymes and small molecules. Most significantly, the pullulan tablets provide exceptional protection for the entrapped reagents against thermal denaturation or chemical modification, thereby allowing room-temperature storage for extended periods of time. Equally important, the tablet strategy provides a general platform for carrying out bioassays with minimal steps and user intervention, which is ideal for resource-limited regions, particularly in the developing world.

Received: March 11, 2014

Published online: April 24, 2014

Keywords: carbohydrates · encapsulation · enzymes · pullulan · stabilization

- [1] T. Arakawaa, S. J. Prestrelskia, W. C. Kenneya, J. F. Carpenter, *Adv. Drug Delivery Rev.* **2001**, *46*, 307–326.
- [2] K. D. Miller, R. Barnette, R. W. Light, *Chest J.* **2004**, *126*, 1933–1937.
- [3] a) F. Caruso, M. Lehmann, R. Renneberg, D. Trau, Vol. US20040014073A1, **2004**; b) N. Milani, *Apidologie* **1995**, *26*, 415–429; c) R. A. Setterquist, G. K. Smith, *Nucleic Acids Res.* **1996**, *24*, 1580–1581; d) V. Siegmund, O. Adjei, P. Racz, C. Berberich, E. Klutse, F. Vloten, T. Kruppa, B. Fleischer, G. Bretzel, *J. Clin. Microbiol.* **2005**, *43*, 271–276.
- [4] a) C. Ó'Fágáin, *Enzyme Microb. Technol.* **2003**, *33*, 137–149; b) A. Y. Kolosova, W.-B. Shim, Z.-Y. Yang, S. A. Eremin, D.-H. Chung, *Anal. Bioanal. Chem.* **2006**, *384*, 286–294; c) M. K. Goyal, I. Roy, A. Amin, U. C. Banerjee, A. K. Bansal, *J. Pharm. Sci.* **2010**, *99*, 4149.
- [5] P. V. Iyer, L. Ananthanarayan, *Process Biochem.* **2008**, *43*, 1019–1032.
- [6] a) M. Shibata, M. Asahina, N. Teramoto, R. Yosomiya, *Polymer* **2001**, *42*, 59–64; b) R. S. Singh, G. K. Saini, J. F. Kennedy, *Carbohydr. Polym.* **2008**, *73*, 515–531; c) A. Imeson, *Food Stabilisers, Thickeners and Gelling Agents*, Wiley, Hoboken, **2011**, pp. 267–274.
- [7] S. Farris, L. Introzzi, J. M. Fuentes-Alventosa, N. Santo, R. Rocca, L. Piergiovanni, *J. Agric. Food Chem.* **2012**, *60*, 782–790.
- [8] A. A. Krumnow, I. B. Sorokulova, E. Olsen, L. Globa, J. M. Barbaree, V. J. Vodyanoy, *J. Microbiol. Methods* **2009**, *78*, 189–194.
- [9] S. Wu, J. Chen, *Int. J. Biol. Macromol.* **2013**, *55*, 254–257.

- [10] a) S. Ciesielski, D. P. Loomis, S. Rupp Mims, A. Auer, *Am. J. Public Health* **1994**, *84*, 792; b) DailyNewsBlog in *Beyond Pesticides* **2013**; c) B. Eskenazi, A. R. Marks, A. Bradman, K. Harley, D. B. Barr, C. Johnson, N. Morga, N. P. Jewell, *Environ. Health Perspect.* **2007**, *115*, 792–798; d) S. Giri, S. B. Prasad, A. Giri, G. D. Sharma, *Mutat. Res.* **2002**, *514*, 223–231; e) S. M. Ross, I. C. McManus, V. Harrison, O. Mason, *Crit. Rev. Toxicol.* **2013**, *43*, 21–44.
- [11] M. Pohanka, M. Hrabanova, K. Kuca, J. P. Simonato, *Int. J. Mol. Sci.* **2011**, *12*, 2631–2640.
- [12] a) J. E. Casida, *Science* **1964**, *146*, 1011–1017; b) H. Soreq, S. Seidman, *Nat. Rev. Neurosci.* **2001**, *2*, 294–302.
- [13] a) N. Hwa-Young, K. Young Ah, L. Yong Tae, L. Hye-Sung, *Anal. Chim. Acta* **2007**, *594*, 37–43; b) S. Jahanshahi-Anbui, P. Chavan, C. Sicard, V. Leung, S. M. Z. Hossain, R. Pelton, J. D. Brennan, C. D. M. Filipe, *Lab Chip* **2012**, *12*, 5079–5085; c) S. Jahanshahi-Anbui, A. Henry, V. Leung, C. Sicard, K. Pennings, R. Pelton, J. D. Brennan, C. D. M. Filipe, *Lab Chip* **2014**, *14*, 229–236; d) M. Yuqing, H. Nongyue, Z. Jun-Jie, *Chem. Rev.* **2010**, *110*, 5216–5234.
- [14] a) K. M. Somashekar, McMaster University (Hamilton), **2013**; b) G. Pico, *Biochem. Mol. Biol. Int.* **1995**, *36*, 1017–1023.
- [15] S. Cotson, S. J. Holt, *Proc. R. Soc. London Ser. B* **1958**, *148*, 506–519.
- [16] U. H. Brinker, J.-L. Mieusset, *Molecular Encapsulation Organic Reactions in Constrained Systems*, Wiley, Vienna, **2010**, chap. 3.
- [17] C. Liu, Q. Jia, C. Yang, R. Qiao, L. Jing, L. Wang, C. Xu, M. Ga, *Anal. Chem.* **2011**, *83*, 6778–6784.
- [18] a) C. Ding, C. R. Cantor, *Proc. Natl. Acad. Sci. USA* **2003**, *100*, 7449–7453; b) F. Feng, L. Liu, S. Wang, *Nat. Protoc.* **2010**, *5*, 1255–1264; c) T. Ishige, S. Sawai, S. Itoga, K. Sato, E. Utsuno, M. Beppu, K. Kanai, M. Nishimura, K. Matsushita, S. Kuwabara, F. Nomura, *J. Hum. Genet.* **2012**, *57*, 807–808; d) R. K. Saiki, D. H. Gelfand, S. Stoffel, S. J. Scharf, R. Higuchi, G. T. Horn, K. B. Mullis, H. A. Erlich, *Science* **1988**, *239*, 487–491; e) R. K. Saiki, S. Scharf, F. Faloona, K. B. Mullis, G. T. Horn, H. A. Erlich, N. Arnheim, *Science* **1985**, *230*, 1350–1354.

Supporting Information

© Wiley-VCH 2014

69451 Weinheim, Germany

Pullulan Encapsulation of Labile Biomolecules to Give Stable Bioassay Tablets**

Sana Jahanshahi-Anbuhi, Kevin Pennings, Vincent Leung, Meng Liu, Carmen Carrasquilla, Balamurali Kannan, Yingfu Li, Robert Pelton, John D. Brennan, and Carlos D. M. Filipe**

ange_201403222_sm_miscellaneous_information.pdf

Supplementary Information

A. Experimental Details

Materials. Acetylcholinesterase (AChE, from *Electrophorus electricus*, EC 3.1.1.7), and indoxyl acetate (IDA) were obtained from Sigma-Aldrich. Pullulan (MW ~200000) was purchased from Polysciences, Inc and malathion was obtained from Fluka. Human serum albumin (HSA; fatty acid and globulin free, ≥99%) was obtained from Sigma-Aldrich (Oakville, ON). Quartz microscope slides were purchased from Chemglass (Vineland, NJ) and cut to approximate dimensions of 8 × 32 mm. Water was purified with a Milli-Q Synthesis A10 water purification system. Buffer salt (Tris 100 mM) and pullulan solutions were filtered using a Pall® syringe filter with 5 µm membrane in order to remove any dust particulate. DNA oligonucleotides were purchased from Integrated DNA Technologies (IDT) and purified by 10% denaturing polyacrylamide gel electrophoresis (dPAGE) before use. Agarose was obtained from Bioshop (Burlington, Canada). The fluorescent images of gels were obtained using Typhoon 9200 variable mode imager (GE healthcare) and analyzed using ImageQuant software (Molecular Dynamics). Taq DNA polymerase (TaqDP) was acquired from Biotools.

Forward Primer: 5'-CAGGT CCATC GAGTG GTAGG A

Reverse primer: 5'-GTACG TTCAG GAGCA GTGCG A

Template: 5'-CAGGT CCATC GAGTG GTAGG AGGAG GTATT TAGTG CCAAG CCATC TCAAA CGACG TCTGA GTCGC ACTGC TCCTG AACGT AC.

Experimental procedures

IDA Tablets, Creation and Activity Test. To test the ability of pullulan to retain IDA activity, 10 µL of 40 mM IDA and 40 µL of 120 g/L pullulan in water were mixed and casted in a polypropylene mold with wells with a size of 3 mm in diameter × 3 mm in depth. The solution was air-dried overnight at 21 °C and 48% RH; tablet formation was considered not fully completed if the tablet could not be removed from the bottom of the well. The resulting tablets were kept at room temperature for different lengths of time before being tested. To test IDA activity, 199 µL of Tris-HCl (100 mM, pH 8) was used to dissolve the pill and 1 µL of fresh 250 U/mL AChE was added. The solution was then transferred to a 96-well plate and the absorbance of the developing blue color was measured at A₆₀₅ on a TECAN Infinite M200 Pro microtiter plate reader.

AChE Tablets, Creation and Activity Test. To test the ability of pullulan to retain AChE activity, 1 µL of 250 U/mL AChE and 40 µL of 120 g/L pullulan were mixed and casted into tablets. The solution was air-dried overnight at 21 °C and 48% RH; tablet formation was considered not fully completed if the tablet could not be removed from the bottom of the well; and the resulting tablets were kept at room temperature for different lengths of time before being tested. To test AChE activity, 195 µL of Tris-HCl (100 mM, pH 8) was used to dissolve the tablet and 5 µL of fresh 80 mM IDA was added. The solution was then transferred to a 96-well plate and the absorbance was measured at A₆₀₅ on TECAN Infinite M200 Pro microtiter plate reader.

Malathion Detection Test. 200 µL of malathion solution was added into the Eppendorf tube followed by the addition of the pullulan-AChE tablet. After 5 minutes of incubation, the pullulan-IDA tablet was added into the Eppendorf tube. The mixture was incubated for 10–15 minutes for development of the blue color; the concentration of malathion was calculated based on the color intensity. Images were obtained using a Galaxy Nexus cellphone camera operated in automatic mode with no flash. The Images were analyzed using ImageJ software by methods described elsewhere^[1]. The concentration range of malathion was 0.01 to 1E-10 M.

PCR. The DNA was amplified by PCR. Each reaction mixture (50 µL) contained Taq polymerase (1.5 U), forward and reverse primer (1 µM each), dNTPs (0.2 mM each of dATP, dCTP, dGTP and dTTP), and template (10 nM). In order to produce the Taq-pullulan tablet samples, the Taq polymerase was dissolved into 20 µL of Milli-Q water containing 10% pullulan and allowed to air-dry overnight at 21 °C and 48% RH. DNA amplification was performed by using the following conditions: 30 s at 94°C, 45 s at 50 °C, 40 s at 72 °C, 18 cycles. PCR product was analyzed by 3% agarose gel electrophoresis.

Preparation of Pullulan-HSA Solutions and Films. Human serum albumin (60 µM final concentration) was dissolved into either 100 mM Tris-HCl (pH 7.5) or 100 mM Tris-HCl containing 10% pullulan. These pullulan solutions, with or without HSA, were carefully pipetted onto the quartz slides (500 µL / slide) and allowed to dry overnight at 21 °C and 48% RH in order to produce the film samples.

Determination of the Water Content in Pullulan Films. The water content of films was done by gravimetric analysis with drying at 130 °C until constant weight. The water content in the films was found to be 0%.

Fluorescence Intensity Measurements. Fluorescence measurements were acquired using a Cary Eclipse fluorescence spectrophotometer. Solution samples were measured in quartz cuvettes and continuously stirred throughout the experiments. Film samples were suspended in quartz cuvettes at a 45° angle to the excitation light using specialized holders which reflected excitation light away from the detector and collected emission through the slide and into the monochromator/PMT.

For fluorescence emission spectra, samples were excited at 295 nm (to ensure that the light was absorbed almost entirely by the lone tryptophanyl residue) and emission was collected at 310 – 450 nm in 1 nm increments, using a 5-nm bandpass for both excitation and emission paths and an integration time of 0.1 s. Spectra from both solution and film-based samples were corrected for light scattering by blank subtraction of signals originating from buffer or pullulan/quartz materials, respectively,

without HSA. All the spectra were also corrected for deviations in emission monochromator throughput and PMT response and smoothed by the Savitzky-Golay method, using a factor of 5 and an interpolated factor of 5.

For thermal denaturation studies, the temperature was raised in ~ 5 °C increments from 20 °C to 90 °C and allowed to equilibrate at each temperature for at least 5 min. The temperature in the cuvette was measured directly with a thermistor probe. Intensity-based unfolding curves are reported as integrated scan intensities, which are normalized to the integrated intensity at the beginning of the experiment (20 °C as 100%) for each sample. Emission scans are measured in relative fluorescence units, RFU, and all values are reported as the average of three separate samples.

B. Supporting Figures

Figure S1: Reaction Rate Studies

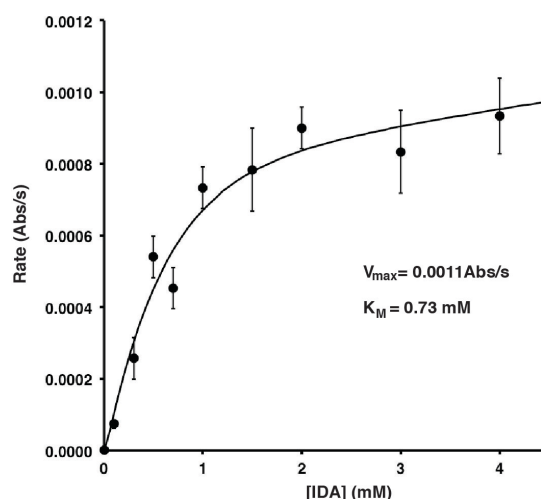


Figure S1. Graph of the reaction rate (abs/s) of AChE and IDA as a function of the IDA concentration from 0 to 4 mM. The reaction rate of AChE tablet with different concentration of IDA was monitored to establish an optimal IDA concentration for pesticide detection experiment. From the data, we chose the concentration of IDA for the pesticide to be 2 mM (which is significantly larger than K_M). The error bars representing the standard deviations based on triplicate repeats.

Figure S2: Thermal Stability Test on HSA

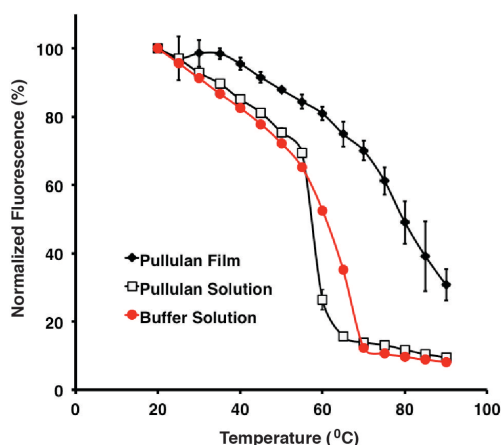


Figure S2. Fluorescence intensity-based thermal unfolding curves for HSA-buffer solution, in HSA-pullulan solution and HSA-pullulan film. Changes in the intrinsic fluorescence from tryptophan (Trp) residues within proteins can be used to provide information on protein conformational stability and unfolding.^[2] Therefore, steady-state fluorescence spectra were measured at various temperatures for HSA-buffer solution, HSA-pullulan solution and HSA-pullulan film (HSA was chosen for this study because it contains a single Trp allowing for unambiguous investigation^[3]). The data shows that the intensity of fluorescence for HSA-buffer and HSA-pullulan solution decreased by more than 90% when the temperature was raised from 20 °C to 90 °C, while that of HSA-pullulan film only decreased by $\sim 70\%$. The unfolding temperature (wherein the Trp intensity is reduced by 50%) was significantly higher for the pullulan-HSA film at ~ 80 °C, versus ~ 60 °C for both HSA-buffer and HSA-pullulan solutions. This study demonstrate that pullulan film significantly enhances the thermal stability by preventing substantial unfolding as a result of molecular confinement in the rigid matrix. This stabilizing effect is only observed in the pullulan film and not in the pullulan solution.

Figure S3: Different Pullulan Concentration for Taq Encapsulation

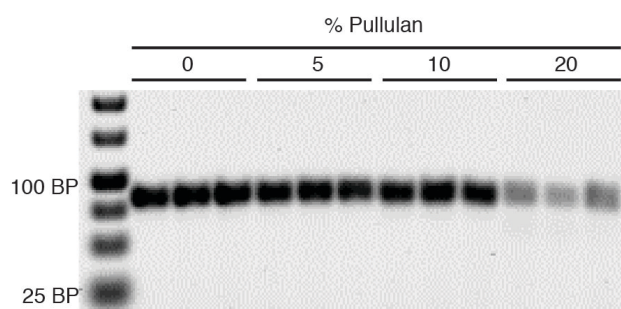
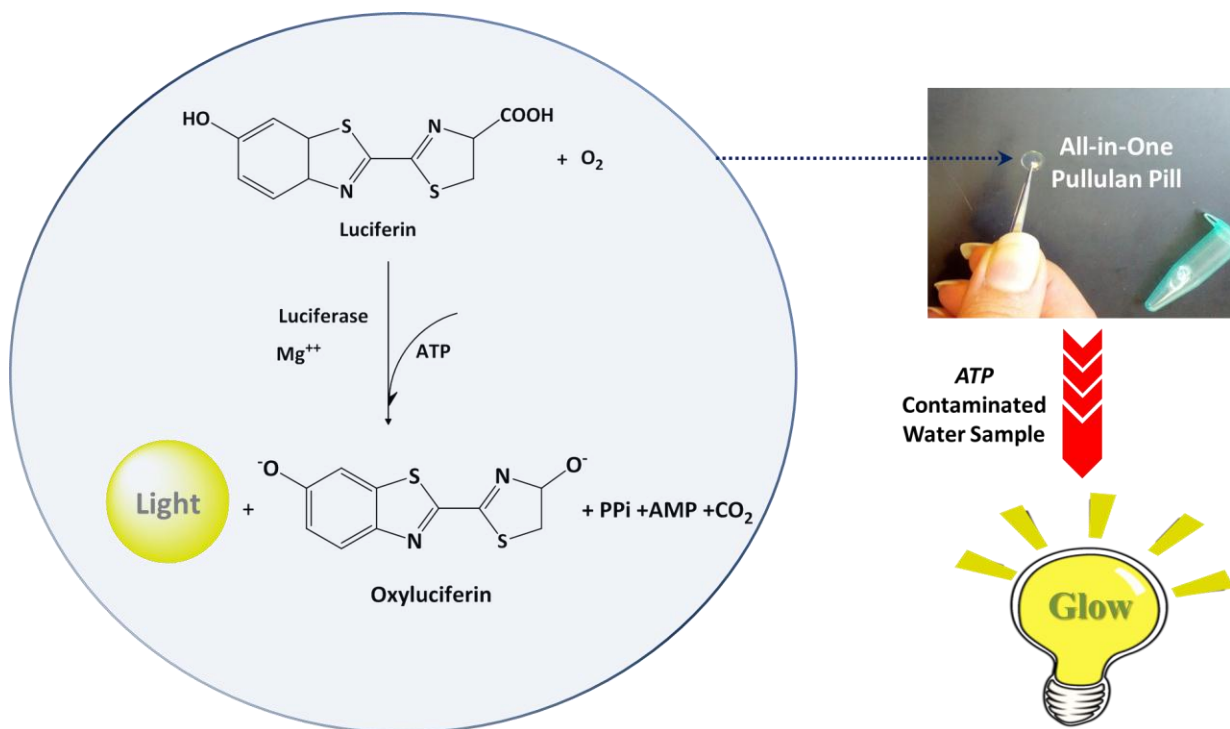


Figure S3. Agarose gel results of PCR products in the presence of different pullulan concentrations. The effect of pullulan concentration on the activity of TaqDP was studied in this experiment. 20 μ L of pullulan solution (50, 100, 150, 200 mg/mL) and 1 μ L of TaqDP were casted into Eppendorf tubes. The activity of TaqDP was tested after one week. The results show that higher concentrations of pullulan up to \sim 10-12% provide better protection of TaqDP. Inefficient protection in higher concentrations of pullulan (\geq 20%) is due to high solution viscosity which causes greater error in the experiments and losing samples during pipetting.

References for Supporting Information:

- [1] a) S. Jahanshahi-Anbui, P. Chavan, C. Sicard, V. Leung, S. M. Z. Hossain, R. Pelton, J. D. Brennan, C. D. M. Filipe, *Lab Chip* **2012**, *12*, 5079-5085; b) S. M. Z. Hossain, R. E. Luckham, A.-M. Smith, J. M. Lebert, L. M. Davies, R. H. Pelton, C. D. M. Filipe, J. D. Brennan, *Anal. Chem.* **2009**, *81*, 5474-5483.
- [2] a) M. S. Hargrove, S. Krzywda, A. J. Wilkinson, Y. Dou, M. Ikeda-Saito, J. S. Olson, *Biochemistry* **1994**, *33*, 11767-11775; b) M. R. Eftink, *Biophysical Journal* **1994**, *66*, 482-501.
- [3] a) D. C. Carter, J. X. Ho, *Adv Protein Chem* **1994**, *45*, 153-203; b) G. Pico, *Biochem Mol Biol Int* **1995**, *36*, 1017-1023.

Chapter 5 ‘All-in-One’ Luminescent Pullulan Pills



20 Word Summary:

Highly stable ready-to-go luminescent pullulan pills which include all required reagents for ATP detection all-in-one.

In Chapter 5, all experiments were planned by myself, and conducted by myself with very helpful assistance from Vincent Leung and Dr. Balamurali Kannan. I analyzed all experimental data and submitted the first draft of the results exhibiting the framework of the paper to Prof. Filipe; Dr. Balamurali Kannan added descriptions and edited later to final version. Prof. Filipe and Prof. Brenan, and Prof. Pelton contributed many helpful suggestions on both experiments and data analysis. This work is a manuscript prepared for submission to a journal.

Highly stable 'All-in-one' luminescent pullulan pills for sensitive ATP detection

Sana Jahanshahi-Anbuhi, Balamurali Kannan, Vincent Leung, Robert Pelton, John D. Brennan,* and Carlos D. M. Filipe*

Abstract: A cost-effective, thermally stable luminescent pills were prepared by encapsulating all the components necessary for the ATP detection in pullulan matrix. These highly soluble pullulan pills readily release all the components in testing solution and retain the glow kinetics to produce stable light for more than an hour. This pill-based detection is sensitive up to 10⁻¹² molar concentration of ATP and will be a convenient way of real-time ATP testing. Other than ATP testing, this general way of stabilizing the highly unstable enzyme can be applied to luciferase-based in-vitro imaging as well..

ATP detection is becoming very common for the cleanliness evaluation in various common samples and surfaces.[1] Numerous methods have been reported in the last decade for ATP detection based on Fluorescence,[2] Aptamer-based detection,[3] quantum dots[4] and electrochemical methods.[5] However, the bioluminescent method using firefly luciferase is the most sensitive and ubiquitous method.[6] The major limitation of this method is the stability of enzyme, luciferase which act as the catalyst.[7] The activity will start decreasing once it is taken in solution even at lower temperature.[8] Various attempts have been made on the stabilization of enzymes such as adding osmolytes/stabilizers[9] and immobilization on solid supports such as pre-coated polymer films,[10] dendrimers,[11] glass rods[12] and sol-gel derived silica supports.[13] None of the methods can retain the activity for a prolonged time period except the sol-gel derived soft glasses which again is enzyme-specific because of the differential interaction of protein and silica. A general protein stabilization method was reported by Li et al which gives a protective liposome coating before sol-gel

encapsulation and thus avoiding the protein-silica interaction during the sol gel process.[14] However, it suffers experimental complexity. Enzyme immobilization involving alkoxy silanes which are covalently tethered to the sugars were able to retain the activity and reusability of luciferase for weeks and provide highly sensitive ATP detection.[7a, 15] In spite of its advantages, the method is quite laborious and has scale-up limitations.

In this work, pullulan, a polysaccharide consists of maltotriose units is used to form 'all-in-one' luminescent pill for ATP detection. All the components such as luciferase, luciferin, MgSO₄, MgCO₃, dithiothreitol, ethylenediaminetetraacetic acid (EDTA), CoA enzyme and tricine buffer which are necessary for the luminescence detection of ATP were taken in pullulan (12% w/v final concentration) and encapsulated to form a stable 'ready-to-use' pill. The stabilizing effect of osmolytes such as sugars and sorbitols have studied for various enzymes.[9b, 16] Recently, pullulan stabilization of acetylcholinesterase and indoxylacetate to form bioassay tablets were reported by our group for real-time pesticide detection.[17]. However, Pullulan encapsulation is not just protecting the enzymes but it also forms a stable, non-hygroscopic and size/shape-tunable pills after drying. When the luminescent pill is treated with ATP in solution, it readily dissolves and releases all the components for luminescence detection (Figure 1).

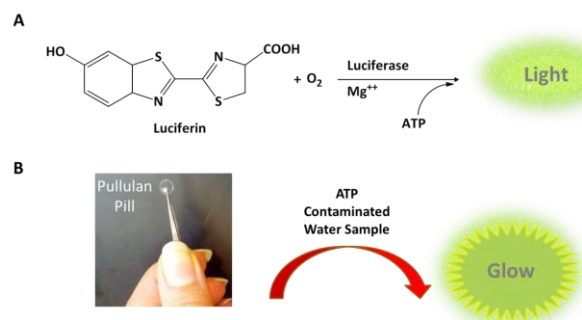


Figure 1. Pill assay for ATP. (a) Firefly luciferase reaction. (b) Operation principle of the assay using 'all-in-one' pullulan pill which generates a "glow-type" luminescent signal

[*] S. Jahanshahi-Anbuhi, Dr. B. Kannan, V. Leung, Prof. Dr. Robert Pelton, Prof. Dr. John D. Brennan, and Prof. Dr. Carlos D. M. Filipe
Departments of Chemical Engineering, and Chemistry & Chemical Biology,
McMaster University
1280 Main Street West, Hamilton, ON, L8S 4M1, Canada. Fax: (905) 521-1350.
Tel: (+1) 905-525-9140 (ext. 27278, 20682).
E-mail: brennanj@mcmaster.ca, filipe@mcmaster.ca

[**]The authors thank the Natural Sciences and Engineering Research Council of Canada and Sentinel Bioactive Paper Network for funding. The authors also thank the Canada Foundation for Innovation and the Ontario Innovation Trust for support of this work. R.P. holds the Canada Research Chair in Interfacial Technologies. J.D.B. holds the Canada Research Chair in Bioanalytical Chemistry and Biointerfaces. The authors would also like to thank Dr. Clemence Sicard for her useful consultation. The authors also acknowledge the McMaster Biointerfaces Institute (BI) where part of the experiments was performed.



Supporting information for this article is available.

To our knowledge, this is the first report in which all the components required for luciferase/luciferin assay were stabilized together as a single pill for the ATP detection. The pills were sensitive up to picomolar concentration of ATP in solution. The stability of the pills at room temperature was conducted by storing the pills at bench top in dark containers. Figure 2a shows the glow kinetics (Luminescent units versus time) of a luminescent pill with 250 μM ATP concentration on a 96 well plate reader (Tecan M1000). Figure 2b shows the stability of pills in comparison with the same components stored in buffer solution without pullulan. It shows that the enzyme loses its activity in buffer solution in few hours. On the other hand, the enzyme and other components in pullulan pills are

found to be stable for 3 weeks at bench top. The stability of enzyme alone was also tested in pullulan pills and is found to be fully active for at least two months when stored at room temperature (Figure S1) which shows that other components in the bioluminescent pill mainly luciferin is losing its activity after three weeks. Luciferin, as a substrate for this oxidative-decarboxylation reaction is also unstable at room temperature and prone to auto-oxidation and photo-degradation.[18] As these pills encapsulate all the required components, it highly benefits by circumventing the laborious preparations each time. It was observed that additives such as dextran and polyethylene glycol were not able to retain the activity as pullulan when they were prepared and tested similarly which shows pullulan has unique stabilizing effect when compared to other polyols.

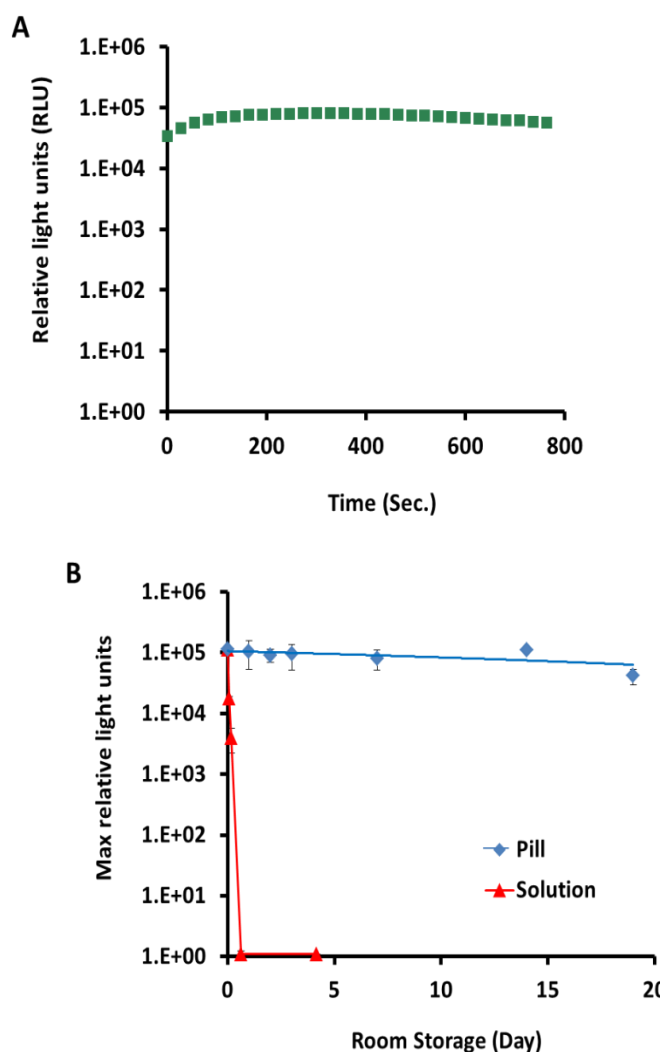


Figure 2. A) Glow kinetics of ‘all-in-one’ pill after one week of preparation and stored at room temperature. B) Stability of the pills over three weeks. The error bar represents triplicate measurements at each time interval.

The thermal stability of luciferase is known to be very low. The luminescent ‘all-in-one’ pills were also tested for thermal stability by incubating the pills at temperatures up to 70 °C. The activity of the pills remains the same up to 70 °C while in solution it decreases even at 30 °C and lost all its activity at 50 °C (Figure 3). This clearly shows that the pullulan protection for luciferase also ensures the retention of activity at elevated

temperatures.

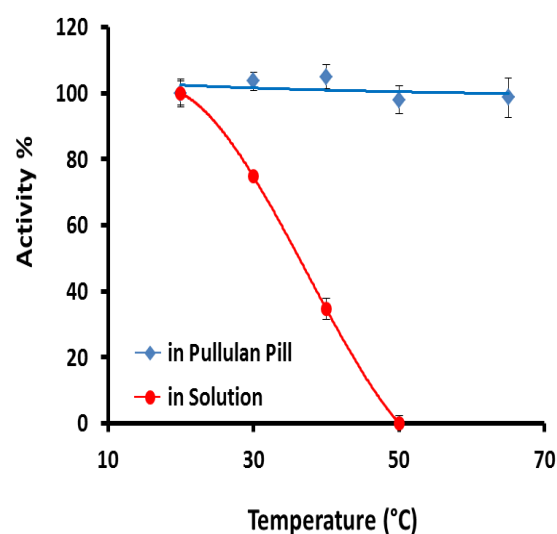


Figure 3. Loss of activity as a function of temperature. Both encapsulated (◆) and native reagents (●) were assessed

The ability of luminescent pills for ATP detection was shown in figure 4. A series of concentration of ATP in tricine buffer was added to the pills and the luminescence intensity was measured in a plate reader. The relative luminescent units (RLU) was plotted for the range of concentration. The limit of detection was found to be 1.5 pM which is comparable to the highly sensitive detection methods that are reported previously.

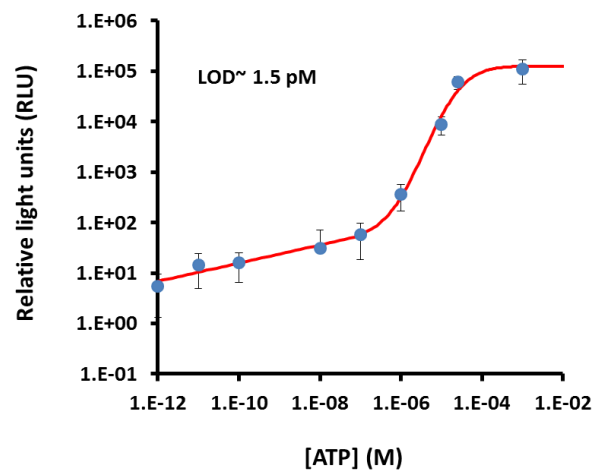


Figure 4. Detection of ATP in solution using ‘all-in-one’ pills. Plot of light intensity versus ATP concentration ranging from 10^{-12} to 10^{-2} M in tricine buffer. The error bar represents triplicate measurements at each concentration.

In summary, a highly strenuous and time-consuming luminescence assay was made single-step by encapsulating all the reagents including highly unstable enzyme and substrate in a single pill using pullulan. All the components are thermally stable in the pills and provides sensitive ATP detection up to picomolar concentration. This cost-effective method (~88 Canadian cents per 100 pills which is more 130 times cheaper than the solution-based commercial assay kits), is also easy to scale-up. This stabilization technique will cover a broad spectrum of application ranging from inexpensive real-time ATP testing to high-throughput screening applications where sensitivity and stable light emission are desired.

Keywords: bioassay • encapsulation • pullulan • ATP detection • luminescent • stabilization

References.

- [1] aE. Amodio, C. Dino, *Journal of Infection and Public Health* **2014**, *7*, 92-98; bG. R. Siragusa, W. J. Dorsa, C. N. Cutter, L. J. Perino, M. Koohmaraie, *J. Biolumin. Chemilumin.* **1996**, *11*, 297-301; cN. Omidbakhsh, F. Ahmadpour, N. Kenny, *PLoS ONE* **2014**, *9*, e99951; dM. T. La Duc, R. Kern, K. Venkateswaran, *Microb Ecol* **2004**, *47*, 150-158.
- [2] aH. Wang, W.-H. Chan, *Organic & Biomolecular Chemistry* **2008**, *6*, 162-168; bY. Kanekiyo, R. Naganawa, H. Tao, *Chemical Communications* **2004**, 1006-1007.
- [3] aW. Yao, L. Wang, H. Wang, X. Zhang, L. Li, *Biosensors and Bioelectronics* **2009**, *24*, 3269-3274; bY. Wang, B. Liu, *Analyst* **2008**, *133*, 1593-1598; cS. Sitaula, S. D. Branch, M. F. Ali, *Chemical Communications* **2012**, *48*, 9284-9286; dY. He, Z. G. Wang, H. W. Tang, D. W. Pang, *Biosens. Bioelectron.* **2011**, *29*, 76-81.
- [4] aH. Huang, Y. Tan, J. Shi, G. Liang, J.-J. Zhu, *Nanoscale* **2010**, *2*, 606-612; bG. Jie, J. Yuan, J. Zhang, *Biosensors and Bioelectronics* **2012**, *31*, 69-76.
- [5] aX. Zuo, S. Song, J. Zhang, D. Pan, L. Wang, C. Fan, *Journal of the American Chemical Society* **2007**, *129*, 1042-1043; bY. Z. Lin, T. L. Chang, C. C. Chang, *Sens. Actuator B-Chem.* **2014**, *190*, 486-493.
- [6] S. V. Khlyntseva, Y. R. Bazel', A. B. Vishnikin, V. Andruch, *J Anal Chem* **2009**, *64*, 657-673.
- [7] aJ. A. Cruz-Aguado, Y. Chen, Z. Zhang, N. H. Elowe, M. A. Brook, J. D. Brennan, *Journal of the American Chemical Society* **2004**, *126*, 6878-6879; bM. R. Ganjalikhany, B. Ranjbar, S. Hosseinkhani, K. Khalifeh, L. Hassani, *J. Mol. Catal. B-Enzym.* **2010**, *62*, 127-132.
- [8] R. Herbst, U. Schafer, R. Seckler, *J. Biol. Chem.* **1997**, *272*, 7099-7105.
- [9] aT. O. Street, D. W. Bolen, G. D. Rose, *Proc. Natl. Acad. Sci. U. S. A.* **2006**, *103*, 17064-17064; bJ. K. Kaushik, R. Bhat, *J. Biol. Chem.* **2003**, *278*, 26458-26465.
- [10] N. Y. Filippova, A. F. Dukhovich, N. N. Ugarova, *J. Biolumin. Chemilumin.* **1989**, *4*, 419-422.
- [11] S. A. Miller, E. D. Hong, D. Wright, *Macromol. Biosci.* **2006**, *6*, 839-845.
- [12] Y. Lee, I. Jablonski, M. Deluca, *Anal. Biochem.* **1977**, *80*, 496-501.
- [13] aM. R. N. Monton, E. M. Forsberg, J. D. Brennan, *Chem. Mat.* **2012**, *24*, 796-811; bT. R. Besanger, J. D. Brennan, *J. Sol-Gel Sci. Technol.* **2006**, *40*, 209-225; cD. Avnir, T. Coradin, O. Lev, J. Livage, *J. Mater. Chem.* **2006**, *16*, 1013-1030.
- [14] Y. Li, W. T. Yip, *Journal of the American Chemical Society* **2005**, *127*, 12756-12757.
- [15] aT. Y. Lin, C. H. Wu, J. D. Brennan, *Biosens. Bioelectron.* **2007**, *22*, 1861-1867; bX. H. Sui, J. A. Cruz-Aguado, Y. Chen, Z. Zhang, M. A. Brook, J. D. Brennan, *Chem. Mat.* **2005**, *17*, 1174-1182.
- [16] aP. H. Yancey, M. E. Clark, S. C. Hand, R. D. Bowlus, G. N. Somero, *Science* **1982**, *217*, 1214-1222; bJ. C. Lee, S. N. Timasheff, *J. Biol. Chem.* **1981**, *256*, 7193-7201.
- [17] S. Jahanshahi-Anbuhi, K. Pennings, V. Leung, M. Liu, C. Carrasquilla, B. Kannan, Y. Li, R. Pelton, J. D. Brennan, C. D. M. Filipe, *Angewandte Chemie International Edition* **2014**, *53*, 6155-6158.
- [18] S. Inouye, *Methods Enzymol.* **2000**, *326*, 165-174.

Supplementary Information

Highly stable ‘All-in-one’ bioluminescent pill for sensitive ATP detection

Sana Jahanshahi-Anbuhi, Balamurali Kannan, Vincent Leung, Robert Pelton, John D. Brennan, and Carlos D. M. Filipe**

A. Experimental Details

Materials. Luciferase, Luciferin, Co-enzyme A (CoA), Adenosine triphosphate (ATP), Tricine, Magnesium Carbonate (MgCO₃), Magnesium Sulfate (MgSO₄), DL-Dithiothreitol (DTT), [Ethylenediaminetetraacetic acid](#) (EDTA), and Dextran (MW ~ 148000) were purchased from Sigma-Aldrich. Polyethylene glycol (PEG, MW~6000) was purchased from Fluka. Pullulan (MW~200’000 Da) was purchased from Polysciences.

Preparation of ‘all-in-one’ Pullulan Pill. All reagents for the luciferase assay except for adenosine triphosphate (ATP) were casted in a single pullulan pill. For the pullulan pills aqueous solutions of 10 mM Luciferin, 100 mM Luciferase, 27 mM Coenzyme A (CoA), 170 mM Dithiothreitol (DTT), 10 mM [Ethylenediaminetetraacetic acid](#) (EDTA), 107 mM MgCO₃, and 267 mM MgSO₄ were prepared. 200 μL of each solution was added to 8 mL of 12 w/v% Pullulan solution. Lastly, for each pill 47 μL of the final solution was pipetted onto a PET film and dried in a glove box under nitrogen. The casted pills were then stored at room temperature.

Buffer preparation. A buffer solution containing ATP was prepared to test the activity of the luciferase pills. For the buffer solution, 16 mL of water was added to 2 mL of 2.5 mM ATP and 2 mL of 200 mM Tricine and the pH was adjusted to pH 7.8.

Stability at room storage condition. Once the pills are completely dried, they were collected in dark bottles. The pills were stored at room temperature and the activity of the pills was tested over time. On the day the pills were prepared, the activity of the fresh pullulan and reagent

solution was tested. 47 μL of the solution and 100 μL of the buffer were added to a 96 well-plate and the luminescence was measured using the TECAN M1000. On subsequent days, the activity of the pills was measured by placing a single pill into a well and 100 μL of ATP buffer. Each test was performed with three repeats.

ATP Detection Assay. The sensitivity of the luciferase assay was also investigated. To determine the detection limit of the assay, different ATP buffers were prepared with concentration ranging from 0 μM to 1000 μM .

Thermal stability. Reagents in solution and pullulan Pills were incubated at each temperature set point for 30 minutes in a hot plate. After that, they were allowed to cool till room temperature is reached. Then the luminescence reading was taken using 100 μL of 250 μM ATP (in tricine buffer)

Stability in Dextran/PEG. The effect of other polymers and polysaccharides on luciferase activity was investigated. Dextran and PEG pills were prepared using the same procedure as the pullulan pills. In place of pullulan solution, 12 w/v% Dextran and 12 w/v% PEG solutions were used to create dextran and PEG pills respectively.

For comparison, the same study was repeated with dextran and polyethyleneglycol as additives. (PEG and Dextran cannot be used as stabilizer as they do not preserve the luciferase, data not shown).

B. Supporting Figures

Figure S1: Only luciferase in pullulan pill

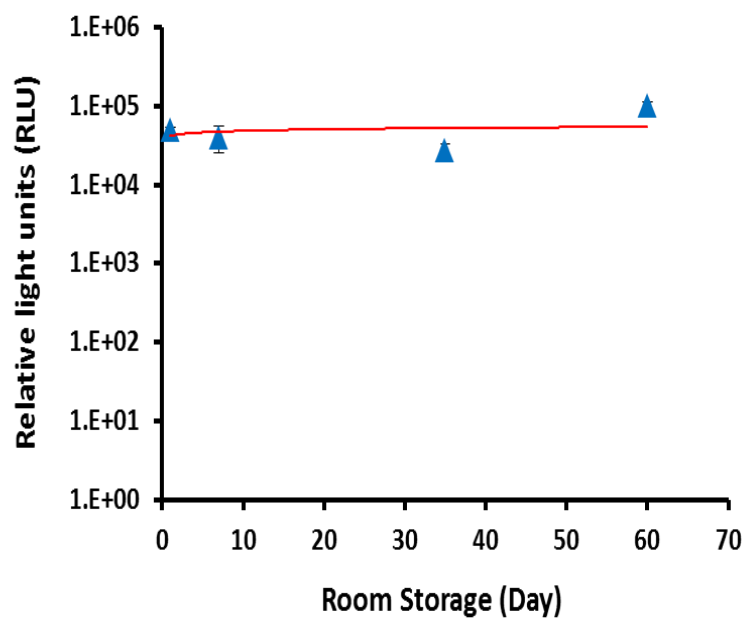


Figure S1. Evaluation of long-term stability of only luciferase in pullulan pills when stored at room temperature. The error bars representing the standard deviations based on triplicate repeats.

Figure S2: Effect of other polymers and polysaccharides on reaction behavior

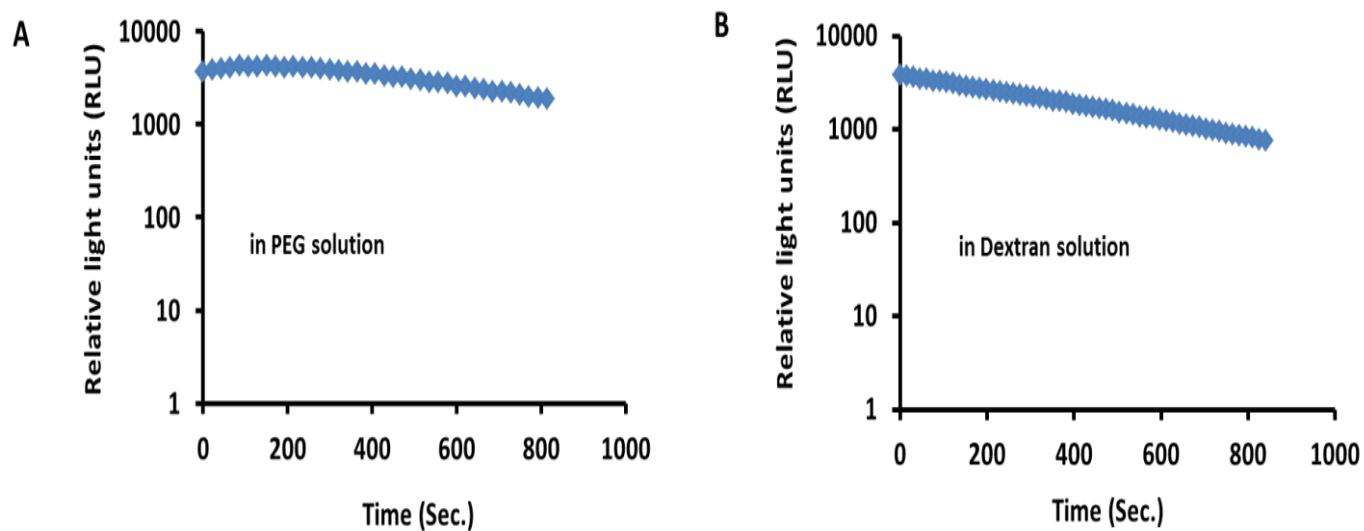


Figure S2. Reaction type when a) PEG, b) Dextran is used instead of pullulan.

Figure S3: Stability in Dextran Pills

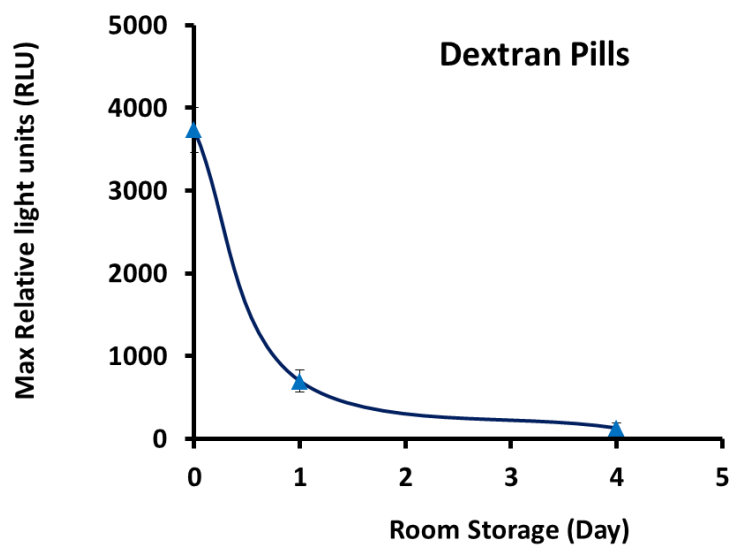
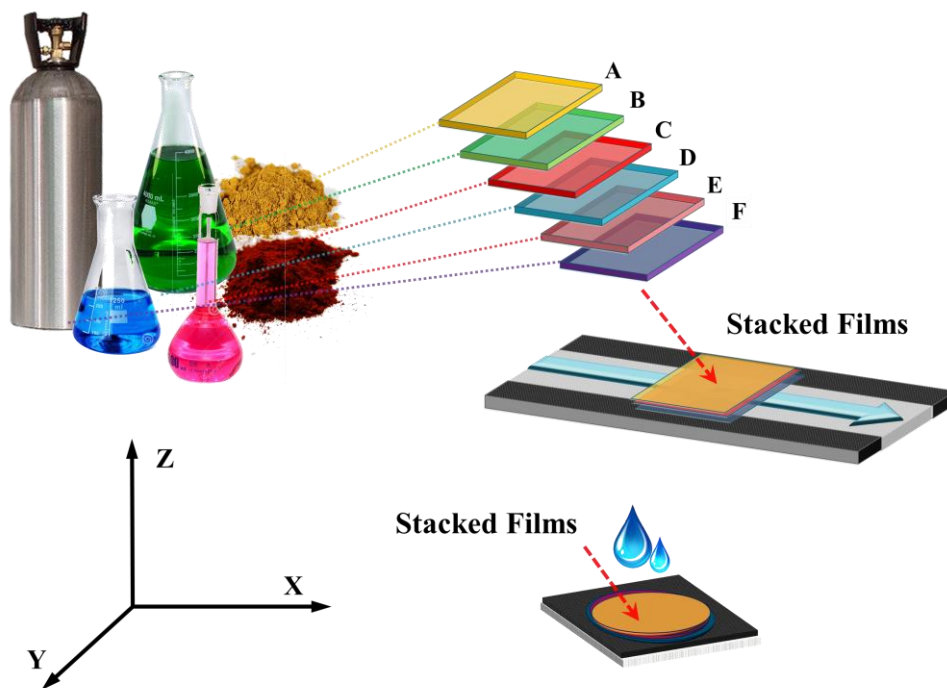


Figure S3. Stability of luminescence pills in dextran pills stored at room storage. Dextran is not preserving the luminescence reagents as good as pullulan

Chapter 6 Automatic Time Dependent Reagent Delivery in Paper-Based Microfluidics Devices



20 Word Summary:

Pullulan films may be loaded with desired reagents to provide multi-directional and sequential release mechanism which can be used to convert complex, multi-step chemical reactions to a simplified, scalable paper-based device while retaining control of the reaction rates and timing.

In Chapter 6, I initiated this project. Demonstration on *E. coli* detection was performed by myself with assistance Tracy Jingyun Wang who provided me with CPRG printed paper, and Dawn White who prepared the *E. coli* sample solutions, and Kevin Pennings. Demonstration on time dependent pH manipulation was performed by myself with very helpful assistance from Kevin Pennings. Polymer screening and testing the dissolution rate of different polymer films was performed with assistance from Karen Giang and Vince Leung. Dr. Balamurali Kannan contributed the idea of the Simon Reagents assay; I helped him to make the reagent-pullulan films and assemble it on paper devices, analyzing the related data and making the relevant figures. Prof. Filipe and Prof. Brenan, and Prof. Pelton gave many helpful suggestions on experiments. This work is a manuscript prepared for submission to Angew. Chem.

Automatic Time Dependent Multi-Reagents Delivery in Paper-Based

Microfluidics Devices Sana Jahanshahi-Anbuhi, Balamurali Kannan, Kevin Pennings, Vincent Leung, Jingyun Wang, Karen Giang, Dawn White, Robert Pelton, John D. Brennan,* and Carlos D. M. Filipe*

Abstract: Water soluble biopolymer, pullulan is used to entrap reagents and deliver them sequentially in lateral and z-direction to create paper based point-of-care sensors. The key advantage of this method includes the entrapment of labile and volatile reagents and stabilize them by forming thin films with pullulan. These pullulan films can be strategically pasted on a paper strip in different directions to form colorimetric sensors. The sequential release of entrapped reagents was shown using a simple demonstration which allows manipulation the pH of the lateral flow stream. Proof-of-principle demonstrations include (1) using Simon's reagents which is widely used for methamphetamine detection; and (2) creating ready-to-use assay kit for detection of *E. coli*.

Pullulan, an edible polysaccharide made up of maltotriose units has demonstrated very promising results in the stabilization of biomolecules & labile reagents, [1] nanoparticles etc., [2] [3]. The high water solubility and inert nature of pullulan makes it extremely useful in various fields from food packaging to biosensor applications. In addition to the ability to control fluid flow in the paper based microfluidic systems, [4] pullulan films can also be used for the delivery of multiple reagents. In this work, the fabrication of ready-to-use paper-based sensors are reported. The paper-based sensors have the capability to perform multi-steps operations such as buffering, cell-lysing and chromogenic reactions using pullulan as a binder for making reagent pellets. Direct immobilization of reagents on paper is not feasible in many applications especially given the instability of reagents in the storage or working conditions. Using pullulan as a

binder for reagents serves two major purposes. First, it stabilizes the reagents by protecting them from oxidative and/or thermal degradation. Second, pullulan can be used to control the rate and order of reagents delivery. These paper-based sensors with pullulan films have the ability to provide sequential release of reagents in both later flow and z-directional flow, allowing for a simple method for multistep reactions and assays. In this work, we demonstrate the capabilities of these paper-based sensors by successfully detecting the presence of *E. coli* using a CPRG-based colorimetric assay [5] and the detection drugs with secondary amines, such as methamphetamine, using the Simon's reagent[6] [7].

The presence of bacterial pathogens in beverages and food can cause serious illness in humans. Herein, we report a single step paper-based assay for the detection of coliforms using the CPRG-based colorimetric assay as described by Hossain et al.[5] The sensor consists of B-PER, Lysozyme and DNase casted into a pullulan disc and a CPRG treated paper. The resultant paper-based sensor can detect the presence of *E. coli* by simply applying the sample solution onto the sensor in a one-step process.

Simon's reagent is one of the most common reagents used to detect controlled substances such as methamphetamine, amphetamine, etc. It consists of acetaldehyde, sodium nitroprusside and sodium carbonate to react with secondary amines to produce a blue color. [8] The secondary amine forms enamine with acetaldehyde followed by the reaction with sodium nitroprusside to form immonium ion which subsequently hydrolyze to give the blue-colored Simon-Awe complex. This test is typically performed by adding individual reagents on the test substance to produce the color change. A paper based test for this type of reaction will avoid transporting volatile reagents to the field which greatly increase the convenience and user-friendliness of the test. Furthermore, the incorporation of pullulan films helps facilitate the sequential release of the different reagents which simplifies in the multi-step assay into a single step procedure. As a model for methamphetamine, diethylamine (DEA) was chosen as the analyte to avoid tedious procedure in procuring the controlled substance. Using this Simon reagent paper-strip, a linear range of DEA concentration and the limit of detection (LOD) was determined quantitatively.

Delivery of Multiple Reagents, Multidirectional Flow and Sequential Release

The pullulan films can facilitate multidirectional flow and sequential release of reagents. Pullulan films can be layered and adhered with a thin layer of water to form a 3D layered stack. When water flow through paper, the layered stack dissolves from the bottom upwards, releasing the entrapped reagents in order. This demonstrates the possibility of not only the release of multiple reagents but the sequential release of reagents using pullulan films.

In addition, this pattern shows flow in both a lateral direction

[*] S. Jahanshahi-Anbuhi, Dr. B. Kannan, K. Pennings, V. Leung, Dr. J. Wang, K. Giang, D. White, Prof. Dr. Robert Pelton, Prof. Dr. John D. Brennan, and Prof. Dr. Carlos D. M. Filipe
Departments of Chemical Engineering, and Chemistry & Chemical Biology.
McMaster University
1280 Main Street West, Hamilton, ON, L8S 4M1, Canada. Fax: (905) 521-1350.
Tel: (+1) 905-525-9140 (ext. 27278, 20682).
E-mail: brennanj@mcmaster.ca, filipe@mcmaster.ca

[**]The authors thank the Natural Sciences and Engineering Research Council of Canada and Sentinel Bioactive Paper Network for funding. The authors also thank the Canada Foundation for Innovation and the Ontario Innovation Trust for support of this work. R.P. holds the Canada Research Chair in Interfacial Technologies. J.D.B. holds the Canada Research Chair in Bioanalytical Chemistry and Biointerfaces. The authors would also like to thank Dr. Clemence Sicard for her useful consultation. The authors also acknowledge the McMaster Biointerfaces Institute (BI) where part of the experiments was performed.



Supporting information for this article is available.

through the paper and vertical direction through the pullulan film simultaneously. Controlled multidirectional flow is a unique capability of the pullulan bridges.

The delivery of multiple reagents from pullulan films is depicted in Figure 1a. Pullulan solutions with different dyes were cast and allowed to dry for pattern construction. Placing two films with different dye colors side by side allowed for un-mixed dye release on distinct sides of the channel.

Various pullulan film patterns were also constructed in addition to the side by side configuration. Figure 1b shows a 'checkered' pattern film, where different colored films were cut and adhered to a plain film backing, and in Figure 1c is a sample of layer-by-layer stack pattern. The ease of assembly indicates that these patterns can be easily manipulated and that the pullulan film system provides the possibility of multiple reagent delivery.

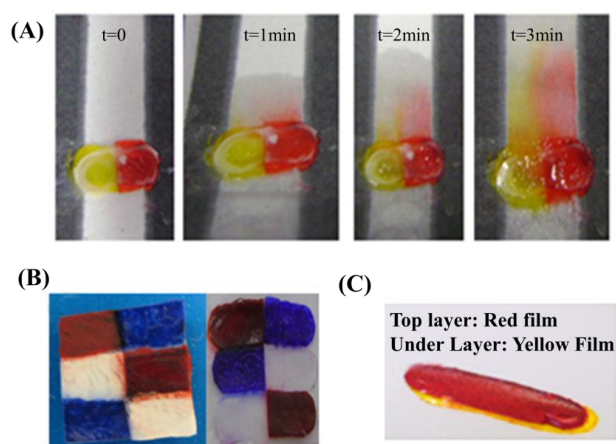


Figure 1(a) Pictures of dye being released from a 2-tone/side-by-side red and yellow bridge. (b) Examples of Pullulan bridge formations and a 'checkered' pattern. (c) Stack pattern

pH Adaptor. The use of a variable pH device was selected as a visual proof-of-concept, while it is suggested that the pullulan films may be loaded with desired reagents for step-wise or time dependent reactions.

The pullulan films can be layered together with films at different pH. Placing the stack of pullulan films was onto a paper device providing the possibility of manipulating the pH of the stream throughout the paper. Experimental details are provided in the Supporting Information.

As shown in Figure 2a, to run the test, the solution was passed through the paper, and the change in pH can be observed by the colorimetric changes of the pH indicator paper. Figure 2b shows the step-by-step changes of the pH in the upper stream provided by stack of pullulan films at pH of 2, 4, 6, and 8 (Related video is provided in the Supporting). The time of the pH change can be delayed or regulated by simply adding neutral pullulan films, Figure 2c.

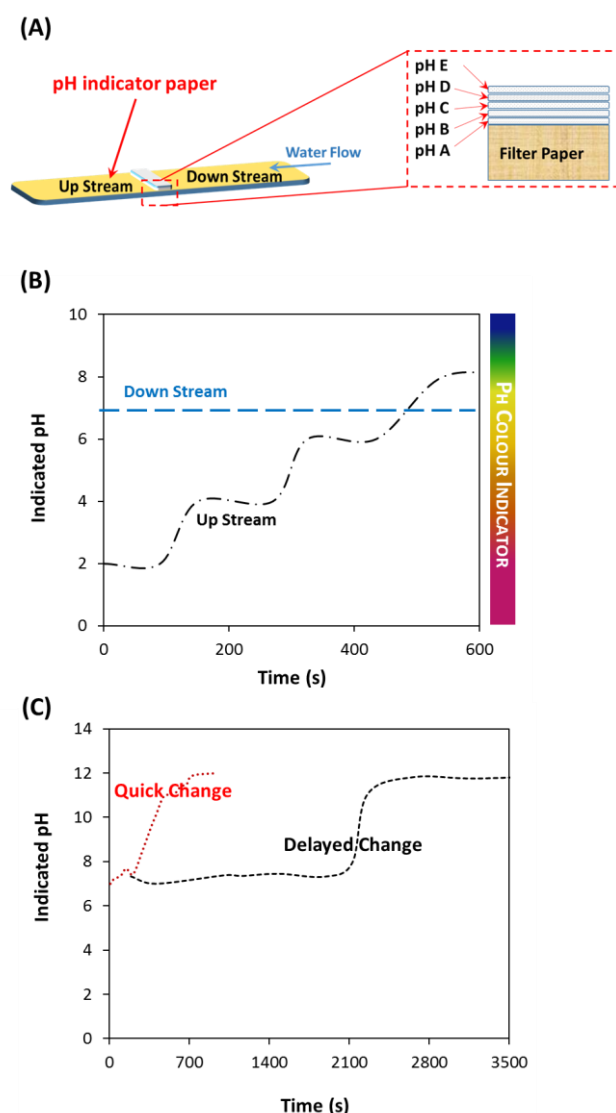


Figure.2 pH adaptor. Sequential release of pullulan films on a paper-based device. (a). Schematic set up (b) pH change versus time for a pullulan system consist of pullulan films layers at pH 2, 4, 6 and 8 (c) Quick step change in pH by having a combination of 4 pullulan films respectively at pH 7, 7, 12, and 12 in compare with having delayed change when there is 7 films respectively at pH 7, 7, 7, 7, 12, 12, and 12.

Simon reagent strip for lateral flow detection Lateral Flow Pattern

To demonstrate the ability of pullulan to sequentially release the entrapped reagents for lateral flow detection, a simple system for secondary amines using Simon's reagent was chosen. It is one of the common reagents used to detect methamphetamine. Acetaldehyde and Sodiumnitroprusside (SNP) were entrapped in pullulan films and placed sequentially along a paper channel (Figure 3). When the analyte solution (sec amine) is wicked through this channel, initially the amine reacts with acetaldehyde forms enamine and it subsequently reacts with SNP to form blue color Simon-Awe complex. This multi-steps reaction is summarized reaction in Figure 3C:

i) As the solution passes the first pullulan film containing acetaldehyde, 2^o amines present in the solution react with acetaldehyde to form an enamine.
 ii) When solution passes the next film containing SNP and sodium carbonate, the enamine reacts with the sodium nitroprusside to form an imine.
 iii) As the sodium carbonate dissolves, and it dissociates into HCO₃⁻, allows the imine to hydrolyze, forming the Simon-Awe complex, which is a deep blue/purple colour.
 The role of pullulan is to stabilize the reagents in thin films and allow reacting sequentially for the detection of sec. amine. Acetaldehyde is volatile, water soluble compound and has boiling point of 20°C. However, acetaldehyde can be entrapped in pullulan film and being stored at room temperature.

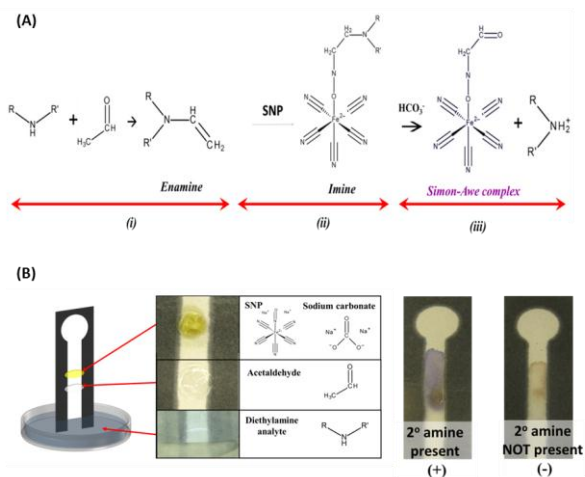


Figure.3 Simon reagent test for detection of secondary amine in paper based devices. (a) Chemical reaction. (b) Lateral flow design and actual images of the positive/negative test's result.

Z-Directional Flow Pattern

Pullulan films containing reagents can also be stacked in z-direction in a systematic order to create the sensor without reacting with each other. This can be utilized when the lateral flow detection is not possible or time consuming. Simon reagent is pasted on paper strip in such a way where the bottom film is SNP/SC and top film is acetaldehyde. When the analyte (Diethylamine) is spotted on the top film (acetaldehyde), it reacts to form enamine and the consequent reaction with SNP/SC film to form blue color as shown in Figure 4A.

A series of DEA solution was prepared with various concentration ranging from 100 ug/mL to 50 mg/mL and 20 uL of each solution was spotted on circular paper strip allowing z-directional flow. The blue color intensity was analysed for each concentration and plotted against the concentration, Figure 4B. The linear dependency of concentration with color intensity falls in the range between 1 mg/mL and 10 mg/mL.

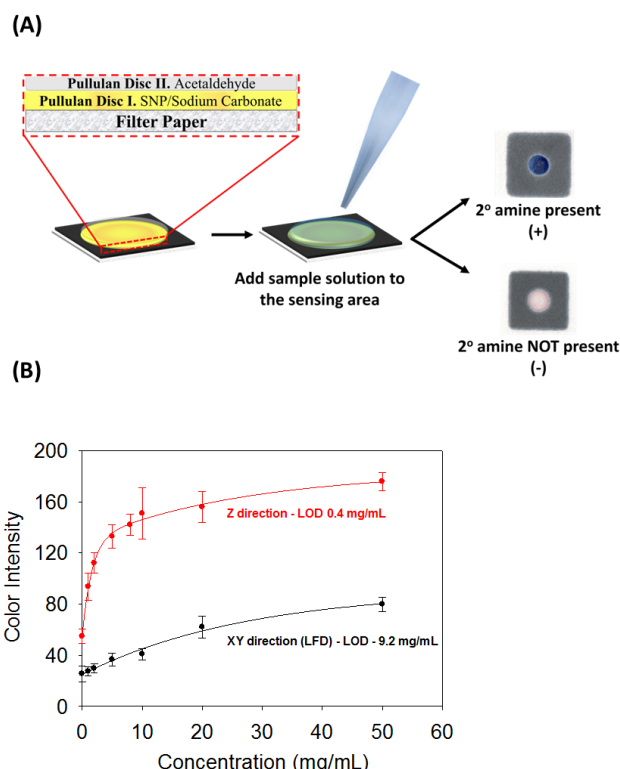


Figure.4 Simon reagent test. (a) Z-directional flow (spot test) design. (b) Color intensity vs. secondary amine for both "lateral flow" and "spot test" designs.

A Paper-Based Sensor for the Detection of *E. coli*.

The assay kit consists of two parts, a B-PER pullulan pill and a CPRG paper as shown in Figure 5A, B. The test can be run simply by introducing the water sample to the assay kit followed by 40 min incubation. The sensor will turn a red/purple color in the presence of *E. coli* and a light yellow color in the absence of *E. coli*.

To achieve quantitative colorimetric detection of *E. coli* smartphone camera or mobile scanner and image-processing software (such as ImageJ) [9] can be used. Figure 5 shows a plot of the color intensity versus concentration of *E. coli*. This simple, equipment free method can be used to detect *E. coli* at levels as low as 5×10⁵ cfu/mL.

c

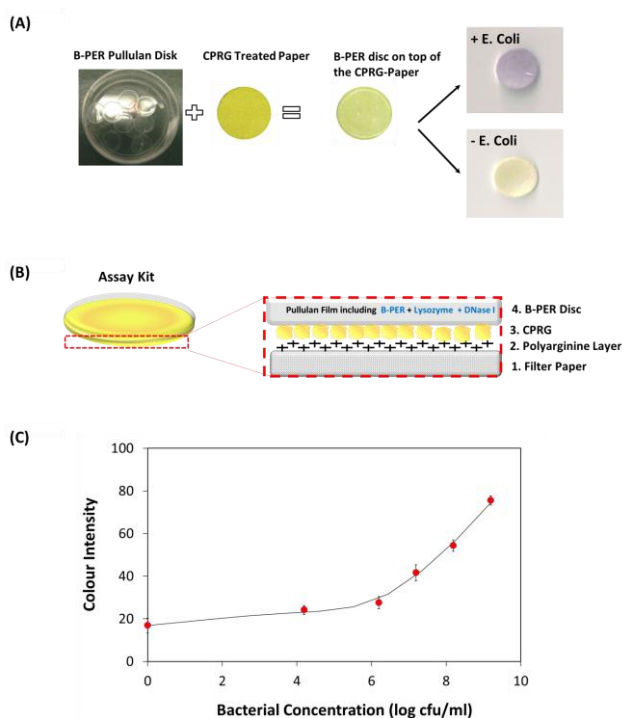


Figure.5 *E. coli* detection using paper based device

In summary, Labile and volatile reagents are immobilized and stabilized by forming pullulan films. The reagents thus stabilized can be sequentially released in a time-dependent fashion on a paper strip to form paper based sensors. This time dependent reagent deliverer allows the user to manipulate fluid movement in all three directions (x,y and z directions) to create multi-step reactions and assays. Using this technology, paper based analytical devices is created for the detection of *E. coli*, and the secondary amine. Construction of the secondary amine was demonstrated with Simon reagent which includes acetaldehyde, a highly volatile compound trapped in pullulan. Low concentration (20 ug) detection of diethylamine which is analogous is methamphetamine was shown using the paper based sensor. These type of sensors fabricated with pullulan-entrapped reagents will avoid handling such labile and volatile reagents on the field. This concept can simplify the detection systems which involves complex tandem reactions to simple ready-to-use sensors.

Keywords: Bioassay • pullulan • *E. coli* detection • Simon Reagents • Multidirectional Flow, Biactive Paper-Based Microfluidic Devices, Reagent Delivery

References.

- [1] S. Jahanshahi-Anbuhi, K. Pennings, V. Leung, M. Liu, C. Carrasquilla, B. Kannan, Y. Li, R. Pelton, J. D. Brennan, C. D. M. Filipe, *Angewandte Chemie* 2014, n/a-n/a.
- [2] M. Ganeshkumar, T. Ponrasu, M. D. Raja, M. K. Subamekala, L. Suguna, *Spectrochimica Acta Part A: Molecular and Biomolecular Spectroscopy* 2014, 130, 64-71.
- [3] P. Kanmani, S. T. Lim, *Carbohydrate Polymers* 2013, 97, 421-428.
- [4] S. Jahanshahi-Anbuhi, A. Henry, V. Leung, C. Sicard, K. Pennings, R. Pelton, J. D. Brennan, C. D. M. Filipe, *Lab Chip* 2014, 14, 229-236.
- [5] S. M. Z. Hossain, C. Ozimok, C. Sicard, S. D. Aguirre,

M. M. Ali, Y. F. Li, J. D. Brennan, *Analytical and Bioanalytical Chemistry* 2012, 403, 1567-1576.

[6] S. SUZUKI, T. INOUE, T. NIWAGUCHI, *Journal of Chromatography* 1983, 267

[7] A. Chooduma, N. N. Daeida, *Drug Test. Analysis* 2011, 1-6.

[8] K. A. L. Kovar, M., *United Nations: Scientific and Technical Notes* 1989, SCITEC/6.

[9] aS. Jahanshahi-Anbuhi, P. Chavan, C. Sicard, V. Leung, S. M. Z. Hossain, R. Pelton, J. D. Brennan, C. D. M. Filipe, *Lab Chip* 2012, 12, 5079-5085; bS. Jahanshahi-Anbuhi, A. Henry, V. Leung, C. Sicard, K. Pennings, R. Pelton, J. D. Brennan, C. D. M. Filipe, *Lab Chip* 2014, 14, 229-236; cC. Liu, Q. Jia, C. Yang, R. Qiao, L. Jing, L. Wang, C. Xu, M. Ga, *Anal. Chem.* 2011, 83, 6778-6784.

Supplementary Information

Automatic Time Dependent Multi-Reagents Delivery in Paper-Based Microfluidics Devices

Sana Jahanshahi-Anbuhi, Balamurali Kannan, Kevin Pennings, Vincent Leung, Jingyun Wang, Karen Giang, Dawn White, Robert Pelton, John D. Brennan, and Carlos D. M. Filipe**

A. Experimental Details

Material. Acetaldehyde, Sodiumnitroprusside, Sodium carbonate, TSB (Tryptic Soy Broth), poly-arginine (MW>70kDa), CPRG (chlorophenol Red- β -D-galactopyranoside, and Allura Red were received from Sigma-Aldrich. Pullulan (PI20, molecular mass of 200 kDa) was obtained from Hayashibara Co, Ltd, Okayama, Japan. Hydrophobic spray (Heavy-Duty Water Proofer, SOFSOLE, available at sport accessories stores). PET films (Polyester 50 Film, 0.004" thick, clear, Part # 8567k44) were purchased from McMaster-CARR (Hamilton, ON, Canada).

PH Adapter:

A pH adapter was constructed to demonstrate the sequential release of pullulan films on a paper-based device. The pullulan films were prepared by casting pullulan solution on a PET sheet, as demonstrated in Figure S1. Strips of 0.5 cm \times 2 cm tape were placed onto the PET sheet and the PET sheet was treated with a hydrophobic . The strips of tape were then removed, thus leaving hydrophilic areas on the PET sheet for casting the pullulan films. In order to create pullulan films with different pH several 12% pullulan solutions were prepared with pH ranging from 2-12 were created. HCl and NaOH were used to adjust the solution to the desired pH. 150 μ L of the pullulan solution was then added to the hydrophilic area using a pipette. The solution was then air dried to form a film, Figure 1S.

The pullulan films were then layered together with films at different pH. Given the self-sealing property of pullulan 1 μ L of 20% pullulan solution was placed on each corner of the film in

order to secure the pullulan films onto each other. In the same way, the stack of pullulan films was placed onto a pH indicator paper.

To run the test, the solution was passed through the paper, and the change in pH can be observed by the colorimetric changes of the pH indicator paper. The time of the pH change can be delayed or regulated by simply adding neutral pullulan films.

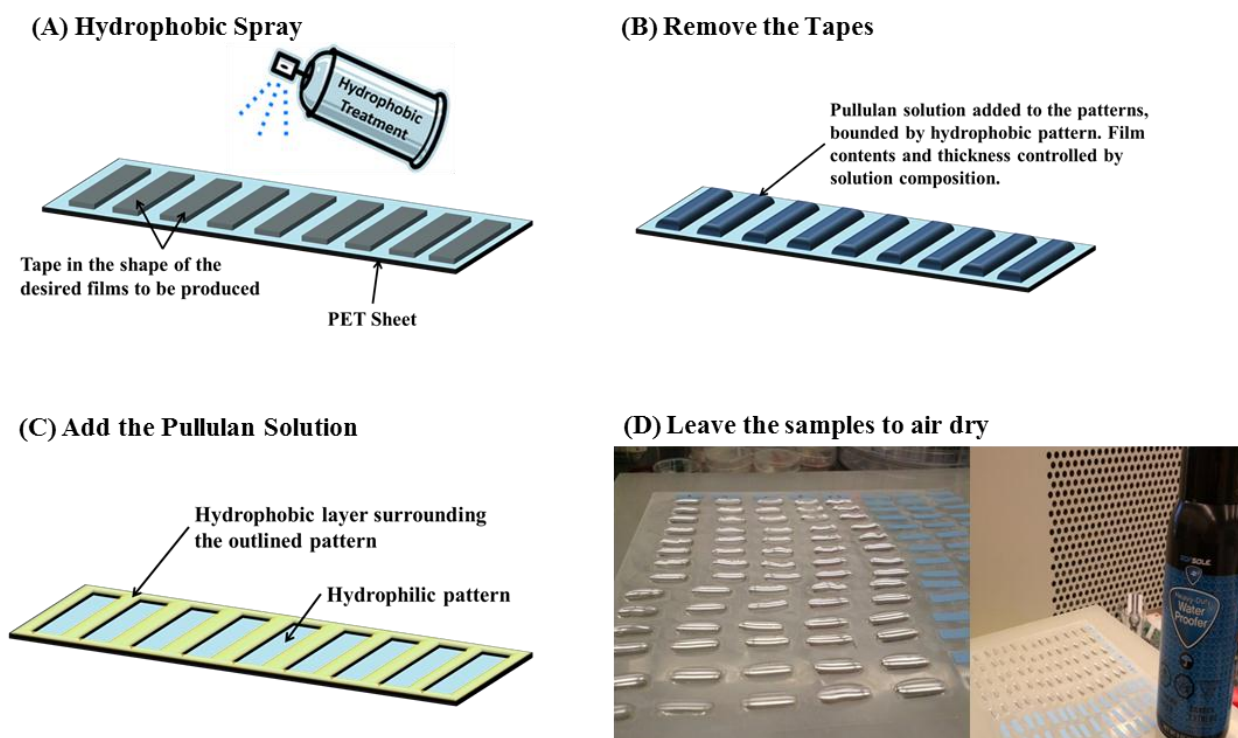


Fig.S1 Creating pullulan films in desired shape and dimension

A Paper-Based Sensor for the Detection of *E. coli*:

The sensor consists of two parts, a B-PER pullulan pill and a CPRG paper.

The CPRG Paper. 2 wt% poly-arginine (MW>70kDa) and 9 mM CPRG (chlorophenol Red- β -D-galactopyranoside) dissolved in water were sequentially printed onto the Whatman #1 filter paper using Canon thermal inkjet printer with the “high print quality” setting.

The B-PER pill lyses any bacterial cells in the sample solution and in the presence of β -galactosidase, CPRG will be hydrolyzed to produce a red-colored product. Each B-PER pullulan pill was casted from 32 μ L of 5% pullulan and 3 μ L of B-PER buffer solution. The B-PER buffer solution was prepared by adding 2 μ L of lysozyme and 2 μ L of DNase to 1 mL of B-PER reagent. The CPRG paper which was prepared by printing CPRG onto Whatman paper and was cut to match the size of the B-PER pill.

The B-PER pill was then attached to the CPRG paper using 1 μ L of 20% pullulan.

To run the test, the sensor can be placed into a container such as a 96-well plate or a 1.5 mL Eppendorf tube cap. Once inside the container, 200 μ L of sample solution was added onto the sensor and incubate for 40 minutes. The sensor will turn a red/purple color in the presence of *E. coli* and a light yellow color in the absence of *E. coli*. The air dried test papers were then imaged using a handheld scanner (Flip Pal 100C Mobile scanner). The color intensity of the sensing zone was quantified using ImageJ software as described elsewhere. [11, 97]

***E. coli* Culture.** *E. coli* (ATCC 25922) was culture overnight in TSB (Tryptic Soy Broth) media for about 20 hrs at 37 °C with shaking rate of 200 rpm. (The 5 ml culture was started with one colony picked from an agar plate. No antibiotic.)

Paper-Based Sensor for the Detection of Secondary Amine:

Acetaldehyde Pullulan Film: 0.5 g of pullulan was dissolved in 5 mL of water. 1 mL of acetaldehyde was added and mixed using a vortex. It was casted as thin films on bench top by pipetting out 10 μ L drops on PET sheets.

Sodium nitroprusside-Sodiumcarbonate Pullulan Film : 0.1 g each of sodiumnitroprusside and sodium carbonate were dissolved in 5 mL water. 0.25 g of pullulan was added and mixed using a vortex. It was casted on bench top water. 1 mL of acetaldehyde was added and mixed using a vortex. It was casted as thin films on bench top by pipetting out 10 μ L drops on PET sheets.

For both lateral flow paper sensor and z-direction flow sensors, the films were stucked in such a way that the analyte will react with acetaldehyde first followed by SNP and sodium carbonate.

Pullulan Kinetics – Absorbance Measurement. The pullulan films were made by mixing 1 mL of 20 g/L dye (Allura Red or Tartrazine) solution with 12 mL of pullulan solution. 2 mL, 4 mL, and 6 mL of the mixed solutions were then cast onto three different petri dishes to create films with varying thicknesses. The solution in the petri dishes was air dried. Once dried, the films were removed from the dishes and weighed. Films were then hole-punched to produce 1 cm × 0.5 cm cut-outs. These cut-outs were weighed and the mass of dye in the cut outs was calculated. A single pullulan film cut-out was added to a 10 mL vial of DI water. From this, 150 μL samples were taken every 15 seconds and placed in Eppendorf tubes. 100 μL of the sample was then added to a 96-well dish. The first sample was taken at time zero, before the film was placed into water. These samples were used to determine the absorbance of the solution at each time to characterize the dye release kinetics.

B. Supporting Figures

To study the release kinetics of the pullulan film, Allura Red was added to the pullulan solution and cast into films as described in the methods section. For sample analysis, serial dilutions of Allura Red dye were prepared to create a standard curve using a spectrometer (Tecan infinite® M1000 plate reader). The absorbance of each sample was then recorded, and the corresponding concentration was calculated using the standard curve.

Figure S2 shows the total mass of Allura Red released from the pullulan film as a function of time for different film thicknesses

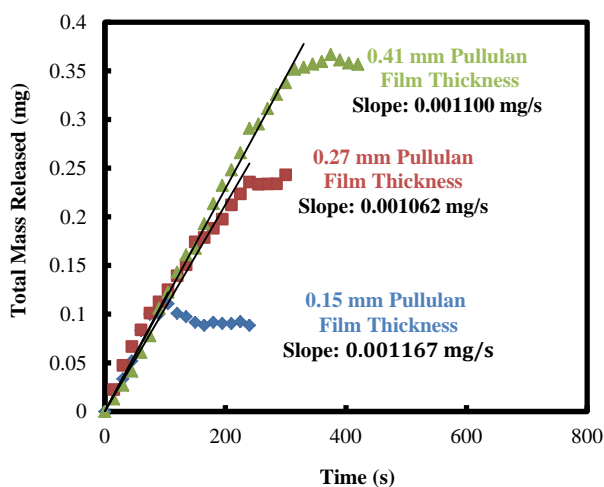


Fig.S2 Release Kinetics for pullulan film. zero order kinetic shown by the total mass of Allura Red release as a function of time.

Furthermore, as depicted in Figure S3, similar kinetic study is done for CMC (Sodium carboxy methyl cellulose, MW 250,000), MC (Methyl cellulose), PVA (Polyvinyl amine, MW 125,000, 87-89% hydrolysis), and HEC (Hydroxylethyl Cellulose). Depends on the application, different polymers may be combined with pullulan films to prolong the releasing process.

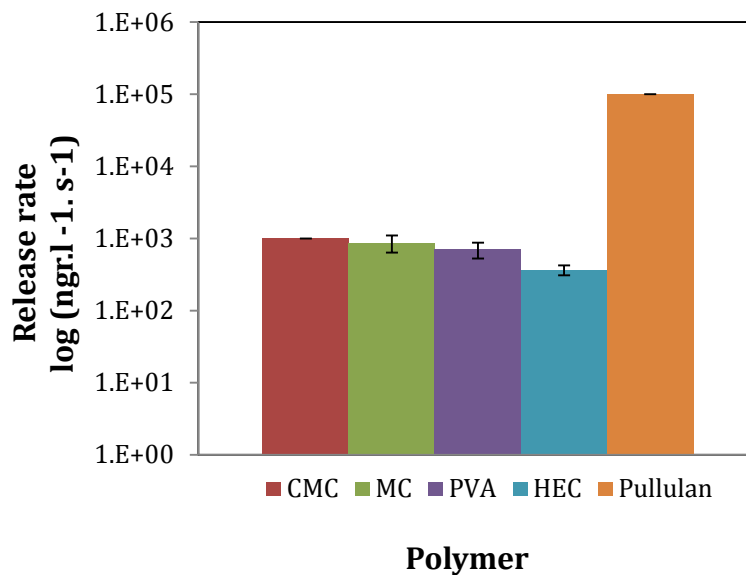


Fig.S3 Release Kinetics for different polymeric films

- [1] W. Van Zijl. Studies on diarrhoeal diseases in seven countries by the WHO Diarrhoeal Diseases Advisory Team. Bulletin of the World Health Organisation. 35 (1966) 249-61.

Chapter 7 Concluding Remarks

The major contributions of this work are given as follows:

☑ From the experimental results reported in *Chapter 2*, it was demonstrated that high speed capillary flow through paper-based channels can be achieved by sandwiching paper between flexible cover slips. The following can be concluded from this work:

- Flexible cover slips have been used to fabricate an accelerator for paper-based microfluidic devices.
- This method increases the elution distance and accelerates the capillary wicking process by more than ten times compared to capillary flow through non-covered paper.
- The height of the liquid increases with $t^{1/3}$.
- This dependence was demonstrated using three different flexible films (PET, Clear Tape back-side and PARAFILM[®] M) and with three different fluids (water and two silicon oils).
- This method provides:
 - A way to control and increase the flow rate.
 - The possibility of having different flow velocities without the use of external energy.
 - These devices can be fabricated with basic tools without compromising the simplicity, low cost, or ease-of-use that is characteristic of paper-based devices.

☑ Furthermore, in *Chapter 3*, it was shown that the volume flow of solution which reaches to a specific zone of paper-based channels can be automatically controlled by using a dissolvable pullulan film in the way of the flow stream. It was demonstrated that:

- A physical gap in paper impedes flow
- Temporary connection made with soluble polymeric bridge

- Flow crossing the valve is stopped at a specified distance and dried within a required time limit
 - Variation of the bridge thickness can provide both time control and allow for tunable volume
 - This technique provides the possibility of controlling the volume of liquid passed through the paper-based analytical devices
 - The valve utility was demonstrated by a one-step, fully automatic implementation of a multi-step pesticide assay requiring timed, sequential exposure of an immobilized enzyme layer to separate liquid streams.
- ☑ In addition, a new generation of biosensors, labelled as LAB-ON-PILLS is introduced and discussed in *Chapters 4* and *5*. It is shown that:
- Pullulan film provides a barrier from the environment (most notably it is oxygen impermeable).
 - Using water soluble pullulan biopolymer, a method is described for stabilizing materials for long term storage at room temperature.
 - Encapsulating substrate and enzymes inside the pullulan pills not only immobilize the substrate/enzyme and increases their stability and time of life but also provides a pill-shape sensor which is more user friendly.
 - Pullulan is used to entrap AChE, IDA, Taq polymerase enzyme, luciferase and luciferin and the resulting bioreagent pills are stable for long term storage at room condition.
 - AChE and IDA pullulan-based pills are utilized for point-of-care detection of pesticides.
 - All-in-one luminescent pills are utilized for stabilization of highly unstable firefly luciferase, and preloading of all required components for detection of ATP.

- These highly soluble luminescent pills readily release all the components in testing solution and retain the glow kinetics to produce stable light for more than an hour.
 - Pullulan-based bioreagent pills are stable both at ambient conditions as well as at elevated temperature.
 - This method provides valuable savings on storage, shipping and distribution.
- ☑ In addition to utilizing pullulan films as a flow cut-off system and stabilizing bioreagents, in *Chapter 6* it is suggested that the pullulan films may be loaded with desired reagents (even if they are volatile or unstable) and being systematically arranged or combined for step-wise or time dependent reactions, resulting in a 'ready-to-use' sensor.
- Development of multidirectional flow and sequential release of reagents in vertical direction or lateral flow within paper-based microfluidic devices is facilitated using this technique without compromising the simplicity and low cost of paper-based devices.
 - As a visual proof-of-concept, and showing the ability of the proposed system to control the reagent delivery, a device for manipulating the pH of the flow was demonstrated.
 - Using this sequential release technique, both: (a) A ready-to-use *E. coli* assay kit involving cell lysing and an enzymatic reaction, and (b) Simon reagent test for quantitative measurement of secondary amine (methamphetamine) are demonstrated.
- ☑ A simple technique has been developed for pullulan pill manufacturing by simply printing on flexible films, with or without patterns. In this method there is no need to have molds with different shapes and sizes. This method includes mixing the reagent with pullulan solution and:
- Casting the solution on flexible PET sheet and let it dry which result in circle shape films. The films may be dried under air or under an inert gas such as nitrogen, as

each bioreagent requires.

- For other desired patterns (rather than the circle shape pills) the pullulan solution can be added to patterns bounded by hydrophobic pattern. Film contents and thickness are controlled by solution composition.